



Universitat Autònoma de Barcelona

**ADVERTIMENT.** L'accés als continguts d'aquesta tesi queda condicionat a l'acceptació de les condicions d'ús establertes per la següent llicència Creative Commons:  [http://cat.creativecommons.org/?page\\_id=184](http://cat.creativecommons.org/?page_id=184)

**ADVERTENCIA.** El acceso a los contenidos de esta tesis queda condicionado a la aceptación de las condiciones de uso establecidas por la siguiente licencia Creative Commons:  <http://es.creativecommons.org/blog/licencias/>

**WARNING.** The access to the contents of this doctoral thesis it is limited to the acceptance of the use conditions set by the following Creative Commons license:  <https://creativecommons.org/licenses/?lang=en>

Doctoral Thesis

D-[113–122]apoJ mimetic peptide as a therapy  
against atherosclerosis. *In vitro* and *in vivo*  
approaches

Andrea Patricia Rivas Urbina

Doctoral Program in Biochemistry, Molecular Biology and Biomedicine  
Department of Biochemistry and Molecular Biology  
Universitat Autònoma de Barcelona  
Institut de Recerca de l'Hospital de la Santa Creu i Sant Pau

Barcelona, October 2021



D-[113–122]apoJ mimetic peptide as a therapy  
against atherosclerosis. *In vitro* and *in vivo*  
approaches

Andrea Patricia Rivas Urbina

Doctoral Program in Biochemistry, Molecular Biology and Biomedicine

Department of Biochemistry and Molecular Biology

Universitat Autònoma de Barcelona

Institut de Recerca de l'Hospital Sant Pau

Directors:

José Luis Sánchez Quesada, PhD.

Institut de Recerca de l'Hospital de la Santa Creu i Sant Pau

Jordi Ordóñez Llanos, MD, PhD.

Institut de Recerca de l'Hospital de la Santa Creu i Sant Pau

Department of Biochemistry and Molecular Biology. Universitat Autònoma  
de Barcelona





Universitat Autònoma de Barcelona  
Department of Biochemistry and Molecular Biology  
Doctoral Program in Biochemistry, Molecular Biology and Biomedicine

**D-[113–122]apoJ mimetic peptide as a therapy against  
atherosclerosis. *In vitro* and *in vivo* approaches**

Report presented by Andrea Patricia Rivas Urbina in order to complete the requirements to be granted the degree of Doctor of Philosophy in Biochemistry, Molecular Biology and Biomedicine, by Universitat Autònoma de Barcelona.

This thesis has been carried out in the Cardiovascular Biochemistry group in the Research Institute of Hospital de la Santa Creu i Sant Pau, co-directed by Dr. José Luis Sánchez Quesada and Dr. Jordi Ordóñez Llanos.

Dr. José Luis Sánchez Quesada  
Institut de Recerca de l'Hospital  
de la Santa Creu i Sant Pau

Dr. Jordi Ordóñez Llanos  
Institut de Recerca de l'Hospital  
de la Santa Creu i Sant Pau  
Department of Biochemistry and  
Molecular Biology. Universitat  
Autònoma de Barcelona

Andrea Patricia Rivas Urbina  
Institut de Recerca de l'Hospital  
de la Santa Creu i Sant Pau



- *A Papi, mi ángel.*



## ■ CONTENTS



## ■ TABLE OF CONTENTS

■ <b>CONTENTS</b>	<b>9</b>
■ <i>TABLE OF CONTENTS</i> .....	11
■ <i>INDEX OF FIGURES</i> .....	15
■ <i>INDEX OF TABLES</i> .....	17
■ <i>ABBREVIATIONS</i> .....	19
■ <i>ABSTRACT</i> .....	23
■ <i>RESUMEN</i> .....	25
■ <i>GRAPHICAL ABSTRACT</i> .....	27
 CHAPTER I.....	 29
■ <b>INTRODUCTION</b>	<b>29</b>
1. Atherosclerosis.....	31
1.1 Atherosclerosis development .....	33
2. Mouse models of atherosclerosis .....	38
2.1 LDL receptor-deficient (LDLR-KO) mice.....	41
3. Lipoproteins and Lipoprotein Metabolism .....	44
3.1 Chylomicrons .....	48
3.2 VLDL.....	49
3.3 HDL.....	50
3.4 LDL .....	53
4. LDL and Atherosclerosis .....	55
4.1 Oxidized LDL (oxLDL).....	57
4.2 Desialylated LDL.....	58
4.3 Glycated LDL (glyLDL).....	59
4.4 Small-dense LDL (sdLDL).....	60
4.5 Carbamylated LDL .....	60



4.6	Electronegative LDL [LDL(-)].....	61
4.7	Aggregated LDL (agLDL).....	61
5.	Apolipoprotein J (ApoJ) or Clusterin (CLU).....	63
6.	Mimetic Peptides.....	66
6.1	ApoA-I mimetic peptide .....	66
6.2	ApoE mimetic peptide .....	67
6.3	ApoJ mimetic peptide.....	68
CHAPTER II.....		71
▪	<b>HYPOTHESIS AND OBJECTIVES</b>	<b>71</b>
CHAPTER III.....		77
▪	<b>MATERIALS AND METHODS</b>	<b>77</b>
1.	Peptides	81
2.	Animal study design	81
3.	Lipoprotein isolation	82
4.	LDL subfraction separation	85
5.	Plasma and lipoprotein characterization	86
6.	<i>In vitro</i> modification of LDL	89
7.	Methods for monitoring LDL aggregation	91
8.	Binding of D-[113–122]apoJ peptide to LDL	92
9.	Susceptibility to oxidation of LDL and HDL	93
10.	Electronegativity of LDL	94
11.	Cholesterol efflux capacity of HDL	94
12.	Evaluation of atherosclerotic lesions	95
13.	Quantitative RT-PCR analyses	96
14.	Statistical analysis	98

CHAPTER IV .....	99
▪ <b>ORIGINAL PUBLICATIONS</b>	<b>99</b>
PUBLICATION 1 .....	103
PUBLICATION 2 .....	117
CHAPTER V .....	141
▪ <b>GLOBAL DISCUSSION</b>	<b>141</b>
CHAPTER VI .....	153
▪ <b>CONCLUSIONS</b>	<b>153</b>
▪ <b>REFERENCES</b>	<b>157</b>
▪ <b>ACKNOWLEDGEMENTS</b>	<b>179</b>



## ■ INDEX OF FIGURES

Figure 1. Mononuclear phagocytes in atherogenesis. ....	33
Figure 2. Coronary fibrous cap atheroma in a 24-year-old man. ....	35
Figure 3. Thin fibrous cap. ....	36
Figure 4. (A) Healed plaque rupture. (B) Stenosis of the anterior descending coronary artery in a 40-year old man. ....	37
Figure 5. Overview of current mouse models of atherosclerosis. ....	40
Figure 6. Aortic sinus lesion morphology in LDL-R KO mice. ....	43
Figure 7. Lipoprotein structure .....	45
Figure 8. Classes of Lipoproteins.....	46
Figure 9. Lipoprotein metabolism.....	48
Blue arrows refer to points of action of the respective enzymes in blue.	48
Figure 10. Chylomicron structure. ....	49
Figure 11. VLDL structure.....	50
Figure 12. HDL structure.....	51
Figure 13. LDL structure. ....	54
Figure 14. OxLDL. Oxidized product-induced native LDL oxidation and modifications of apoB amino acids.....	58
Figure 15. Glycosylation: modification of LDL and apoB by advanced glycosylation end-products (AGEs).....	59
Figure 16. Carbamylation.....	60

Figure 17. Aggregation and fusion of LDL.....	62
Figure 18. ApoJ structure.....	65
Figure 19. D-[113–122]apoJ peptide structure. ....	69
Figure 20. Experimental design. ....	82
Figure 21. Radding and Steinberg formula.....	84
Figure 22. Schematic view of SDS-PAGE process of protein samples...	88

## ■ INDEX OF TABLES

Table 1. Major types of lesions of atherosclerosis.....	38
Table 2. Lipoprotein Classes.....	45
Table 3. Scheme of LDL modification .....	56
Table 4. Methodology used in each of the publications presented. P: publication. ....	80
Table 5. Lipoprotein density distribution .....	84
Table 6. Step salt gradient for LDL (+) and LDL (-) isolation by FPLC....	86



## ■ ABBREVIATIONS

ABCA1: ATP-binding cassette transporter A1

agLDL: aggregated LDL

ALT: alanine aminotransferase

Apo: apolipoproteins

ApoE-KO: apolipoprotein E knock out mice

AST: aspartate aminotransferase

BHT: butylated hydroxytoluene

CD: circular dichroism

cDNA: complementary deoxyribonucleic acid

CER: ceramide or N-acetylsphingosine

CETP: cholesteryl esters transfer protein

CHD: coronary heart disease

CLU: clusterin

CVD: cardiovascular diseases

DLS: dynamic light scattering

DNA: deoxyribonucleic acid

EDTA: ethylenediaminetetraacetic acid

ELISA: enzyme-linked immunosorbent assay

FC: free cholesterol

FFA: free fatty acids

FH: familial hypercholesterolemia

FPLC: fast protein liquid chromatography

GAG: glycosaminoglycans

GGE: non-denaturing polyacrylamide gradient gel electrophoresis

GP: generalized polarization



HDL: high-density lipoprotein  
HDL-C: high-density lipoprotein cholesterol  
HL: hepatic lipase  
IDL: intermediate-density lipoprotein  
KBr: potassium bromide  
LCAT: lecithin-cholesterol acyltransferase  
LDL: low-density lipoprotein  
LDL(+): electropositive low-density lipoprotein  
LDL(-): electronegative low-density lipoprotein  
LDL-R: LDL receptor  
LDLR-KO: LDL receptor knock-out  
LOX-1: lectin-like-oxidized LDL receptor-1  
LPC: lysophosphatidylcholine  
LPL: lipoprotein lipase  
LRP: LDL receptor-related protein  
MMPs: matrix metalloproteinases  
MI: myocardial infarction  
NEFA: non-esterified fatty acids  
ox-LDL: oxidized LDL  
OCT: optimal cutting temperature compound  
ORO: oil red O  
PBS: phosphate saline buffer  
PC: phosphatidylcholine  
PGs: proteoglycans  
PL: phospholipids  
PLC: phospholipase C  
qRT-PCR: quantitative real-time polymerase chain reaction  
RNA: ribonucleic acid  
ROS: reactive oxygen species  
RT: room temperature  
SD: standard deviation

SDS-PAGE: sodium dodecylsulphate polyacrylamide-gel electrophoresis

sdLDL: small dense LDL

SEC: size exclusion chromatography

SEM: standard error of the mean

SM: sphingomyelin

SMase: sphingomyelinase

SREBPs: sterol regulatory element binding proteins

SRBI: scavenger receptor

TEM: transmission electron microscopy

TG: triglycerides

THP1: human monocytic cell line derived Taken from an acute monocytic leukemia patient

THP1-CD14: THP1 overexpressing CD14

TLC: thin layer chromatography

TNF $\alpha$ : tumor necrosis factor-alpha

VLDL: very-low-density lipoprotein

WD: western-type diet

WT: wild type



## ■ ABSTRACT

Mimetic peptides are potential therapeutic agents for atherosclerosis prevention. D-[113–122]apolipoprotein (apo) J (D-[113–122]apoJ) is a 10-residue class G\* peptide from apolipoprotein J (apoJ); it possesses anti-inflammatory and anti-atherogenic properties. This prompted us to study its effect on the *in vitro* and *in vivo* aggregation process of low-density lipoprotein (LDL) particles, an early event in the evolution of atherosclerosis. We also analyzed the effect of this peptide in low-density lipoprotein receptor knockout mice (LDLR-KO) on the development of atherosclerosis and lipoprotein function.

For *in vitro* studies, LDL particles in presence or absence of D-[113–122]apoJ peptide were incubated at 37 °C with sphingomyelinase (SMase) or were left to aggregate spontaneously at room temperature. The aggregation process was analyzed by size-exclusion chromatography (SEC), native gradient gel electrophoresis (GGE), absorbance at 405 nm, dynamic light scattering (DLS), and transmission electronic microscopy (TEM). Additionally, circular dichroism was employed to determine changes in the secondary structure of apoB. At an equimolar ratio of D-[113–122]apoJ peptide to apoB-100, D-[113–122]apoJ inhibited both SMase-induced or spontaneous LDL aggregation. All methods showed that this peptide retarded the progression of SMase-induced LDL aggregation at long incubation times. No effect of D-[113–122]apoJ on apoB secondary structure was observed. Binding experiments showed that this peptide presents low affinity for native LDL but it binds readily to LDL during the first stages of aggregation.

For *in vivo* studies, female LDLR-KO mice fed an atherogenic Western-type diet were treated for eight weeks with D-[113–122]apoJ peptide, a scrambled peptide, or vehicle. Peptides were dispensed subcutaneously three days per week. After euthanasia, blood was collected and the aortic arch was studied for the presence of atherosclerotic lesions. Lipoproteins were isolated and their composition and functionality were analyzed. The area of atherosclerotic lesions was 43% lower with D-[113–122]apoJ treatment than with the vehicle or scramble. The lipid profile was similar between groups, but the high-density lipoprotein (HDL) of D-[113–122]apoJ-treated mice had a higher antioxidant capacity and increased ability to promote cholesterol efflux than the control group. Moreover, low-density lipoprotein (LDL) from D-[113–122]apoJ-treated mice was more resistant to induced aggregation and presented lower electronegativity than in mice treated with D-[113–122]apoJ.

These results demonstrate that D-[113–122]apoJ peptide not only prevents *in vitro* and *in vivo* SMase-induced LDL aggregation but also prevents the extent of atherosclerotic lesions in mice models, which could be partially explained by the improvement of lipoprotein functionality. Our results open the possibility for the use of this mimetic peptide as a therapeutic tool.

## ▪ RESUMEN

Los péptidos miméticos son potenciales agentes terapéuticos para la prevención de la aterosclerosis. D- [113-122] apoJ es un péptido de clase G\* de 10 residuos de la apolipoproteína J (apoJ); posee propiedades antiinflamatorias y anti-aterogénicas. Esto nos ha llevado a estudiar su efecto sobre el proceso de agregación *in vitro* e *in vivo* de partículas de las lipoproteínas de baja densidad (LDL), el cual es un evento temprano en la evolución de la aterosclerosis. También analizamos el efecto de este péptido en ratones knockout del receptor de lipoproteínas de baja densidad (LDLR-KO) sobre el desarrollo de la aterosclerosis y la función de las lipoproteínas.

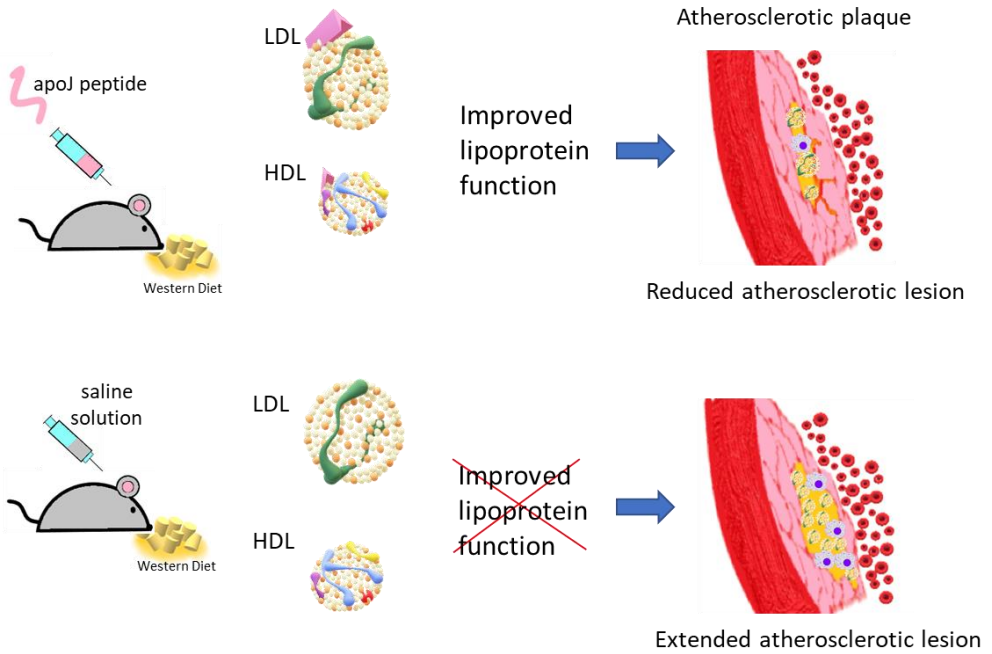
Para los estudios *in vitro*, las partículas de LDL en presencia o ausencia del péptido D- [113-122] apoJ se incubaron a 37 ° C con esfingomielinasa (SMasa) o se dejaron agregar espontáneamente a temperatura ambiente. El proceso de agregación se analizó mediante cromatografía de exclusión por tamaño (SEC), electroforesis en gel de gradiente nativo (GGE), absorbancia a 405 nm, dispersión dinámica de luz (DLS) y microscopía electrónica de transmisión (TEM). Además, se empleó dicroísmo circular para determinar cambios en la estructura secundaria de apoB. El péptido D- [113-122] apoJ inhibió la agregación de LDL tanto inducida por SMasa como espontánea en una proporción equimolar de péptido D- [113-122] apoJ a apoB-100. Todos los métodos mostraron que este péptido retardaba la progresión de la agregación de LDL inducida por SMasa en tiempos de incubación prolongados y no se observó ningún efecto de D- [113-122] apoJ sobre la estructura secundaria de apoB. Los experimentos de unión mostraron que este péptido presenta baja afinidad por la LDL

nativa, pero se une fácilmente a la LDL durante las primeras etapas de agregación.

Para los estudios *in vivo*, ratones LDLR-KO alimentados con una dieta aterogénica de tipo occidental se trataron por vía subcutánea (tres días a la semana) durante ocho semanas con péptido D- [113-122] apoJ, un péptido scramble o un vehículo. Al finalizar el tratamiento y después de la eutanasia, se extrajo sangre y se estudió el arco aórtico en busca de lesiones ateroscleróticas. Se aislaron las lipoproteínas y se analizó su composición y funcionalidad. Se observó que el área de las lesiones ateroscleróticas fue un 43% menor con el tratamiento con D- [113-122] apoJ que con el vehículo o scramble. El perfil lipídico fue similar entre los grupos, pero la lipoproteína de alta densidad (HDL) de los ratones tratados con D- [113-122] apoJ tenía una mayor capacidad antioxidante y una mayor capacidad para promover el eflujo de colesterol que el grupo control. Además, la lipoproteína de baja densidad (LDL) de ratones tratados con D- [113-122] apoJ fue más resistente a la agregación inducida y presentó menor electronegatividad que en los ratones tratados con D- [113-122] apoJ.

Estos resultados demuestran que el péptido D- [113-122] apoJ no solo previene la agregación de LDL inducida por SMasa *in vitro* e *in vivo*, sino que también previene la extensión de las lesiones ateroscleróticas en modelos de ratones, lo que podría explicarse parcialmente por la mejora de la funcionalidad de las lipoproteínas. Nuestros resultados abren la posibilidad del uso de este péptido mimético como herramienta terapéutica frente la arteriosclerosis.

# GRAPHICAL ABSTRACT







- **INTRODUCTION**



## **1. Atherosclerosis**

Cardiovascular disease (CVD) is the leading cause of mortality worldwide, accounting for 17.3 million deaths each year. The primary cause of the majority of CVD patients is atherosclerosis, a disease that is characterized by the accumulation of lipids and immune-cell containing plaques in the intima of large and mid-sized arteries [1]. Atherosclerosis is a progressive inflammatory disease, which leads to the development of atherosclerotic plaques that cause a reduction of the arterial lumen. Frequently, these plaques persist stable for years, but can quickly become unstable, rupture, and prompt thrombus formation. Consequently, besides the limitation of the vessel lumen, the existence of atherosclerotic plaques is related to an increased risk of acute cardiovascular events such as myocardial infarction (MI) and stroke [2].

Epidemiological studies have revealed numerous risk factors for atherosclerosis. These can be categorized into factors with an important genetic component, and those that are mostly environmental. The relative abundance of the different plasma lipoproteins appears to be of primary importance, as increased levels of atherogenic lipoproteins are a prerequisite for most forms of the disease. The interactions between risk factors aggregate another level of complexity to the atherosclerosis process. Frequently, these are not simply additive; for example, the effects of hypertension on coronary heart disease (CHD) are considerably amplified if cholesterol levels are high [3].

Atherosclerosis develops progressively through the continuous evolution of arterial wall lesions centered on the accumulation of cholesterol-rich lipids and the accompanying inflammatory response. Many studies support that inflammatory mechanisms are related to atheroma formation. Leukocyte recruitment and proinflammatory cytokines contribute to the initial stage of

atherogenesis [1, 4]. Briefly, this pathophysiological process implicates different steps: (1) endothelial cells face inflammatory activation; (2) blood monocytes and other leukocytes access the atheroma; (3) chemokines and chemoattractant proteins take part in the recruitment of further inflammatory cells into the intima; (4) monocytes differentiate to macrophages and internalize lipoprotein particles and generate foam cells, which is a hallmark of the nascent atheroma; (5) inflammatory cytokines, reactive oxygen species, and other mediators are secreted by foam cells; (6) macrophages can suffer apoptosis, establishing the so-called lipid or 'necrotic core' of the atherosclerotic lesion; (7) phagocytes actions increase the local inflammatory response, by producing matrix metalloproteinases (MMPs), which degrade extracellular matrix macromolecules that lend to the strength of the plaque fibrous cap; (8) fracture of a weakened fibrous cap permits blood to contact another macrophage product, the potent pro-coagulant protein tissue factor (Figure 1).

Different innate immune processes can drive superficial erosion, another sort of thrombotic event. Thus, inflammation leads to atherosclerosis and prompts thrombotic plaque complications, which usually cause stroke, myocardial infarction (MI), and cardiovascular death [4, 5].

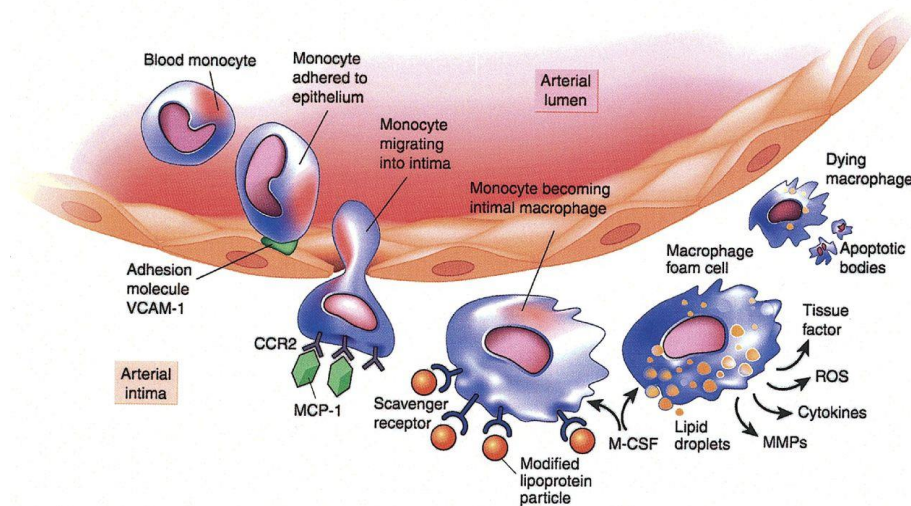


Figure 1. **Mononuclear phagocytes in atherosclerosis.**

Taken from [5]

## 1.1 Atherosclerosis development

As atherosclerosis development progresses, the processes and histologic changes become progressively complex and can vary significantly among individuals. In the natural course of atherosclerosis, spontaneous regression of early-stage lesions may occur, but the intermediate and advanced stages seem to be continuously progressive. This concept of a developmental continuum of plaque changes is useful as an aid to understanding the potential steps of atherosclerosis development. Although our current molecular understanding of these steps and their integration is fragmentary, their general outline supports crucial interplay among lipid accumulation, lipid oxidation, and inflammation.

The continuous development of atherosclerosis usually is described as an extended series of histologic changes:

- Early Fatty Streak Development: it begins in childhood and adolescence [6-8]. The initial step occurs when low-density lipoprotein (LDL) particles in the blood enter the arterial intima, where, if LDL levels are increased, they accumulate [9]. Then, they are oxidized and modified by enzymes into proinflammatory particles, which cause the reaction of the innate inflammatory system within the intima [10]. These earliest changes in the arterial wall occur at the branch of arteries, where adaptive intimal thickening appears in response to normal hemodynamic stresses.

Inflammation begins when the endothelial cells become activated and secrete adhesion molecules, and the smooth muscle cells secrete chemokines and chemoattractants, which together pull monocytes, lymphocytes, mast cells, and neutrophils into the arterial wall [11]. Also, the intimal smooth muscle cells secrete proteoglycans, collagen, and elastic fibers into the extracellular space. Upon entry, monocytes transform into macrophages, take up lipids as multiple small droplets, and become foam cells. Isolated foam cells, multiple layers of foam cells, and isolated extracellular pools of lipids are not considered advanced-stage lesions. These early changes are microscopic and may progress to gross visibility. At this stage, these lipid changes can be reversed. Atherosclerosis is believed to start when the lipid accumulation appears as confluent extracellular lipid pools and extracellular lipid cores with decreased cellularity [12].

- Early Fibroatheroma: occurs in persons in their teens and 20s [8, 13-15]. Macrophage foam cells, other activated inflammatory cells, and smooth muscle cells from arteries accumulate. Macrophages take a controlling role in plaque development, but inflammation may become unchecked and excessive. Extracellular proteoglycans, secreted by smooth muscle cells, bind lipids and gradually increase their lipid-binding capacity by extension of their disaccharide arms. Some factors promote the death of

macrophages and smooth muscle cells. The necrotic debris provokes further inflammation.

Increasing accumulation of extracellular lipid coalesces into pools and causes cell necrosis. This progressively alters the normal structural design of the intima until it is completely disrupted. These enlarging pools form lipid-rich necrotic cores that dominate the central part of the intima, ultimately occupying 30% to 50% of arterial wall volume. Fibrous tissue is added to form a fibrous cap over the lipid-rich necrotic cores and just under the endothelium at the blood interface. This forms the fibrous plaque lesions that develop to become the dominant lesion (Figure 2).

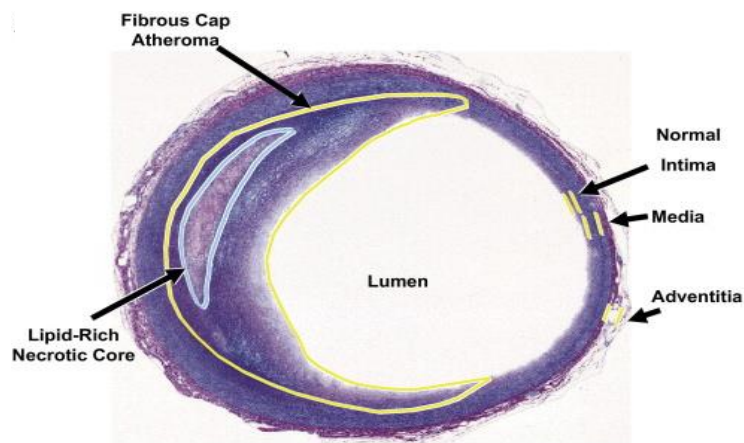


Figure 2. **Coronary fibrous cap atheroma in a 24-year-old man.**

Taken from [8]

- Advancing Atheroma. Thin-Cap Fibroatheroma and Its Rupture: advancing atheroma occurs in persons aged  $\geq 55$  years. In this phase of plaque development, a thin-cap fibroatheroma (TCFA) develops and may rupture [15-17]. The fibrous cap at some sites becomes thin and weakened when proteolytic enzyme activity continues unchecked and dissolves the fibrous tissue. This thin cap is susceptible to rupture, which exposes the



thrombogenic interior arterial wall and produces a thrombus that extends into the arterial lumen. These intramural hemorrhages provoke increased fibrous tissue. This lesion usually is labeled a vulnerable plaque because of the risk of rupture and life-threatening thrombosis. These lesions appear at about age 55 to 65 years, just before the peak incidences of myocardial infarction and stroke (Figure 3).

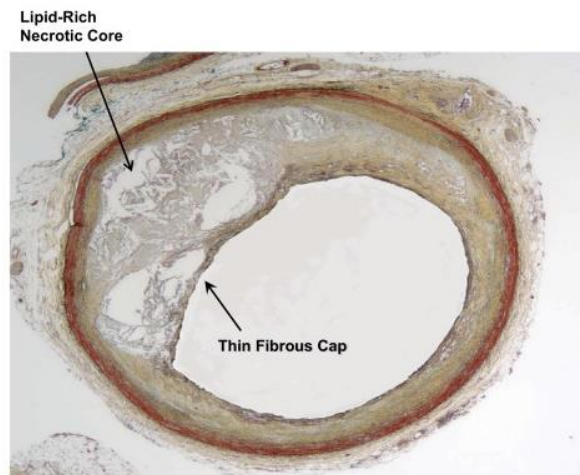


Figure 3. **Thin fibrous cap.**

Taken from [8]

- Complex Lesion Development: many ruptures of thin fibrous caps are clinically silent in that they heal by forming fibrous tissue matrices of cells, collagen fibers, and extracellular space but may rupture again with thrombus formation [8, 13, 15]. These cyclic changes of rupture, thrombosis and healing may recur as many as 4 times at a single site in the arterial wall, resulting in multiple layers of healed tissue (Figure 4A). Calcium deposits in the wall occur throughout all these steps, initially as small aggregates, and later as large nodules. Plaques may rupture into the lumen and expose the nodules, which become sites for thrombosis.

Erosion of endothelium, underlain by some of the changes described previously or with no underlying histologic abnormality, may occur, resulting in thrombosis. The increasing mass of some plaques alone may become enough to form significant stenosis that may cause lethal ischemia simply through flow restriction (Figure 4B). All these changes may be significantly influenced by risk factors, notably the stresses of local hemodynamics and blood flow patterns, hypertension, tobacco smoking, and diabetes, as well as genetically determined arterial susceptibility or resistance to atherosclerosis [18]. The mechanisms of these risk factors in influencing atherosclerosis are the target of intensive investigation by molecular pathology, along with proteomics and genomics, conducted to determine the exact molecular biological processes involved in their development.

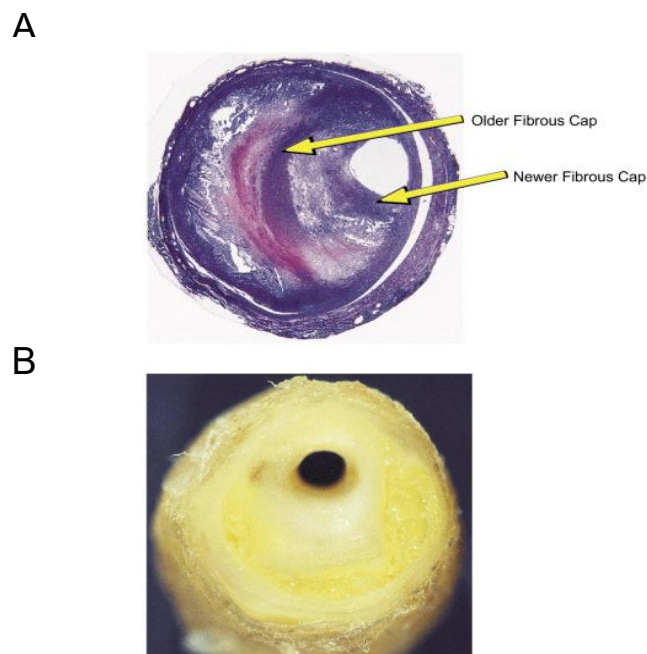


Figure 4. (A) Healed plaque rupture. (B) Stenosis of the anterior descending coronary artery in a 40-year old man.

Taken from [8]

Also, it is useful to condense lesion development into classes of plaques that are grossly visible. This classification is summarized in Table 1.

Major types of lesions of atherosclerosis		
Lesion Name	Lesion Description by Histopathology	Thrombosis
Nonatherosclerotic intimal lesions		
1. Intimal thickening	The normal accumulation of SMCs in the intima with the absence of lipid or macrophage foam cells	Thrombus is absent
2. Intimal xanthoma or fatty streaks	Subendothelial accumulation of foam cells in intima without necrotic core or fibrous cap; animal and human data show that such lesions usually regress	Thrombus is absent
Progressive atherosclerotic lesions		
1a. Pathologic intimal thickening	SMCs in a proteoglycan-rich matrix with areas of extracellular lipid accumulation without necrosis	Thrombus is absent
1b. With erosion	Luminal thrombosis, plaque same as above	Thrombus most often mural and infrequently occlusive
2a. Fibrous cap atheroma	Well-formed necrotic core with overlying fibrous cap	Thrombus is absent
2b. With erosion	Luminal thrombosis; plaque same as above, no communication of thrombus with necrotic core	Thrombus most often mural and infrequently occlusive
3. TCFA	A thin fibrous cap infiltrated with macrophages and lymphocytes, rare SMCs, and an underlying necrotic core	Absent, with intraplaque hemorrhage/fibrin
a. With rupture	Fibroatheroma with cap disruption; luminal thrombus communicates with underlying necrotic core	Thrombus usually occlusive
4. Calcified nodule	Eruptive nodular calcification with underlying fibrocalcific plaque	Thrombus usually nonocclusive
5. Fibrocalcific plaque	Collagen-rich plaque usually with significant stenosis; contains large areas of calcification with few inflammatory cells; necrotic core may be present	Thrombus is absent

SMC=smooth muscle cell; TCFA= thin-cap fibroatheroma

Table 1. Major types of lesions of atherosclerosis.

Taken from [12]

## 2. Mouse models of atherosclerosis

Mouse and rabbit models have been mostly used, followed by pigs and non-human primates. Each one of these models has its advantages and limitations. Animal models of atherosclerosis are based on accelerated plaque formation due to a cholesterol-rich/Western-type diet, manipulation of genes involved in the cholesterol metabolism, and the introduction of additional risk factors for atherosclerosis. The mouse has become the predominant species to study experimental atherosclerosis because of its fast reproduction, ease of genetic manipulation, and its ability to monitor atherogenesis in a reasonable time frame [19, 20].

Nevertheless, mice are quite resistant to the development of atherosclerosis because of their different lipid profile as compared to humans. Consequently, genetic manipulation of their lipid metabolism is required [20, 21].

In mice, most of the cholesterol is transported in high-density lipoprotein (HDL)-like particles. Consequently, mice have only low concentrations of atherogenic LDL and very low-density lipoprotein (VLDL). Lipoproteins, their structure, and their function will be described in detail in the following section.

Mice deficient in the receptor clearing these LDL particles (LDLR-KO) develop considerably higher plasma levels of cholesterol than wild-type mice. Apolipoprotein E (ApoE) is a glycoprotein that acts as a ligand for receptors that clear chylomicrons and VLDL remnants. Deficiency in this apolipoprotein also leads to increased plasma levels of total cholesterol, mainly in the VLDL and chylomicron fractions [22], which are increased fourfold by a high-fat or Western-type diet (WD) [23]. Both mouse models have widely been used to study the mechanisms underlying the initiation and progression of atherosclerosis.

Atherosclerotic lesions in mice are developed in regions of the vasculature subjected to low or oscillatory shear stress [19, 24]. Preference sites in the mouse are the aortic root, lesser curvature of the aortic arch, and branch points of the brachiocephalic, left carotid and subclavian arteries. However, on a high-cholesterol diet, apoE-KO mice develop plaques faster and with a more advanced phenotype as compared to LDLR-KO mice [25], making the apoE-KO model extensively used in experimental atherosclerosis studies.

There are also other mouse models of atherosclerosis, the most used are described in detail in Figure 5.













	Model	Lipid profile	Plaque distribution and characteristics (20 weeks WD)	Advantages & limitations
ApoE <sup>-/-</sup>	<p>Disruption of the ApoE gene</p> 	<p><b>Plasma cholesterol:</b> 400-600 mg/dl on ND &gt;1000 mg/dl on WD</p> <p><b>Lipoproteins:</b> ↑↑ VLDL ↑ LDL ↓ HDL</p>	 <p><b>Fibrous plaques:</b> Smooth muscle cells Extracellular matrix Inflammatory cells Necrotic core</p>	<ul style="list-style-type: none"> <li>➢ Develops atherosclerosis on ND</li> <li>➖ No human-like lipid profile</li> <li>➖ ApoE plays a role in inflammation → influence plaque development</li> <li>➖ No spontaneous plaque rupture, thrombosis and complications</li> </ul>
LDLR <sup>-/-</sup>	<p>Disruption of the LDL receptor gene</p> 	<p><b>Plasma cholesterol:</b> 200-300 mg/dl on ND &gt;1000 mg/dl on WD</p> <p><b>Lipoproteins:</b> ↑ VLDL ↑↑ LDL = HDL</p>	 <p><b>Fibrous plaques:</b> Smooth muscle cells Extracellular matrix Inflammatory cells Necrotic core</p>	<ul style="list-style-type: none"> <li>➢ Human-like lipid profile (LDL)</li> <li>➢ Functional ApoE → no impact on inflammation</li> <li>➖ Complex lesion development requires a WD</li> <li>➖ No spontaneous plaque rupture, thrombosis and complications</li> </ul>
ApoE <sup>-/-</sup> LDLR <sup>-/-</sup>	<p>Disruption of the ApoE and the LDL receptor gene</p> 	<p><b>Plasma cholesterol:</b> 400-600 mg/dl on ND &gt;1000 mg/dl on WD</p> <p><b>Lipoproteins:</b> ↑↑ VLDL ↑↑ LDL ↓ HDL</p>	 <p><b>Fibrous plaques:</b> Smooth muscle cells Extracellular matrix Inflammatory cells Necrotic core</p>	<ul style="list-style-type: none"> <li>➢ Develops atherosclerosis on ND</li> <li>➖ No spontaneous plaque rupture, thrombosis and complications</li> </ul>
ApoE3-Leiden	<p>ApoE3-Leiden mutation via DNA construct (ApoE, ApoC1) from the ApoE3-Leiden proband</p> 	<p><b>Plasma cholesterol:</b> 100-200 mg/dl on ND &gt;1000 mg/dl on WD</p> <p><b>Lipoproteins:</b> ↑↑ VLDL ↑ LDL ↑ HDL (only on WD)</p>	 <p><b>Fibrous plaques:</b> Smooth muscle cells Extracellular matrix Inflammatory cells Necrotic core</p>	<ul style="list-style-type: none"> <li>➢ Functional ApoE → no impact on inflammation</li> <li>➖ Complex lesion development requires a WD</li> <li>➖ No spontaneous plaque rupture, thrombosis and complications</li> </ul>
PCSK9-AAV	<p>Single Adeno-Associated Virus-mediated gene transfer of mutant PCSK9</p> 	<p><b>Plasma cholesterol:</b> 300 mg/dl on ND &gt;1000 mg/dl on WD</p> <p><b>Lipoproteins:</b> ↑ VLDL (only on WD) ↑ LDL = HDL</p>	 <p><b>Fibrous plaques:</b> Smooth muscle cells Extracellular matrix Inflammatory cells Necrotic core</p>	<ul style="list-style-type: none"> <li>➢ No genetic modification needed</li> <li>➖ Lesion development requires a WD</li> <li>➖ No spontaneous plaque rupture, thrombosis and complications</li> </ul>
ApoE <sup>-/-</sup> Fbn1 <sup>C1039G/+</sup>	<p>ApoE<sup>-/-</sup> mice X mice with a mutation in the Fbn1 gene (C1039G)</p> 	<p><b>Plasma cholesterol:</b> 400-600 mg/dl on ND &gt;1000 mg/dl on WD</p> <p><b>Lipoproteins:</b> ↑↑ VLDL ↑ LDL ↓ HDL</p>	 <p><b>Rupture-prone plaques:</b> ↓ Smooth muscle cells ↓ Extracellular matrix ↑ Inflammatory cells ↑ Necrotic core Neovascularisation Haemorrhage</p>	<ul style="list-style-type: none"> <li>➢ Accelerated plaque development</li> <li>➢ Spontaneous plaque rupture with complications (MI, stroke) and sudden death</li> <li>➢ Intra-plaque neovascularisation and haemorrhage present</li> <li>➖ Male mice on WD die prematurely due to aneurysm rupture</li> </ul>

Figure 5. Overview of current mouse models of atherosclerosis.

Taken from [2]

## 2.1 LDL receptor-deficient (LDLR-KO) mice

The LDL receptor (LDL-R) is a membrane receptor (160 kDa), which mediates the endocytosis of cholesterol-rich LDL and thus maintains the plasma level of LDL. It also mediates the cellular uptake of apolipoprotein B- and E- containing lipoproteins. LDL receptor deficiency along with mutations in the gene encoding for the LDL receptor count for the phenotypic events described in familial hypercholesterolemia (FH) [26]. Mice with targeted inactivation of the LDL receptor were created in 1993 [27, 28]. The LDLR-KO model in atherosclerosis susceptible C57BL/6 genetic background is very widely used to study atherosclerosis with a variety of physiological and genetic interventions [29] and is the model used in the second part of this thesis.

Compared to wild-type mice, LDLR-KO mice maintained on chow diet exhibit moderately elevated levels of LDL but develop no or only minimal atherosclerosis [28, 30], even in mice fully inbred into the C57BL/6 background [31, 32]. However, the addition of fat and cholesterol to the diet results in significant increases in the level of VLDL and VLDL remnants as well as further increases in LDL levels, and the relatively rapid development of advanced atherosclerosis over 2 to 3 months. Thus, a high cholesterol diet with or without a high fat is needed to provide the hyperlipidemic drive for atherogenesis. Regarding lipoprotein particles, the increase is higher among intermediate-density lipoprotein (IDL) and LDL-sized particles, whereas high-density lipoprotein (HDL) and triglycerides remain unaffected [27, 28]. It is worth mentioning that this is different from apoE-KO mice, in which cholesterol is primarily accumulated in large lipoprotein particles such as chylomicron remnants, VLDL and IDL particles [23, 33]. The response to high-fat/high cholesterol Western-type diets shows a remarkable change in the lipoprotein profile of these mice with a high probability for atherosclerotic lesion development.

The major accumulating lipoprotein in the plasma of LDLR-KO mice fed high cholesterol, low-fat diet is LDL [34], and with the high cholesterol high fat diet, VLDL is also elevated [35]. The VLDL in this model is much more triglyceride-rich than is the case for the apoE-KO mice. LDLR-KO mice fed the Western-type diet for 12 weeks show a very good correlation between aortic root lesion size and VLDL cholesterol concentration [36]. The plaques that develop in LDLR-KO mice are similar to those seen in ApoE-KO mice [37]. A Western-type diet induces larger and more advanced lesions with a collagen-rich fibrous cap, a necrotic core containing cholesterol clefts and cellular enrichment adjacent to the lumen [34]. The plaque development happens in a time-dependent manner, initially in the proximal aorta, and expanding toward the distal aorta. Similar to humans, the locations where the blood flow is disturbed are more prone to atherosclerotic lesions [37]. By creating LDLR-KO and ApoE-KO mice homozygous for the human ApoB-100 allele, total plasma cholesterol levels of approximately 300 mg/dl were found on a normal diet. LDLR-KO ApoB<sup>100/100</sup> mice developed more atherosclerotic lesions than the ApoE-KO ApoB<sup>100/100</sup> mice, even with a normal diet [30, 38].

An example of atherosclerotic lesions in LDLR-KO mice fed a regular chow diet or high-fat diet is shown in Figure 6.

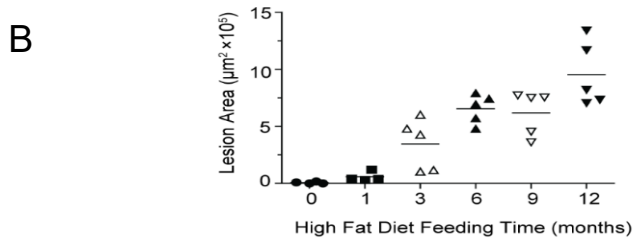
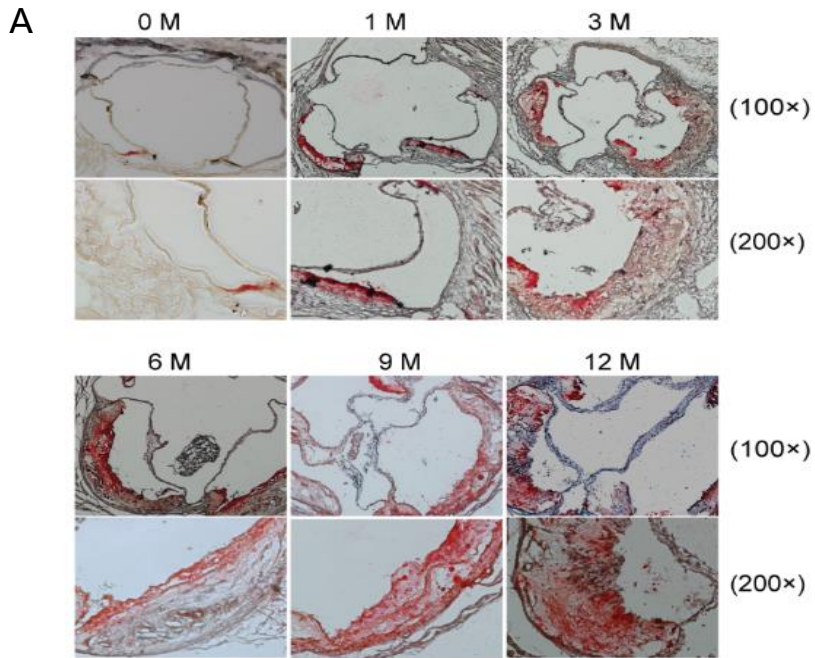


**Figure 6. Aortic sinus lesion morphology in LDL-R KO mice.**

**A)** Representative sections in LDL-R KO mice fed CD (0 M) or HFD for 1 to 12 months stained with Oil Red-O and hematoxylin. **(B)** Lesion area was quantified using computer software IPP6.0.

Taken from [39]



The LDLR-KO mouse model has certain advantages compared to apoE-KO mice. First, plasma cholesterol is mainly carried by LDL particles, which generate a more human-like lipid profile. Second, the absence of the LDL receptor does not have an impact on inflammation as compared to ApoE deficiency. Therefore, atherosclerotic plaque development in this mouse model is based on elevated plasma lipid levels and not caused by other functions linked to the LDL receptor [20]. Third, the LDLR-KO mouse model shares the characteristics detected in human familial hypercholesterolemia, which is caused by the absence of functional LDL receptors [40, 41].

### **3. Lipoproteins and Lipoprotein Metabolism**

Lipids (cholesterol, triacylglycerols, and phospholipids) are transported in blood as part of lipoprotein particles. Lipoproteins are formed from lipid and protein molecule complexes. Lipoproteins are spherical particles, with a center core made of cholesterol ester and triacylglycerol molecules. These are surrounded by an outer shell composed of unesterified cholesterol and phospholipids with the fatty acids oriented toward the core of the particle. Incorporated in this outer shell are specific proteins known as apolipoproteins. As a part of its main functions, lipoproteins transport and deliver fatty acids, triacylglycerol, and cholesterol to and from target cells in many organs [42]. The general structure of lipoproteins is shown in Fig. 7.

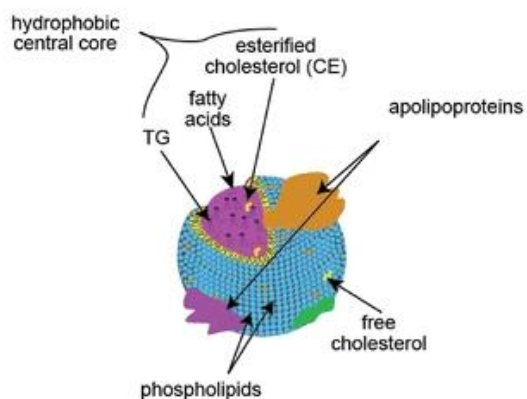


Figure 7. **Lipoprotein structure**

Taken from [43]

Lipoproteins have been classified based on their hydrated density, size and apolipoprotein composition (Table 2 and Figure 8 and 9).

Lipoprotein	Density (g/ml)	Size (nm)	Major Lipids	Major Apoproteins
Chylomicrons	<0.930	75-1200	Triglycerides	Apo B-48, Apo C, Apo E, Apo A-I, A-II, A-IV
Chylomicron Remnants	0.930- 1.006	30-80	Triglycerides Cholesterol	Apo B-48, Apo E
VLDL	0.930- 1.006	30-80	Triglycerides	Apo B-100, Apo E, Apo C
IDL	1.006- 1.019	25-35	Triglycerides Cholesterol	Apo B-100, Apo E, Apo C
LDL	1.019- 1.063	18- 25	Cholesterol	Apo B-100
HDL	1.063- 1.210	5- 12	Cholesterol Phospholipids	Apo A-I, Apo A-II, Apo C, Apo E
Lp (a)	1.055- 1.085	~30	Cholesterol	Apo B-100, Apo (a)

Table 2. **Lipoprotein Classes**

Taken from [44]

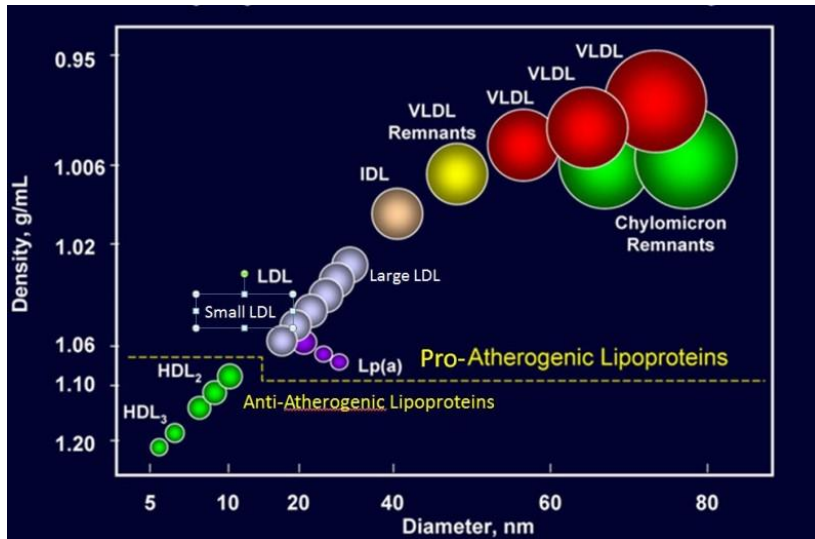


Figure 8. **Classes of Lipoproteins**

Taken from [44]

Lipoproteins have an exogenous and endogenous pathway (Figure 9). In the exogenous pathway, dietary lipids that are absorbed from the intestine via the systemic circulation are transported by chylomicrons. Chylomicrons (triglyceride-rich) are catabolized by the endothelium-associated lipoprotein lipase (LPL) and free fatty acids (FFA) are generated. These FFA are taken up by the liver, muscle, and adipose tissues. Through this catabolic process, chylomicrons reduce their size and become chylomicron remnants, which are taken up via the LDL-R and the LDL receptor-related protein (LRP) by the liver.

In the endogenous pathway (Figure 9) triglyceride-rich very-low-density lipoprotein (VLDL) particles are assembled and produced by the liver. These particles transport triglycerides from the liver to peripheral tissues. Once the triglycerides are hydrolyzed by LPL, the VLDL particles are

transformed to IDL, which are taken up by the liver or can be additionally hydrolyzed by hepatic lipase (HL), also called hepatic triglyceride lipase (HTGL), to form LDL particles. Through this process, the particles become depleted of triglycerides but preserve significant cholesterol amounts [45].

LDL is responsible for cholesterol transport from the liver to peripheral tissues. Through the LDL receptor, the apolipoprotein apoB-100 is responsible for the recognition and uptake of LDL particles. This process clears 60 to 80% of total LDL. The residual LDL is removed by other receptors, such as LRP, or by scavenger receptors. Via scavenger receptors on macrophages and vascular smooth muscle cells, oxidized LDL (ox-LDL) particles can be uptaken. These macrophages are transformed into foam cells, which is a major step in the development of atherosclerosis, when they are overloaded with cholesteryl esters [46]. When LDL becomes lipid depleted, small dense LDL (sdLDL) is produced. sdLDL has a lower affinity for the LDL-R but is more susceptible to oxidative modification, being more atherogenic than larger LDL particles [47].

HDL plays an important function in reverse cholesterol transport, which shuttles cholesterol from peripheral cells to the liver [48], an efficient path that relieves the peripheral cells from cholesterol burden (Figure 9).

HDL precursor particles are secreted by the liver and intestine and absorb free cholesterol from cell membranes, this process is mediated by ATP binding cassette transporter 1 (ABCA1) and the apolipoproteins in HDL, apoA-I, and apoA-IV. ApoA-I activates the enzyme lecithin-cholesterol acyltransferase (LCAT), which is responsible for the esterification of the free cholesterol accepted by the HDL particles to allow more efficient packaging of the cholesterol for transport. HDL3 particles are transformed into larger HDL2 particles by the progressive acquisition of cholesteryl

esters and other apolipoproteins [48, 49]. There are three different routes that reverse cholesterol can take. First, the liver via LDL-R can take up large HDL particles with several copies of apoE [50]. Also, the liver can selectively take up the accumulated cholesteryl esters from HDL via scavenger receptor B1 [51]. Third, the cholesteryl ester transfer protein (CETP) moves cholesteryl esters from HDL to triglyceride-rich lipoproteins [48].

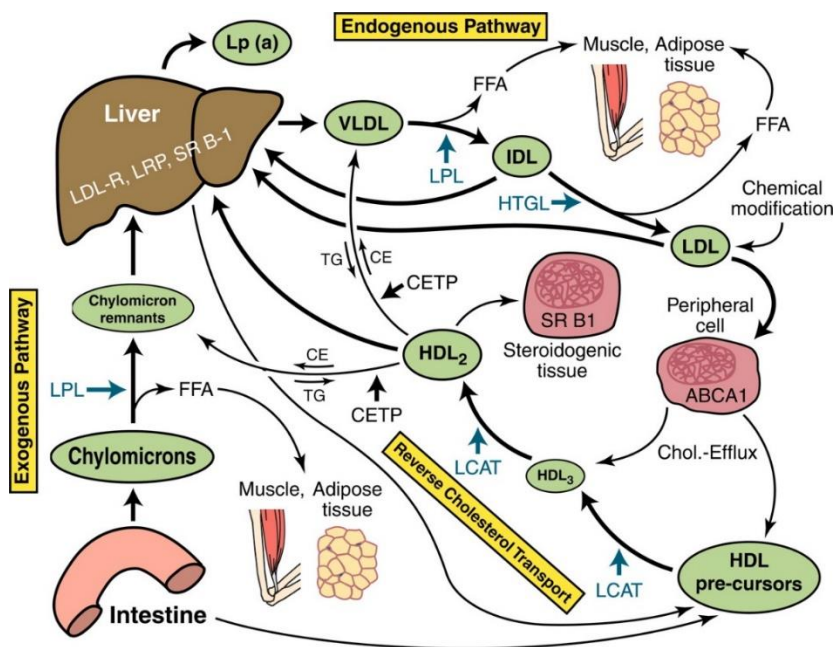


Figure 9. Lipoprotein metabolism.

Blue arrows refer to points of action of the respective enzymes in blue.

Taken from [52]

### 3.1 Chylomicrons

Chylomicrons are large triglyceride particles produced by the intestine, which transport dietary triglycerides and cholesterol to peripheral tissues

and the liver. ApoB-48 is the core structural protein, containing one apoB-48 molecule in each chylomicron (Figure 10) [45]. The size of chylomicrons depends on the amount of fat ingested. A high-fat meal produces large chylomicron particles, due to the increased amount of triglyceride being transported. However, in the fasting state, the chylomicrons particles are small because of carrying decreased quantities of triglyceride and their concentration is very low.

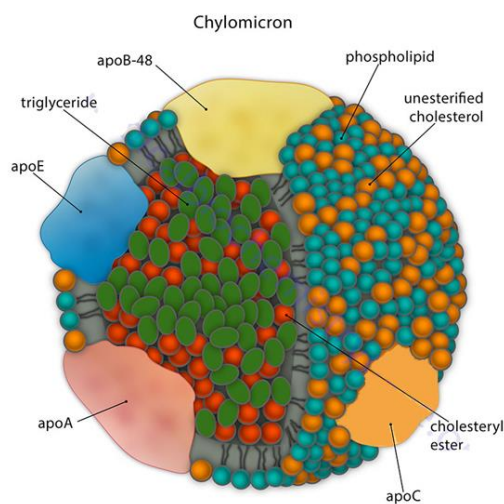


Figure 10. **Chylomicron structure.**

Taken from [53]

### 3.2 VLDL

VLDL is produced and secreted by hepatocytes, being the major transporter from the liver of endogenously produced triacylglycerol. Each VLDL particle contains one apoB-100 molecule, which is a large hydrophobic protein and the main structural component of VLDL, IDL and LDL. VLDLs are also triglyceride-rich and contain other apolipoproteins as apoC-II, apoC-III and apo E (Figure 11). Though unlike chylomicrons, they

are smaller, contain fewer triglycerides, and now carry apoB-100 (physiologic ligand for the LDL receptor) instead of apoB-48. However, it is important to mention that mouse VLDL and LDL contain apoB-48. LPL (of which apoC-II is a cofactor) reduces VLDL triglyceride content further, leaving the particles progressively smaller, denser, and more cholesterol-enriched as the cascade moves down to IDL formation [54].

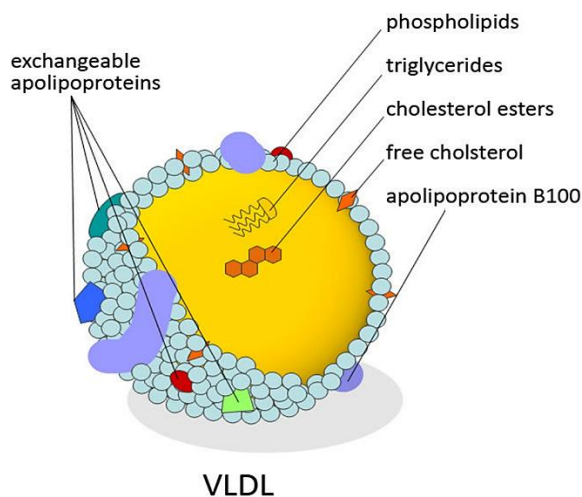


Figure 11. **VLDL structure.**  
Taken from [53]

### 3.3 HDL

HDL particles are rich in cholesterol and phospholipids and undergo constant remodeling and recycling (Figure 12). Each major component, apolipoproteins, phospholipids, cholesteryl esters and triglycerides follow a different metabolic pathway, depending on the organ or tissue. ApoA-I is the main structural protein, and each HDL particle might contain several

apoA-I molecules. Some HDL particles contain apoA-II, and other less abundant apolipoproteins and enzymes associated with HDL are found on only a small fraction of HDL particles. Hence, HDL particles are very diverse and heterogenous, depending on the presence or absence of numerous proteins [55]. Some HDL's accessory proteins such as paraoxonase and apoL-I are associated with apoA-I's antioxidant activity [56].

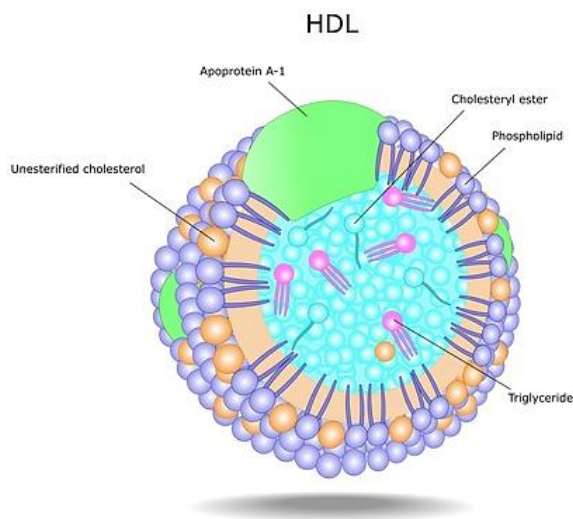


Figure 12. **HDL structure.**  
Taken from [57]

HDL particles play an important role in cholesterol transport from peripheral tissues to the liver, which is known as reverse cholesterol transport, one potential mechanism considered key to its atheroprotection. Cholesterol efflux capacity (CEC) is an important in vitro assay that measures the ability of an individual's HDL to promote cholesterol efflux from cholesterol donor cells, for example, macrophages [58]. This capacity has emerged as a



better predictor of cardiovascular (CV) risk compared to merely plasma HDL-cholesterol (HDL-C) levels [59].

HDL is also known to exert anti-inflammatory, antioxidant, anti-thrombotic and, anti-apoptotic properties, which could also contribute to their capacity to prevent atherosclerosis [60]. There is strong evidence showing that the atheroprotective actions of HDL include its ability to protect LDL from oxidation by free radicals. In fact, HDL potently protects both lipid and protein moieties of LDL, inhibiting the accumulation of primary and secondary peroxidation products [61, 62].

HDL function can be measured in several in vitro assays [55, 63]. There are cell-based and cell-free assays to assess the anti-inflammatory and antioxidant activities of HDL [64]. LDL added to endothelial cells co-cultured with smooth muscle cells suffers oxidation and stimulates expression of monocyte chemotactic factors and rises monocyte binding and transmigration. The addition of HDL can block this response, which is indicative of HDL's antioxidant and anti-inflammatory activities [65]. However, HDL from patients facing an acute phase reaction did not show antioxidant activity nor monocyte chemotaxis inhibition but increased it, exhibiting a pro-inflammatory activity [66]. This means that HDL could also become dysfunctional.

Exist an inverse correlation between HDL-C levels and CHD risk, which suggests that high HDL-C plasma levels protect from atherosclerosis [67]. Thus, many studies aimed at understanding the valuable role of HDL-C levels in human pathology. However, it has been demonstrated from experimental mice and clinical trials, that HDL particle functionality is considerably more important for atheroprotection than HDL-C levels alone [55, 67, 68].

### 3.4 LDL

VLDL particles that are not eventually removed from the circulation in the form of IDL are converted to LDL. LDL carries most of the cholesterol that is in the circulation. The LDL particles have an average diameter of 22-28 nm, and they are composed of an amphipathic phospholipid surface layer and a hydrophobic lipid core. Each LDL particle contains a single apoB-100 molecule, which is partially embedded in the surface lipid monolayer. The layer is composed of about 400 unesterified cholesterol (UC) molecules and 800 phospholipid molecules, of which around 500 are phosphatidylcholine (PC) and 200 sphingomyelin (SM) [69]. Additionally, the surface also contains about 80 molecules of lysophosphatidylcholine (LPC) and a few phosphatidylethanolamine and ceramide molecules [70]. The lipid core includes around 1600 CE, 200 UC, and 170 TG molecules [71]. The main apolipoprotein is B-100 (Figure 10), which represents approximately 98% of the protein mass in LDL. There are, however, several other plasma proteins that can provisionally be associated with LDL particles in circulation, although their concentration is very low in LDL. Proteomic analyses have detected by different techniques over 50 proteins, in addition to apoB-100 [72-74]. They include the apolipoproteins regulating lipoprotein metabolism and lipid transport (apoC-II, apoC-III, apoE, apoA-I, apoA-IV, and apoF), proteins related to inflammation (apoD, apoJ, apoM, serum amyloid A4, paraoxonase 1, prenylcysteine oxidase 1, migration inhibitory factor-related protein 8, and retinol-binding protein), thrombosis (fibrinogen a chain), the complement system, and antimicrobial functions and innate immunity (lysozyme C, a-1 antitrypsin, apoL-1, and transthyretin) [47]. Thus, LDL consists of a spectrum of particles varying in composition, size, and density.

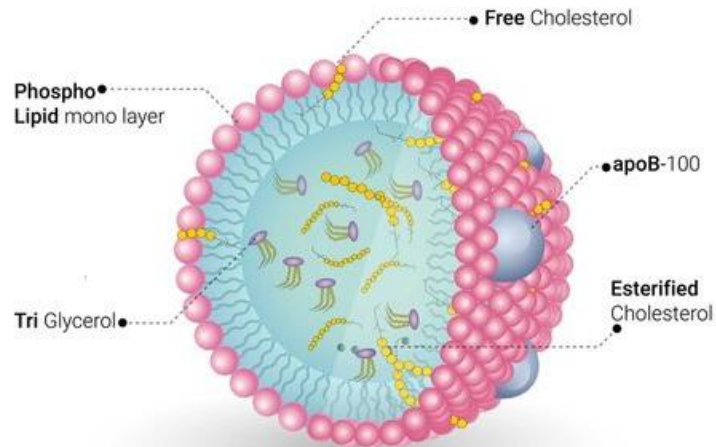


Figure 13. LDL structure.

LDL is a spherical particle with a diameter of 220 nm and a mass of ~3,000 kDa. Each particle contains ~1,500 molecules of cholesteryl ester in an oily core that is shielded from the aqueous plasma by a hydrophilic coat composed of ~800 molecules of phospholipid, ~500 molecules of unesterified cholesterol, and 1 molecule of a 500 kDa protein, apoB.

Taken from [75]

The rate of LDL production and the rate of LDL clearance define the LDL plasma concentration. Both rates are regulated by LDL receptors number in the liver. The LDL production rate from VLDL is partly determined by the hepatic LDL receptor activity, with high LDL receptor activity resulting in a decrease of LDL production due to an increase of IDL uptake. However, low LDL receptor activity will result in an increase in LDL production formation due to a decrease in IDL uptake. Regarding LDL clearance, 70% of circulating LDL is cleared through hepatocyte LDL receptor-mediated endocytosis, and the rest is taking up by extrahepatic tissues [76]. A rise in the number of hepatic LDL receptors increases LDL clearance, leading to

a decrease in plasma LDL levels. A reduction in hepatic LDL receptors slows LDL clearance leading to an increase in plasma LDL concentrations [77].

The quantities of liver LDL receptors are mostly regulated by the cholesterol content of the hepatocyte. When cell cholesterol levels are low, inactive sterol regulatory element binding proteins (SREBPs), are cleaved into active transcription factors and stimulate the transcription of the LDL receptor and other genes, including HMG-CoA reductase, the rate-limiting enzyme in cholesterol synthesis. When cellular cholesterol levels rise, the SREBPs remain in an inactive form and do not stimulate LDL receptor synthesis. Additionally, cholesterol in the cell is oxidized and these oxidized sterols activate LXR, a nuclear hormone receptor that stimulates the transcription of E3 ubiquitin ligase, which mediates the ubiquitination and degradation of the low-density lipoprotein receptor. As a result, the cell can sense the availability of cholesterol and regulate LDL receptor activity. Finally, the LDL receptor is targeted for degradation by PCSK9, a protein that binds to the LDL receptor and enhances LDL receptor degradation in the lysosomes. Thus, the endogenous lipoprotein pathway enables the movement of triglycerides synthesized in the liver to muscle and adipose tissue. It also gives a pathway for the transport of cholesterol from the liver to peripheral tissue [44, 78].

#### **4. LDL and Atherosclerosis**

As mentioned at the beginning of the chapter, subendothelial lipid accumulation plays a crucial role in the development of atherosclerotic lesions in the arterial cells.

Extra and intracellular lipid accumulation primarily of cholesterol esters leading to the formation of foam cells is not only one of the initial

manifestations of atherosclerosis, but also the triggering event of the atherosclerotic lesion development [79]. The 100 years-old [80] proposed hypothesis of cholesterol retention in the artery wall linked to the high levels of total cholesterol, that cause the onset and progression of atherosclerosis is not applied anymore. Later, it was demonstrated that lipid accumulation in the arterial intima is associated with high levels of the atherogenic LDL cholesterol [81, 82]. LDL circulating in human blood is the main source of lipids accumulated in the arterial walls. However, not all LDL particles are atherogenic, native non-modified LDL does not cause lipid accumulation in the arterial wall [83]. In contrast, the existence of LDL subfractions susceptible to multiple atherogenic modifications (enzymatic and non-enzymatic) define LDL atherogenicity [84, 85]. Several studies highlighted the evidence of modified LDLs in atherosclerotic lesions in both animal and human tissues. Orekhov and coworkers reported that LDL acquires atherogenic properties after 3h of incubation with blood plasma from atherosclerotic patients (Table 3), and its atherogenic potential increases during the incubation until 36h when the maximum was reached [84].

1 h	3 h	6 h	12 h	24 h	36 h	48 h
↓	↑	↓	↓	↓	↑	↑
Sialic acid		Free cholesterol	Size	Triglycerides	Electronegativity	Apo B-bound cholesterol
↑			↓			↑
% of desialylated LDL			Cholesteryl esters			Susceptibility to oxidation
			↓			↑
			Phospholipids			Fluorescence
						↓
						Vitamin E

Table 3. **Scheme of LDL modification**

Taken from [86]

Different types of atherogenic modification of LDL have been discovered in the blood of atherosclerotic patients, particularly, small-dense, electronegative, oxidized, and desialylated LDL particles [87]. It was

demonstrated that the same LDL particle can suffer multiple modifications developing the properties of small dense, electro-negative, oxidized and desialylated lipoproteins [88]. Therefore, the risk of onset and development of atherosclerosis is dependent on the level of multiply modified LDL and not as much on the concentration of total LDL in the blood. Hence, it is reasonable to believe that this level of modification is a better biomarker of atherosclerosis in comparison with the total LDL level [89].

The mechanisms of **LDL modification** that yield inflammatory effects and their atherogenicity are explained below.

#### **4.1 Oxidized LDL (oxLDL)**

LDL oxidation is likely to occur in the vascular wall but not in the blood. It has been reported non-enzyme-mediated oxidative modifications, involving interaction with proteoglycan, free radical, glycosylation, and also modifications mediated by enzymes as, lipoxygenases and myeloperoxidase. Additionally, depending on the component of LDL that suffers oxidation, modifications can be classified into lipid modification and protein modification [90]. In both cases of enzymatic and nonenzymatic modifications, the physical structure, the chemical properties, and the biological activity of LDL particles can be altered [91].

Under normal conditions, plasma LDL is composed of triglycerides and cholesterol esters with an outer layer composed of phospholipids, free cholesterol, and apoB that hold hydrophobic cholesterol through the blood. However, under oxidative stress, the oxidation of LDL occurs primarily by a process of lipid peroxidation involving the phospholipid molecules and apo-B. In some pathological conditions, apoB-containing lipoproteins in the plasma infiltrate through the injured endothelium into vascular subendothelial intima getting oxidized by the reactive oxygen species

(ROS) generated by the cell metabolism [92-94]. Under these conditions, the native LDL particle is modified into oxLDL (Figure 11) [95].

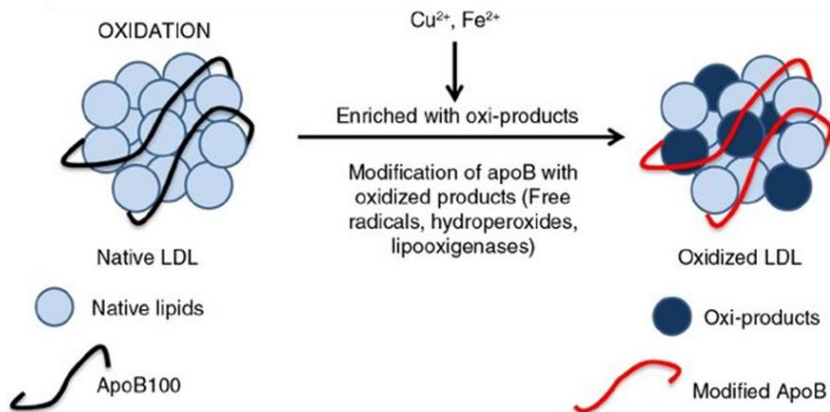


Figure 14. **OxLDL. Oxidized product-induced native LDL oxidation and modifications of apoB amino acids.**

Taken from [96]

## 4.2 Desialylated LDL

Desialylation is probably one of the first steps in a series of several LDL atherogenic modifications in the bloodstream of atherosclerotic patients, and as a result, these LDL particles have a decreased content of sialic acid. Sialic acids are a family of amino sugars that are usually found as terminal oligosaccharide residues present in the LDL apolipoprotein and glycolipid constituents. Different studies have demonstrated that LDL has a 2.5- to 5-fold lower content of sialic acid in patients with coronary artery disease compared with healthy subjects [83]. Sialic acid-poor LDLs have been shown to stimulate intracellular lipid accumulation, and in contrast to native LDL, desialylated LDL can bind to the scavenger receptor, the asialoglycoprotein receptor, and the cellular surface proteoglycans. After

desialylation, other physical and chemical modifications occur, involving a decrease of the cholesterol, triglycerides and phospholipids content, a decrease of the particle size and an increase of the electric charge (Table 3) [86].

### 4.3 Glycated LDL (glyLDL)

The glycosylation process affects the apoB in LDL particles. The irreversible glycation of native LDL begins with the non-enzymatic addition of reducing sugars to the positively charged lysine and/or arginine residues of apoB and continues with the formation of sugar-amino acid products, known as advanced glycation end-products (AGE) (Figure 12) [97]. This mechanism of modification is highly relevant in diabetes and insulin resistance [98].

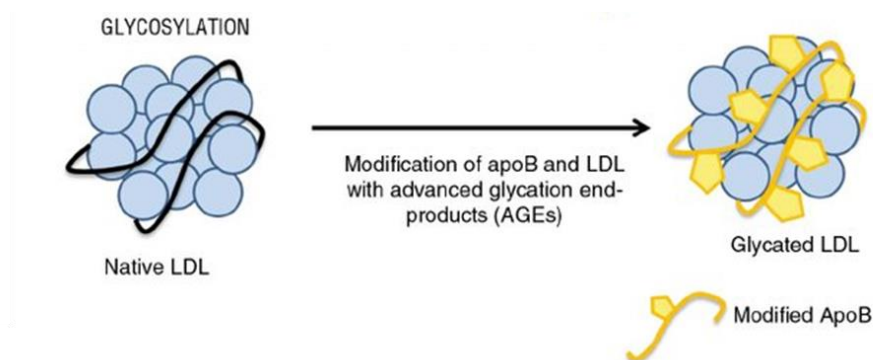


Figure 15. **Glycosylation: modification of LDL and apoB by advanced glycosylation end-products (AGEs).**

Taken from [96]



#### 4.4 Small-dense LDL (sdLDL)

These LDL particles present decreased size and increased density compared to normal large LDL particles. Metabolic studies have revealed that sdLDL particles originate after the delipidation of very large atherogenic VLDL by LPL and HL [99, 100]. The circulation mean lifetime of these particles is longer than that of large LDL particles which are cleared with more efficacy through the LDL receptor [101]. Consequently, circulating sdLDL particles suffer several atherogenic modifications (desialylation, glycation, and oxidation) which increase their atherogenicity [90].

#### 4.5 Carbamylated LDL

Carbamylation is a nonenzymatic modification of a protein by cyanate (Figure 13) [102]. It has been demonstrated that carbamylated LDL induces endothelial dysfunction via endothelial nitric oxide synthase (eNOS) uncoupling, being consequently, an increased source of ROS [103, 104]. It has been also reported that carbamylation of LDL renders these particles more susceptible to oxidation [105].

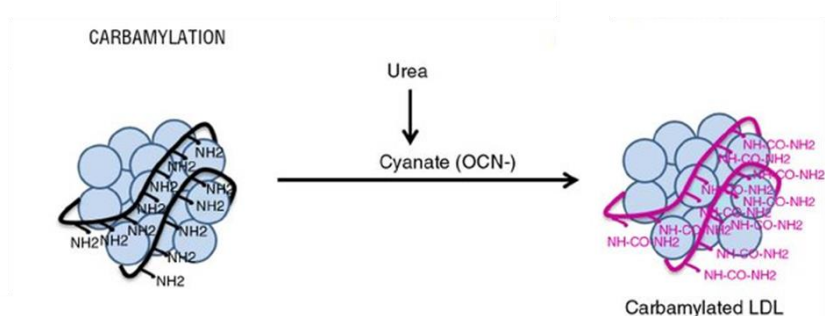


Figure 16. Carbamylation. Urea dissociates to cyanate and reacts irreversibly with the N-terminal group of amino acids.

Taken from [96]

#### **4.6 Electronegative LDL [LDL(-)]**

A common characteristic of the previously mentioned LDL modifications is an increase in the electronegative charge of the LDL particles. Different studies described that electronegative LDL [LDL(-)] exhibits numerous atherogenic properties, which include increased oxidative level, increased aggregation and loss for LDL-R affinity [106-108]. Also, LDL(-) promotes inflammatory responses, apoptosis and cell proliferation [109, 110]. LDL(-) is a heterogeneous combination of particles due to its multiple origins, which includes not only modified LDL particles but also LDLs with size, density, and composition alterations. They show different compositions and properties, being their negative charge a common characteristic between them [105].

Electronegative LDL could considerably contribute to the development of CHD, despite being a small percentage of total plasma LDL. In the plasma of diabetic individuals and other individuals with high CHD risk, the relative proportion of LDL(-) is increased [111]. The LDL(-) percentage is increased in pathologies as FH, hypertriglyceridemia, type 1 and type 2 diabetes, obesity, renal failure, insulin resistance and metabolic syndrome (MS) [105]. Furthermore, LDL(-) is associated with the size of atherosclerotic lesions [112].

#### **4.7 Aggregated LDL (agLDL).**

As it is mentioned throughout the chapter, LDL particles move into the arterial intima and bind to the extracellular matrix, they become modified by proteases, lipases, and oxidizing enzymes. Modification of the surface structure of an LDL particle might cause the loss of particle stability, and this will affect the interactions between the LDL particles, leading to their aggregation and subsequent fusion (Figure 11) [113].

The most relevant mechanism for LDL aggregation in the arterial wall environment is lipolysis, mainly mediated by sphingomyelinase (SMase) [114, 115]. SMase is secreted by endothelial cells and macrophages and in areas of the atherosclerotic lesion is hyper-expressed. It is possible to modify LDL particles in vitro with this enzyme, originating aggregated particles that resemble lipoproteins isolated from atherosclerotic lesions, including the increased ceramide content that is present in very large LDL aggregates [113, 115-117].

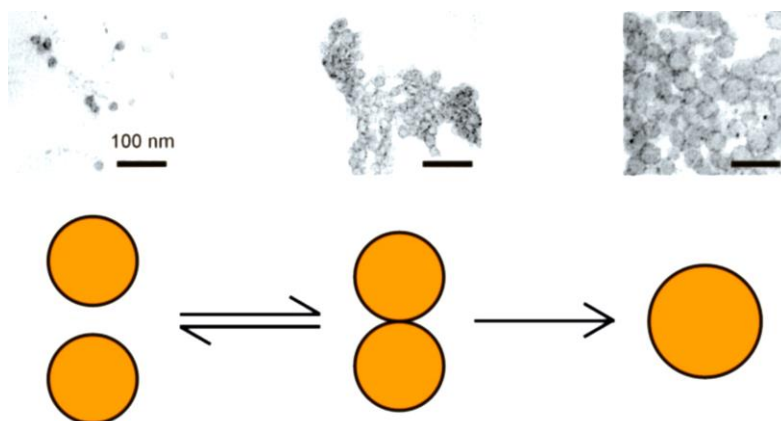


Figure 17. **Aggregation and fusion of LDL.**  
**Native LDL, Aggregated LDL and Fused LDL (Taken from left to right).**

Taken from [113]

The LDL particles isolated from atherosclerotic lesions have a lower PC and a higher LPC content compared to plasma LDL [118], suggesting that their phospholipids have been oxidatively altered or hydrolyzed by phospholipase A2. Both enzymes, Phospholipase A2 and SMase induce changes in the conformation of apoB-100 [119, 120]. Regarding SM hydrolysis, LDL aggregation is mediated via protein-protein interactions

which occur after lipolysis-induced conformational changes in apoB-100 [120].

Also, proteolytic enzymes present in human atherosclerotic lesions have been shown to induce aggregation and/or fusion of LDL particles in vitro, increasing the interaction of these LDL particles with the components of the extracellular matrix present in the arterial intima [113].

Modified LDL particles could bind to antibodies and aggregate. The majority of circulating oxidized LDL particles are found as oxLDL immune complexes, and their concentration is associated with atherosclerosis and cardiovascular events [121, 122]. These immune complexes could be also formed inside the intima, where modified lipoproteins accumulate, and be part of atherosclerosis lesions [123].

## **5. Apolipoprotein J (ApoJ) or Clusterin (CLU)**

ApoJ (also known as clusterin, CLU) is a heterodimeric glycoprotein of 70–80 kDa, linked by five disulfide bonds, constituted of  $\alpha$  and  $\beta$  subunits produced by a single cleavage from the protein precursor (Figure 12). It is expressed in several tissues and all human fluids [124, 125]. Plasma apoJ mainly appears as a soluble protein or as a part of a lipid-poor subclass of HDLs [126], although recent proteomic analyses also revealed that it is bound to LDL and VLDL [73, 127]. Clusterin is implicated in numerous physiological processes such as complement inhibition, sperm maturation, lipid transportation, tissue remodeling, membrane recycling, stabilization of stressed proteins in a folding-competent state, and the inhibition or promotion of apoptosis. ApoJ is upregulated under a variety of pathological conditions, including aging, atherosclerosis, diabetes, and degenerative diseases [128-130]. Additionally, it has been associated with cancer promotion and metastasis [131].

In plasma, apoJ coexists in HDL particles with apoA-I and apoE, which might play an essential role in RCT from peripheral tissues to the liver [124]. ApoJ was detected in the intima, as well as in the media layer, in early stages of atherosclerosis but not in normal aortic walls [132]. It has been demonstrated that apoJ has a protective role in atherosclerosis and induces cholesterol and phospholipid export from macrophage-foam cells [133].

Exist two alternatively spliced forms of the CLU gene that encode for secretory CLU (sCLU) or nuclear CLU (nCLU). What we know as apoJ specifically corresponds to sCLU. The secretory form appears to be cytoprotective [134] while nCLU migrates to the nucleus on cytotoxic stress to trigger cell death [135]. Regarding the cytoprotective effect of sCLU (apoJ), there is increasing evidence that apoJ is induced by stress and acts as an extracellular chaperone similar to small heat shock proteins [136]. It means that apoJ is a protein that regulates the correct folding of maturing proteins or prevents the aggregation of denatured proteins [137].

The primary structure of apoJ is highly conserved between different species and after its first isolation, an amphipathic character was described [138]. Regarding secondary structural elements, an  $\alpha$ -helical content of up to 60% was calculated [139, 140]. On the tertiary structure level, apoJ fits the family of intrinsically disordered proteins, meaning that it partially lacks a defined tertiary structure, consequently exposing hydrophobic regions, towards the external space [141]. This allows for binding to other molecules via hydrophobic interactions.

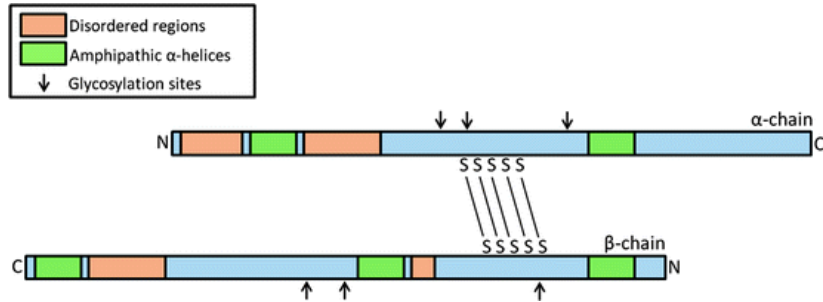


Figure 18. **ApoJ structure**  
Taken from [142]

During vascular damage, apoJ was found to accumulate in the human serum of diabetes type II patients, during myocardial infarction, or in the artery wall during atherosclerosis [128, 143]. It is present in mouse and human atherosclerotic lesions, but not in normal arterial tissue [132, 144].

In tissue cultures apoJ acts as an acceptor of cholesterol from macrophage-derived foam cells, which suggest that this protein at high concentrations in the surrounding environment of stressed cells, has the potential to eliminate cholesterol from damaged cell membranes and then transport it to HDL particles for subsequent clearance through RCT [145]. In another study it was found that apoJ colocalizes with enzymatically modified LDL in atherosclerotic lesions, favoring protective roles through its ability to inactivate C5b-9 complement complexes, and by reducing the cytotoxic effects of modified LDL on cells that gain contact with the lipoprotein [146]. Additionally, our group has previously demonstrated that apoJ plays an active protective role against LDL aggregation [147].

## **6. Mimetic Peptides**

Peptides are fragments of proteins with biological functions. They act as signaling units and interfere with protein-protein interactions, which are essential in biological processes. Generally, a mimetic peptide consists of at least six amino acids, and short peptides should not contain more than 45 amino acids [148]. Mimetic peptides have aroused significant interest due to their unique features and promise in innovative biotherapies. They can mimic the entire protein function and achieve an expected result, but they are much easier and cheaper to produce and manage. Also, mimetic peptides have been shown to have desirable pharmacological profiles and their specificity has been observed to translate into remarkable safety, tolerability, and efficacy profiles in humans [149, 150].

Focus on lipids has been the major strategy used in treating CVD and cholesterol-lowering drugs are the main therapy to prevent atherosclerosis. Other used drugs in CVD include anticoagulants, anti-inflammatory medicines, and beta-blockers. Even that these drugs have shown efficacy, many of them are also associated with varied side effects [151, 152]. Many therapies are currently under study to improve pathological cardiovascular complications, but nowadays there have been very few new drugs approved for treatment. In recent times, an interest in developing peptides and their mimetics for therapeutic intervention has emerged. Peptides that mimic the role of mediators implicated in the pathologic processes during vascular damage have been developed [153], some of them will be described below.

### **6.1 ApoA-I mimetic peptide**

The first apoA-I mimetic peptide was synthesized by Anantharamaiah *et al.* [154]. Later, this 18 amino acid peptide has suffered several modifications

to generate variant mimetic peptides with higher lipid affinity, increased homology to apoA-I, and enhanced anti-atherogenic properties [155]. An example of this is the 4F peptide that replicates the helical and amphipathic portion of apoA-I which is key for its function [156]. D-4F and L-4F, which involve D- and L-isomers of the amino acids, demonstrate similar functionality as apoA-I, D-4F being more stable via oral administration [157]. However, even though this peptide demonstrated effective antioxidant, anti-inflammatory, and atheroprotective effects in experimental models in apoE null mice and human aortic cell cultures, 4F peptides have failed to show some effectiveness in human trials [158-161].

Other apoA-I mimetics have been developed to improve some of the limitations of previous peptides. For example, the 6F peptide, which was also shown to have potent anti-inflammatory, antioxidant, and atheroprotective effects in LDL receptor-null mice but with reduced overall costs for synthesis [162, 163]. Another example is the 5A peptide, in which five amino acids were replaced to decrease its cytotoxicity associated with its high lipid binding affinity [164].

A recently described apoA-I mimetic peptide, named FAMP (Fukuoka University APOA-I mimetic peptide), has been shown to efficiently enhance HDL function in apoE-deficient mice. It has been described to act via ABCA1 in a highly specific manner [165].

## **6.2 ApoE mimetic peptide**

Mimetic peptides based on the apoE structure have been recently designed. The ATI-5261 is a 36 amino acid peptide that induces ABCA1-mediated cholesterol transport and reduces aortic lesion area and plaque lipid content in mice models of atherosclerosis [166].



One of the most characterized apoE mimetic is the Ac-hE18A-NH<sub>2</sub>, constituted of a region of the LDL binding domain of apoE connected to the previously described apoA-I mimetic 18A [167]. This peptide was shown to reduce plasma cholesterol in different animal models with dyslipidemia and had the additional advantage of clearing atherogenic lipoproteins because of the presence of the LDL binding domain [168]. This peptide, under the name AEM-28, is undergoing initial clinical review [169].

### **6.3 ApoJ mimetic peptide**

As previously described, apoJ is another HDL-associated protein. The helices on the apoJ peptide are primarily class G\* amphipathic helices. This G\* class helix holds a random distribution of positively and negatively charged residues on the polar face and it has a broad nonpolar face which allows it to easily bind to phospholipids [170].

Navab *et al.* found several potential G\*amphipathic helices in apoJ and synthesized and tested seven of these structures [171]. Six of them were anti-inflammatory, but only two were as efficient as the intact apoJ protein. These peptides were synthesized from D-amino acids and investigated for their ability to inhibit atherosclerosis in apoE null mice after oral administration. As a result, only the sequence D-[113–122]apoJ (Figure 13), which is the peptide that we studied in this project of thesis, inhibited the lesion formation in apoE null mice [171].

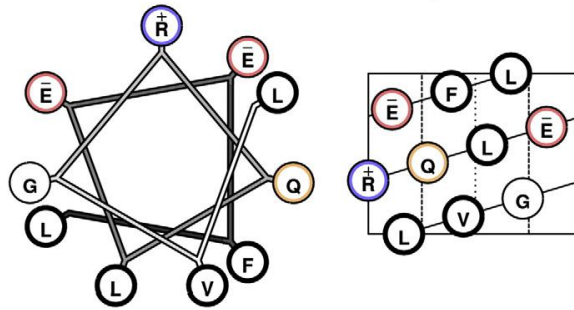
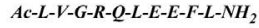


Figure 19. D-[113–122]apoJ peptide structure.

Taken from [172]

Oral administration of the 10-aminoacid D-[113–122]apoJ peptide reduced atherosclerosis by 70%. In comparison with D-4F peptide, after an oral dose, D-[113–122]apoJ associated with HDL more slowly and was also cleared from plasma much more slowly. Consequently, a single oral dose of D-[113–122]apoJ improved the anti-inflammatory properties of apoE null mice HDL. In monkeys, oral D-[113–122]apoJ peptide reduced lipoprotein lipid hydroperoxides and improved HDL inflammatory properties [171].

This thesis will add to the existing D-[113–122]apoJ evidence, significant studies that not only confirm the already promising functions of this peptide but new data regarding its involvement in atherosclerosis.



- **HYPOTHESIS AND OBJECTIVES**



A growing interest in the application of mimetic peptides as therapeutic agents has been raised in the last years. Experimental evidence suggests that peptides derived from apolipoproteins, such as apoA-I, apoE, and apoJ-derived peptides, are potential therapeutic agents against atherosclerosis. Most of these peptides promote cholesterol efflux and enhance the antiatherogenic functions of the HDL.

ApoJ is a glycoprotein that is mainly associated in plasma with HDL, but it also can be transported by LDL and VLDL. ApoJ has been detected in the aortic wall during early stages of atherosclerosis, which is considered an antiatherogenic mechanism. D-[113–122]apoJ, a mimetic peptide derived from the amino acid sequence of apoJ, displays anti-inflammatory and anti-atherogenic properties in the experimental model of apoE knockout mice. It has been reported that this synthetic peptide enhances the anti-inflammatory capacity of the HDL and reduces lipid hydroperoxide content *in vivo* and *in vitro* conditions. However, the direct effect of this peptide on LDL has not been studied yet. This is relevant since the development of atherosclerotic lesions in humans is mainly mediated by the cholesterol transported in LDL particles.

However, the *in vitro* and *in vivo* action of D-[113–122]apoJ peptide on LDL remains poorly explored. This is in part because of its high association with HDL and the difficulty to obtain an important amount of LDL particles for analysis in most mice models of atherosclerosis.

D-[113–122]apoJ peptide administration has been proven to reduce atherosclerosis. It was previously demonstrated that apoJ prevents the LDL aggregation process induced by SMase *in vitro*, we, therefore, hypothesized that the D-[113–122]apoJ peptide might also prevent this process.

Since LDL is the main lipoprotein found in atherosclerotic lesions and LDL aggregation is an important process during atherosclerosis development, we tested the hypothesis that D-[113–122]apoJ peptide administration could improve the functional properties of LDL *in vitro*, and also that the peptide could retard the atherosclerosis progression in a suitable mouse model *in vivo*.

Based on the existing knowledge of apoJ and the D-[113–122]apoJ mimetic peptide, the objectives of this thesis were the following:

1. To study *in vitro* the putative inhibitory effect of D-[113–122]apoJ mimetic peptide on spontaneous and SMase-induced LDL aggregation.
2. To elucidate the molecular mechanisms involved in the inhibition of LDL aggregation mediated by D-[113–122]apoJ mimetic peptide.
3. To determine the effect of D-[113–122]apoJ peptide administration on aortic atherosclerosis in LDLR-KO mice.
4. To explore the lipoprotein function in LDLR-KO treated mice, by analyzing the:
  - a. Pro- and antioxidant capacity of mice lipoproteins.
  - b. Cholesterol efflux capacity of HDL.
  - c. LDL aggregation process induced by SMase.
  - d. Electronegativity of LDL.

5. To evaluate the potential role of D-[113–122]apoJ on liver inflammation through the analysis of inflammation-related genes.





- MATERIALS AND METHODS



Specific methods and procedures of each research design are summarized in Table 4 and detailed described afterward.

METHOD	Paper	Paper
	1	2
1. Peptides	X	X
2. Animal study design		X
3. Lipoprotein isolation		
3.1 Human lipoprotein isolation	X	
3.2 Mice lipoprotein isolation		X
4. LDL subfraction separation	X	
5. Plasma and lipoprotein characterization		
5.1 Lipid composition	X	X
5.2 Protein composition	X	X
5.3 Sodium dodecyl sulphate-polyacrylamide gel electrophoresis (SDS-PAGE)	X	
5.4 Laurdan generalized polarization (GP)	X	
6. <i>In vitro</i> modification of LDL		
6.1 Spontaneous aggregation	X	
6.2 SMase-induced aggregation	X	X
7. Methods for monitoring LDL aggregation		
7.1 Turbidity	X	X
7.2 Size exclusion chromatography (SEC)	X	X
7.3 Non-denaturing gradient gel electrophoresis (GGE)	X	
7.4 Dynamic light scattering (DLS)	X	
7.5 Transmission electronic microscopy (TEM)	X	
8. Binding of D-[113–122]apoJ peptide to LDL	X	
9. Susceptibility to oxidation of LDL and HDL		X
10. Electronegativity of LDL		X
11. Cholesterol efflux capacity of HDL		X

12. Evaluation of atherosclerotic lesions		X
12.1 Oil red O staining		X
13. Quantitative RT-PCR analyses		
13.1 Tissue collection		X
13.2 RNA isolation		X
13.3 cDNA generation		X
13.4 RT-PCR		X
14. Statistical analysis	X	X

Table 4. **Methodology used in each of the publications presented. P: publication.**

## 1. Peptides

The amino acid sequence of D-[113–122]apoJ peptide is Ac-LVGRQLEEF<sub>113</sub>L-NH<sub>2</sub>. The inactive control scrambled peptide (Sc-D-[113–122]apoJ) has the same amino acid composition as D-[113-122]apoJ but in a sequence that does not promote G\* amphipathic helix formation (Ac- LRGVQLLEFE-NH<sub>2</sub>). Both peptides were obtained from Caslo (Kongens Lyngby, Denmark).

## 2. Animal Study Design

LDLR-KO mice from the C57BL/6 background were purchased from Jackson Laboratories (Bar Harbor, ME, USA; #002207).

Fifteen-month-old, female mice were randomly distributed into three groups depending on the received treatment. D-[113–122]apoJ peptide group (n = 12), scrambled peptide group (n = 8) and vehicle group (control, n = 8). The reason for using females is that the development of atherosclerosis is higher in female than in male mice [173].

Mice were housed in a controlled temperature environment (22 °C), exposed to a 12-h light/dark cycle, and food and water were provided ad libitum. Mice fed Western diet (WD) (TD.88137, Harlan Teklad, Madison, WI, USA, containing 21% fat and 0.2% cholesterol). Peptides (10 µg/g body weight) were administered subcutaneously three days per week (200 µg in 100 µL of saline). Weight and food intake were monitored for all experimental groups.

At the end of the study (eight weeks of treatment), mice were kept on a 4h food deprivation, sacrificed, and exsanguinated by cardiac puncture previously anesthetized with isoflurane (Forane®, Abbott). After

euthanasia, blood, heart, and liver were collected. Mice plasmas were obtained by centrifugation at 3,000 g for 10 min. Figure 20 illustrates a flow chart of the experimental design.

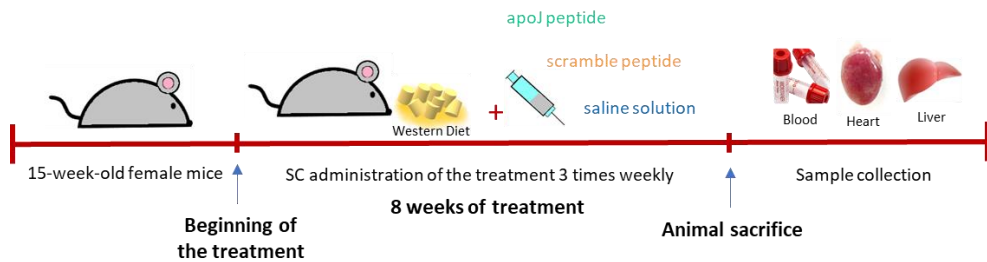


Figure 20. **Experimental design.**

All animal procedures were reviewed and approved by the Institutional Animal Care Committee of the Institut de Recerca de l'Hospital de la Santa Creu i Sant Pau (Procedure N<sup>o</sup> 103), and the methods were conducted in accordance with the approved guidelines.

### **3. Lipoprotein isolation by Sequential Ultracentrifugation**

All lipoproteins were isolated by ultracentrifugation flotation, using the appropriate density.

#### Materials

- Centrifuge tubes of 2.5 mL maximal volume (polycarbonate plastic).
- Centrifuge tubes of 20 mL maximal volume (polycarbonate plastic).
- Ultracentrifuge Beckman.
- Analytical fixed-angle rotor (50.3 and 55.38, Beckman Coulter).
- Lab material (pipettes, tips, eppendorf tubes ...).
- Density Solutions:

*1.006 g/mL density solution:* 0.15 mM chloramphenicol, 0.15 M NaCl, 0.08 g gentamycin. Dissolve all components in distilled water in a final volume of 2 L and adjust pH at 7.4.

*1.019 g/mL density solution:* 9.5 g of potassium bromide (KBr) to 500 mL of density solution 1.006 g/mL (KBr is just directly added to this volume of 1.006 g/mL solution).

*1.050 g/mL density solution:* 6.54 g KBr to 100 mL of density solution 1.006 g/mL (KBr is just directly added to this volume of 1.006 g/mL solution).

*1.063 g/mL density solution:* 8.53 g KBr to 100 mL of density solution 1.006 g/mL (KBr is just directly added to this volume of 1.006 g/mL solution).

*1.340 g/mL density solution:* 57.40 g KBr to 100 mL of density solution 1.006 g/mL (KBr is just directly added to this volume)

All density solutions contained 1mM ethylenediaminetetraacetic acid (EDTA) and 2  $\mu$ M butylated hydroxytoluene (BHT), and ultracentrifugation steps were performed at 4 °C to prevent lipoperoxidation.

### **3.1 Human lipoprotein isolation**

The obtention of human plasma samples for this study was approved by the Ethics Committee of the Hospital de la Santa Creu i Sant Pau.



Pooled plasma of healthy volunteers was obtained after their informed consent. Cholesterol and triglycerides were measured to ensure that all the samples were normolipemic.

Lipoproteins were isolated using potassium bromide (KBr) gradients by sequential ultracentrifugation (55.38 rotor, Beckman Coulter, Fullerton, CA, USA) for 24 hours at 100,000 g at 4 °C [174] in accordance with their density as shown in Table 5.

<b>LIPOPROTEIN</b>	<b>DENSITY</b>
VLDL	<1.019 g/mL
LDL	1.019-1.050 g/mL
HDL	1.063-1.210 g/mL

Table 5. Lipoprotein density distribution

The density to isolate each lipoprotein fraction was reached by adding the proper amount of KBr following the formula of Radding and Steinberg [175] (Figure 20). The density of plasma generally is assumed to be 1.006 g/mL.

$$X = V (d_f - d_i) / (1 - (0.312 \times d_f))$$

Figure 21. Radding and Steinberg formula. Where X = g of KBr, V = mL of plasma, di = initial density, df = final density, 0.312 = partial specific volume of KBr mL/g

Taken from [175]

For LDL isolation, the first isolation step at a density of 1.019 g/mL was performed to remove VLDL and IDL. Then, total LDL was isolated at 1.050 g/mL to avoid contamination with Lp(a) and oxidized LDL.

### 3.2 Mice lipoprotein isolation

VLDL (density <1.019 g/mL), LDL (density 1.019–1.063 g/mL), and HDL (density 1.063–1.210 g/mL) were isolated from each mice plasma by sequential ultracentrifugation, using KBr for density adjustment, at 100,000 g for 24 h at 4 °C with an analytical fixed-angle rotor (50.3, Beckman Coulter, Fullerton, CA, USA). Once calculated the needed quantity in g of KBr, these were added to the plasma sample using the concentrated density solution 1.340 g/mL as follow:

VLDL isolation

$$gKBr = \frac{Vf(df-di)}{1-(0.312*df)} = \frac{2.5 \text{ mL}(1.019-1.006)}{1-(0.312*1.019)} = 0.05gKBr$$

$$mL \text{ 1.340 density solution} = \frac{0.05gKBr * 117.9 \text{ mL}}{57.4gKBr} = 0.103mL$$

For the isolation of LDL and HDL, the above-mentioned calculations are used but with their respective densities.

### 4. LDL subfraction separation

LDL holds a small amount of LDL(-), which displays a phospholipase C (PLC)-like activity [176], which could interfere with our aggregation studies. Hence, in SMase-induced aggregation studies, total LDL was sub-fractionated in native LDL (LDL[+]) and LDL(-).

Isolated LDL was dialyzed against Buffer A (Tris-HCl 10 mM, EDTA 1 mM, pH 7.4) to remove KBr and sub-fractionated by anion-exchange chromatography using a HiLoad 26/10 Q-Sepharose High-Performance

Column in an ÄKTA Fast Protein Liquid Chromatography (FPLC) system (GE Healthcare).

The method used was a step salt gradient (Table 6) using Buffer A as a binding buffer and Buffer B or salted buffer (Tris-HCl 10 mM, NaCl 1M, EDTA 1 mM, pH 7.4) as an elution buffer.

Buffer volumes	Buffer B (%)
0 – 108 mL (2 cv)	0 %
108 – 161 mL (1 cv)	0 – 10 %
161 – 267 mL (2 cv)	24.5 %
267 – 373 mL (2 cv)	60 %
373 - 479 mL (2 cv)	100 %
479 – 506 mL (0.5 cv)	0 %

Table 6. **Step salt gradient for LDL (+) and LDL (-) isolation by FPLC. Cv: column volume.**

LDL (+) eluted and collected at 0.25 M NaCl (26% B Buffer) and LDL (-) eluted at 0.6 M NaCl (60% B Buffer). Chromatograms were obtained by monitoring absorbance at 280 nm.

## 5. Plasma and lipoprotein characterization

### 5.1 Lipid composition

Plasma lipid profile and lipoprotein composition of major lipids were measured by commercial methods adapted to a Cobas 6000/c501 autoanalyzer (Roche Diagnostics, Basel, Switzerland).

Total cholesterol (TC), triglycerides (TG), aspartate transaminase (AST), alanine transaminase (ALT), and apolipoprotein (apo) B reagents were obtained from Roche Diagnostics (Basel, Switzerland). Total phospholipids

(PL), non-esterified fatty acids (NEFAs), and free cholesterol (FC) reagents were obtained from Wako Chemicals (Richmond, VA, USA). TC, TG, AST, ALT, PL and NEFA, used enzyme-colorimetric assay while apoB employed an immunoturbidimetric assay. The quality control assessment for each of these tests was done at run-time and all of them fell within the acceptable range defined as two times the standard deviation. Mice triglyceride determinations were corrected for the free glycerol present in plasma (Sigma-Aldrich St. Louis, MO).

Cholesterol, triglycerides, and phospholipid content in mice livers was determined after solvent extraction. Liver lipids were extracted with isopropyl alcohol-hexane (2:3, v/v) from 500-1000 mg of the liver. After the addition of sodium sulfate ( $\text{Na}_2\text{SO}_4$ ), the lipid layer was isolated, dried with nitrogen, reconstituted with 0.5% (w/v) sodium cholate (Serva, Heidelberg, Germany) and sonicated using an ultrasound bath (model 5510-MT, Branson Ultrasonics Corp., Danbury, CT, USA) for 10 min (50 Hz) prior to lipid measurements.

## **5.2 Protein composition**

The protein content of each lipoprotein was assessed by bicinchoninic acid technique Pierce <sup>TM</sup> BCA Protein Assay (Thermo Fisher Scientific, Rockford, IL, USA) following the next procedure:

1. On a microplate pipette 25  $\mu\text{L}$  of each standard or unknown sample replicate into a microplate well (working range = 20–2000  $\mu\text{g}/\text{mL}$ ).
2. Add 200  $\mu\text{L}$  of the working reagent to each well and mix the plate thoroughly on a plate shaker for 30 seconds.
3. Cover the plate and incubate at 37°C for 30 minutes.
4. Cool plate to RT. Measure the absorbance at or near 562 nm on a plate reader.

Note: wavelengths from 540–590 nm have been used successfully with this method.

5. Subtract the average 562 nm absorbance measurement of the Blank standard replicates from the 562 nm measurements of all other individual standard and unknown sample replicates.

6. Prepare a standard curve by plotting the average Blank–corrected 562 nm measurement for each BSA standard vs. its concentration in  $\mu\text{g/mL}$ .

Use the standard curve to determine the protein concentration of each unknown sample.

### 5.3 Sodium dodecyl sulphate-polyacrylamide gel electrophoresis (SDS-PAGE)

ApoB degradation was assessed by SDS-PAGE in 7.5% polyacrylamide gels stained with Coomassie Brilliant Blue (see Figure 22).

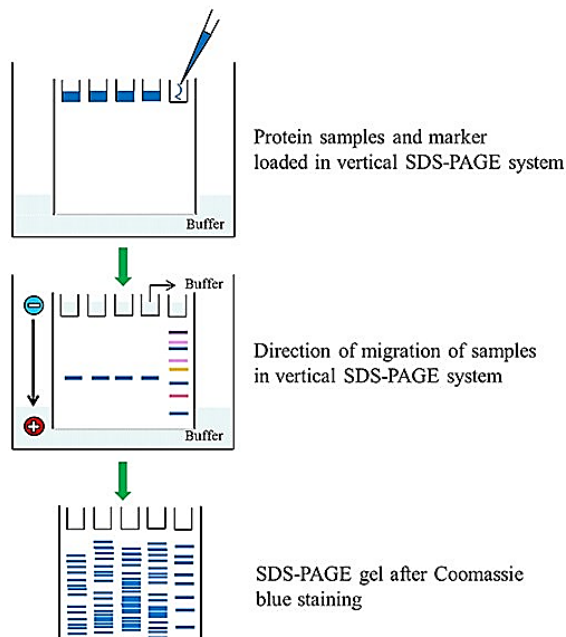


Figure 22. **Schematic view of SDS-PAGE process of protein samples.**

Taken from [177]

## 5.4 Laurdan generalized polarization (GP)

Laurdan (2-dimethylamino-6-lauroylnaphthalene) generalized polarization (GP) fluorescence was used to assess the effect of D-[113–122]apoJ peptide on lipid packaging in the LDL surface. Fluorescence was measured in a Biotek Synergy HT fluorimeter (Biotek Instruments, Winooski, Vermont, USA), using an excitation wavelength at 380 nm and emission wavelengths at 420 and 480 nm, as described in the below procedure:

1. Incubate LDL overnight with D-[113–122]apoJ peptide at RT.
2. Label LDL with 0.3  $\mu\text{L}$  of a 1.34 mM solution of Laurdan in dimethyl sulfoxide (final concentrations: 0.4  $\mu\text{M}$  Laurdan, 0.01% (vol%) DMSO).
3. Equilibrate the sample for 10 minutes at RT.
4. Transfer 200  $\mu\text{L}$  of LDL to a 96-well plate for fluorescence measurement.
5. Measure fluorescence in a fluorimeter (excitation 380nm, emission 420 and 480nm).
6. Following subtraction of the blank, calculate GP with the following equation [178]:

$$GP = \frac{I_{420} - I_{480}}{I_{420} + I_{480}};$$

where  $I_{420}$  and  $I_{480}$  are the emission intensities at 420 and 480 nm, respectively.

## 6. Modification of LDL *in vitro*

### 6.1 LDL spontaneous aggregation

For spontaneous aggregation studies total LDL (including LDL(+) and LDL(-)) was used since LDL(-) acts as a primer for lipoprotein aggregation.

Total LDL (0.5 mg/mL) apoB in buffer A containing was incubated at 25 °C in the absence or presence of D-[113–122]apoJ peptide (apoB/peptide molar ratios of 1:1 and 1:10) for up to 16 days without any external aggregation stimuli [147]. Therefore, the aggregation process occurred spontaneously.

## 6.2 LDL SMase-induced aggregation

In SMase-induced aggregation studies we used LDL(+) since electronegative LDL could interfere with the aggregation studies because its intrinsic phospholipase C (PLC)-like activity.

LDL(+) (0.5 mg/mL apoB) dialyzed in 20 mM Tris (pH 7.4) buffer, containing 150 mM NaCl, 2 mM CaCl<sub>2</sub>, 2 mM MgCl<sub>2</sub>, and 2 μM BHT, was incubated at 37 °C in the presence or absence of D-[113–122] apoJ or scrambled peptide for up to 24 h with SMase from *Bacillus cereus* sp. (Sigma Diagnostics, Livonia, MI, USA) with a final concentration of 5 mU/mL [147]. A molar ratio of 1:1 of apoB/peptide was used. Enzymatic lipolysis was stopped by the addition of 10 mM EDTA.

The same process was applied to study mice LDL aggregation, however, the LDL concentration in mice was 0.6 mmol/L cholesterol, it was dialyzed in phosphate-buffered saline and incubated at 37 °C for 2 h with SMase from *Bacillus cereus* sp. (Sigma Diagnostics, Livonia, MI, USA) at a final concentration of 50 mU/mL in the presence of 2 mM CaCl<sub>2</sub> and 2 mM MgCl<sub>2</sub>.

## **7. Methods for monitoring LDL aggregation**

### **7.1 Turbidity**

Samples' turbidity was determined by measuring absorbance at 450 nm of 100  $\mu$ L of LDLs (0.5 mg/mL apoB) in an AD340 microplate reader (Beckman Coulter, Brea, CA, USA).

### **7.2 Size exclusion chromatography (SEC)**

Size-exclusion chromatography (SEC) was performed for monitoring aggregation using a Superose 6 Increase 5/150 GL column in an AKTA-FPLC system (GE Healthcare Chicago, IL, USA). Fifty  $\mu$ L of human LDL at 0.5 mg/mL apoB and two hundred  $\mu$ L of mice LDL were injected in the column, eluted at a flow rate of 0.3 mL/min, and peaks were detected at 280 nm. This chromatography distinguishes two peaks of LDL, eluting first aggregated LDL (2.5 mL) and later monomeric LDL (3.1 mL).

### **7.3 Non-denaturing gradient gel electrophoresis (GGE)**

The development of aggregated particles was evaluated by non-denaturing polyacrylamide gradient (2–16%) gel electrophoresis after 6 h of electrophoresis at 100 V.

### **7.4 Dynamic light scattering (DLS)**

The detection of the light scattered from the interaction of light with matter gives information related to the physical characteristics of the sample. Volume size distribution of LDL particles was determined by DLS at 633 nm in a Zetasizer NanoZS (Malvern Instruments Limited, Malvern, UK) at a concentration of 0.5 mg/mL apoB. Particle size was obtained from the function of distribution by intensity, while the relative proportion of each



population was derived from the function of distribution by volume, employing the software of the instrument.

## **7.5 Transmission electronic microscopy (TEM)**

TEM was applied to visualize LDLs particles and generate a highly magnified image. LDLs were absorbed and processed for negative staining with 2% potassium phosphotungstate, pH 7.0, on carbon-coated grids. Micrographs were obtained using a Jeol 120-kV JEM-1400 TEM with an Erlangshen ES1000W CCD camera (Gatan, Abingdon, UK).

## **8. Binding of D-[113–122]apoJ peptide to LDL**

The ability of D-[113–122]apoJ peptide to bind to LDL with different levels of aggregation was tested as described below:

One hundred  $\mu\text{L}$  of D-[113–122]apoJ peptide at 1 mg/mL was incubated for 12 h at 4 °C in 96-well plates for fluorescent detection. The peptide not bound was washed out and the free binding sites in wells were blocked with a solution of 20 g/L albumin in PBS for 2 h at 37 °C. Subsequently, LDLs (0.5 g/L apoB) were added in triplicate and incubated with soft agitation for 12 h at 37 °C. Plates were washed four times with PBS, and the quantity of bound LDL was assessed using an Amplex® Red Cholesterol Assay Kit (Sigma Diagnostics, Livonia, MI, USA), according to the manufacturer's instructions. This kit provides a simple fluorometric method for the sensitive quantitation of cholesterol using a fluorescence microplate reader or fluorometer.

To test the effect of aggregation, different LDLs with rising levels of aggregation were used. First, total LDLs were left at room temperature to spontaneously aggregate. Then, we used fresh LDL(+) (aggregation below

1%) and total LDL incubated for 7 days (10–15% of aggregated particles), 12 days (20–25% of aggregated for particles), or 20 days (50–60% of aggregated particles) at room temperature. The level of aggregation was determined by SEC as previously described.

## **9. Susceptibility to oxidation of LDL and HDL**

Mice LDL and HDL susceptibility to copper-induced lipid oxidation and mice HDL capacity to inhibit the oxidative modification of human LDL were measured by monitoring the formation of conjugated dienes at 234 nm, for 7 h at 37° C in a BioTek Synergy HT spectrophotometer (BioTek Synergy, Winooski, VT, USA) [179].

LDL was dialyzed in PBS by gel filtration chromatography on PD-10 columns (GE Healthcare, Chicago, IL, USA) and HDL was dialyzed by Dialysis Cassettes G2 (Thermo Fisher Scientific, Rockford, IL, USA). The oxidation of lipoproteins was started by adding 2.5  $\mu\text{mol/L}$   $\text{CuSO}_4$  in wells containing mice LDL, mice HDL alone or mice HDL in the presence of human LDL (0.1 mmol/L cholesterol in all cases). Conjugated diene kinetics were acquired by continuously monitoring the absorbance at  $\lambda=234$  nm and the maximum slope through the propagation phase of the kinetics was the parameter used to assess the susceptibility of lipoproteins to oxidation.

The antioxidant ability of HDL was expressed as the capacity to decrease the slope of the oxidation kinetics of human LDL alone after the subtraction of the kinetics of mice HDL alone, as previously described [180].

## **10. Electronegativity of LDL**

The electric charge of LDL was determined by anion exchange chromatography in an ÄKTA–FPLC system (GE Healthcare), using a MonoQ 5/50 GL column (GE Healthcare).

First, mice isolated LDL (0.4 mmol/L cholesterol) was dialyzed against buffer A (Tris 10 mmol/L, EDTA 1 mmol/L, pH 7.4). Second, 100 µL of this LDL was injected into the column at a flow rate of 2 mL/min. Two fractions of LDL (native or LDL(+)) and modified or LDL(-)) were separated with a stepwise NaCl gradient using buffer A and buffer B (same composition as buffer A containing 1 M NaCl).

Compared to human LDL, mice LDL fractions eluted at a higher ionic strength. Consequently, LDL(+) eluted at 35% buffer B while LDL(-) eluted at 70% buffer B. Finally, the percentage of these fractions was calculated from the 280 nm peak area integration.

## **11. Cholesterol efflux capacity of HDL**

Cholesterol efflux capacity is an assay that measures the ability of an individual's HDL to promote cholesterol efflux from cholesterol donor cells such as macrophages. This capacity was determined using [<sup>3</sup>H]cholesterol-labeled J774A.1 mouse macrophages (ATCC® TIB67™, Manassas, VA, USA).

First,  $1.5 \times 10^5$  cells/well were seeded in 6-well plates and allowed to grow for three days in RPMI 1640 medium with 2 mM L-Glutamine (Pan Biotech, Aidenbach, Germany) supplemented with 10% fetal bovine serum (FBS) (Pan Biotech) and 100 U/mL penicillin/streptomycin (Dominique Dutscher,

Brumath, France). Next, cells were labeled with 1  $\mu\text{Ci}/\text{well}$  of [ $1\alpha,2\alpha(n)$ - $^3\text{H}$ ]cholesterol (GE Healthcare, Little Chalfont, UK) and 5% FBS for 60 h.

The cells were then equilibrated with 0.2% bovine serum albumin (BSA) in medium overnight and incubated for 4 h with mice HDL (25  $\mu\text{g}/\text{mL}$  protein), previously isolated by ultracentrifugation and dialyzed in PBS.

Lastly, radioactivity was measured in both the medium and the cells, and the percentage of cholesterol efflux from cells was calculated.

## **12. Evaluation of atherosclerotic lesions**

At the end of the experiment, mice were euthanized, and their hearts flushed with saline, embedded in OCT, and immediately flash frozen in dry ice. Frozen sections of 5-10  $\mu\text{m}$  thickness were taken in the region of the proximal aorta, starting from the end of the aortic sinus and the beginning of the aorta.

Atherosclerotic lesion severity was expressed as the area of positive Oil red O staining in four sections separated by 80  $\mu\text{m}$ . The lesion area was quantified using AxioVision V 4.8.1.0 image analysis software (Zeiss, Oberkochen, Germany).

### **12.1 Oil red O staining (ORO)**

This procedure was used to determine the amount of lipid accumulation in the proximal aorta of treated mice following the next steps.

ORO preparation:

1. Dissolve 0.5 g of ORO (Ref. O0625-25G- Sigma Aldrich) in 200 mL of isopropyl alcohol.
2. Warm the solution in a 56°C water bath for 1 h until it is cool.
3. The working solution is prepared prior to use by adding four parts of distilled water to six parts of stock solution.
4. Mix and stand for 10 min.
5. Filter through a fine filter paper.

Procedure:

1. Rinse frozen sections in distilled water.
2. Rinse in 60% isopropyl alcohol prepared with distilled water.
3. Stain in ORO for 10 min.
4. Wash quickly in 60% isopropyl alcohol.
5. Wash in distilled water.
6. Strain in hematoxylin (Ref. HHS32-1L- Sigma Aldrich) for 1 min.
7. Wash in running water.
8. Wash in distilled water.

### **13. Quantitative RT-PCR analyses**

#### **13.1 Tissue collection**

For RNA analysis, organs were collected, weighted and rapidly frozen in liquid nitrogen.

#### **13.2 RNA isolation**

Total liver RNA was obtained using TRIzol LS reagent (Invitrogen, Carlsbad, CA, USA) according to the manufacturer's protocol, and it was purified with an EZ-10 DNAaway RNA Miniprep Kit (Bio Basic, Markham, ON, Canada).

After purification, RNA concentration was determined using a NanoDrop2000 bioanalyzer (Thermo Scientific). The optical density (OD) at  $\lambda=260$  nm was used to determine the RNA concentration in the solution, considering that an  $A_{260}$  of 1.0 is equivalent to about 40  $\mu\text{g/mL}$  of RNA.

The ratio of absorbance at  $\lambda$  260 nm and 280 nm was applied to evaluate the purity of RNA. A ratio of  $\sim 2.0$  is generally accepted as “good” for RNA. If the ratio is considerably lower, it could indicate the presence of protein, phenol or other contaminants that absorb strongly at or near 280 nm.

### **13.3 cDNA generation**

RNA was reverse transcribed to complementary DNA (cDNA). cDNA synthesis is reached by the action of reverse transcriptase, an enzyme capable of creating a single-stranded DNA from an RNA template in the presence of primers. cDNA was generated using EasyScript First-Strand cDNA Synthesis SuperMix (Transgen Biotech, Beijing, China).

### **13.4 Quantitative real-time PCR (RT-PCR)**

Quantitative polymerase chain reaction (qPCR) was applied to amplify cDNA products reverse transcribed from mRNA. A relative quantification method was applied, in which internal reference genes are used to determine fold-variations in the expression of specific genes. The internal reference is a housekeeping gene.

Real-time PCR amplification was performed using the GoTaq(R) Probe qPCR Master Mix (Promega, Madison, WI, USA). Thermal cycling conditions involved 10 min at 95°C, 40 cycles at 95°C for 15 s and 65°C for 1 min.

Specific mouse TaqMan probes (Applied Biosystems, Foster City, CA, USA) were used to analyze gene expression of *Tnf* (Mm99999068\_m1), *Ccl2* (Mcp1, Mm0441242\_m1), *Cd36* (Mm00432403\_m1), and *Cd68* (Mm03047343\_m1). Real-time PCR tests were performed on a C1000 Thermal Cycler linked to a CFX96 Real-Time System (Bio-Rad, Hercules, CA, USA). All analyses were performed in duplicate.

*Gapdh* (Mm99999915\_g1) gene was used as the control housekeeping gene. The relative mRNA expression levels were calculated using the  $\Delta\Delta C_t$  method.

#### **14. Statistical analysis**

GraphPad Prism 6.0 software (GraphPad, San Diego, CA, USA) and the statistical software package R version 3.5.2 ([www.r-project.org](http://www.r-project.org)) were used to perform statistical analyses. For the first publication, results were expressed as mean  $\pm$  SD or as mean  $\pm$  SEM when indicated. Statistically significant differences were assessed by unpaired (Mann-Whitney) or paired (Wilcoxon) non-parametric tests.

Student's t-test was used to compare the differences between two groups. Two-way ANOVA with Tukey's multiple comparisons post-test was used to compare more than two groups (second publication). To analyze the association between atherosclerosis and parameters of lipoprotein function, Spearman's rho correlation was used, considering all variables as non-parametric. Linear regression analyses were performed to explore potential confounding. Data are expressed as the standardized beta coefficient ( $\beta$ ). A  $p$ -value  $< 0.05$  was considered statistically significant.

- ORIGINAL PUBLICATIONS





Publication 1:

**Rivas-Urbina A**, Rull A, Montoliu-Gaya L, Pérez-Cuellar M, Ordóñez-Llanos J, Villegas S, Sánchez-Quesada JL.

Low-density lipoprotein aggregation is inhibited by apolipoprotein J-derived mimetic peptide D-[113-122]apoJ. *Biochim Biophys Acta Mol Cell Biol Lipids*. 2020 Feb;1865(2):158541. doi: 10.1016/j.bbaliip.2019.158541. Epub 2019 Oct 28. PMID: 31672573.

Publication 2:

**Rivas-Urbina A**, Rull A, Aldana-Ramos J, Santos D, Puig N, Farre-Cabrerizo N, Benitez S, Perez A, de Gonzalo-Calvo D, Escola-Gil JC, Julve J, Ordoñez-Llanos J, Sanchez-Quesada JL.

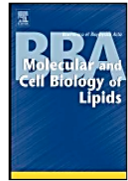
Subcutaneous Administration of Apolipoprotein J-Derived Mimetic Peptide D-[113-122]apoJ Improves LDL and HDL Function and Prevents Atherosclerosis in LDLR-KO Mice. *Biomolecules*. 2020 May 29;10(6):829. doi: 10.3390/biom10060829. PMID: 32485898; PMCID: PMC7356811.



## PUBLICATION 1

Low-density lipoprotein aggregation is inhibited by apolipoprotein J-derived mimetic peptide D-[113-122]apoJ





## Low-density lipoprotein aggregation is inhibited by apolipoprotein J-derived mimetic peptide D-[113–122]apoJ

Andrea Rivas-Urbina<sup>a,b,1</sup>, Anna Rull<sup>a,1,2</sup>, Laia Montoliu-Gaya<sup>b,3</sup>, Montserrat Pérez-Cuellar<sup>a</sup>, Jordi Ordóñez-Llanos<sup>a,b</sup>, Sandra Villegas<sup>b,\*</sup>, Jose Luis Sánchez-Quesada<sup>a,c,\*\*</sup>

<sup>a</sup> Cardiovascular Biochemistry Group, Research Institute of the Hospital de Sant Pau (IIB Sant Pau), Barcelona, Spain

<sup>b</sup> Biochemistry and Molecular Biology Department, Universitat Autònoma de Barcelona, Cerdanyola, Spain

<sup>c</sup> CIBER of Diabetes and Metabolic Diseases (CIBERDEM), Spain



### ARTICLE INFO

#### Keywords:

LDL aggregation  
Mimetic peptides  
Apolipoprotein J  
D-[113–122]apoJ

### ABSTRACT

Mimetic peptides are promising therapeutic agents for atherosclerosis prevention. A 10-residue class G<sup>\*</sup> peptide from apolipoprotein J (apoJ), namely, D-[113–122]apoJ, possesses anti-inflammatory and anti-atherogenic properties. This prompted us to determine its effect on the aggregation process of low-density lipoprotein (LDL) particles, an early event in the development of atherosclerosis. LDL particles with and without [113–122]apoJ peptide were incubated at 37 °C with sphingomyelinase (SMase) or were left to aggregate spontaneously at room temperature. The aggregation process was analyzed by size-exclusion chromatography (SEC), native gradient gel electrophoresis (GGE), absorbance at 405 nm, dynamic light scattering (DLS), and transmission electronic microscopy (TEM). In addition, circular dichroism was used to determine changes in the secondary structure of apoB, and SDS-PAGE was performed to assess apoB degradation. At an equimolar ratio of [113–122]apoJ peptide to apoB-100, [113–122]apoJ inhibited both SMase-induced or spontaneous LDL aggregation. All methods showed that [113–122]apoJ retarded the progression of SMase-induced LDL aggregation at long incubation times. No effect of [113–122]apoJ on apoB secondary structure was observed. Binding experiments showed that [113–122]apoJ presents low affinity for native LDL but binds readily to LDL during the first stages of aggregation. Laurdan fluorescence experiments showed that mild aggregation of LDL resulted in looser lipid packaging, which was partially prevented by D-[113–122]apoJ. These results demonstrate that [113–122]apoJ peptide prevents SMase-induced LDL aggregation at an equimolar ratio and opens the possibility for the use of this peptide as a therapeutic tool.

### 1. Introduction

According to the response-to-retention hypothesis, the initial step in atherogenesis is the entrapment of apolipoprotein B-containing lipoproteins, mainly low-density lipoprotein (LDL), in the subendothelial space [1]. This process is mediated by the interaction between arterial proteoglycans (PGs) in the intima layer and LDL particles that have crossed the monolayer of

endothelial cells by transcytosis. The binding of LDL to PGs is mediated by ionic interactions between the positively charged amino acid residues of apolipoprotein B (apoB) and the negatively charged sulfate and carboxyl groups of glycosaminoglycans (GAGs) [2]. In native LDL, such binding is mediated by a domain present in apoB known as site B (residues 3359–3369), which confers a relatively low capacity to bind to PGs [3]. In turn, native non-aggregated LDL also has the ability to go back to blood

**Abbreviations:** apo, apolipoprotein; BHT, butylated hydroxytoluene; CD, circular dichroism; DLS, dynamic light scattering; EDTA, ethylenediaminetetraacetic acid; GAG, glycosaminoglycans; GGE, non-denaturing polyacrylamide gradient gel electrophoresis; GP, generalized polarization; HDL, high-density lipoprotein; LDL, low-density lipoprotein; LDL(+), electropositive low-density lipoprotein; LDL(-), electronegative low-density lipoprotein; LPC, lysophosphatidylcholine; NEFA, non-esterified fatty acids; PC, phosphatidylcholine; PG, proteoglycan; PLC, phospholipase C; SEC, size exclusion chromatography; SDS-PAGE, sodium dodecylsulphate polyacrylamide-gel electrophoresis; SM, sphingomyelin; SMase, sphingomyelinase; TEM, transmission electron microscopy; TLC, thin layer chromatography

\* Correspondence to: S. Villegas, Protein Design and Immunotherapy Group, Biochemistry and Molecular Biology Department, Universitat Autònoma de Barcelona, Cerdanyola, Spain.

\*\* Correspondence to: J.L. Sánchez-Quesada, Cardiovascular Biochemistry Group, Research Institute of the Hospital de Sant Pau (IIB Sant Pau), Barcelona, Spain.

E-mail addresses: [Sandra.villegas@uab.cat](mailto:Sandra.villegas@uab.cat) (S. Villegas), [jsanchezq@santpau.cat](mailto:jsanchezq@santpau.cat) (J.L. Sánchez-Quesada).

<sup>1</sup> Both authors contributed equally to this work.

<sup>2</sup> Current address: Hospital Universitari Joan XXIII, IISPV, Universitat Rovira i Virgili, Tarragona, Spain.

<sup>3</sup> Current address: Department of Clinical Chemistry and Transfusion Medicine, Institute of Biomedicine, University of Gothenburg, Gothenburg, Sweden.

<https://doi.org/10.1016/j.bbalip.2019.158541>

Received 11 April 2019; Received in revised form 25 September 2019; Accepted 28 September 2019

Available online 28 October 2019

1388-1981/ © 2019 Elsevier B.V. All rights reserved.

circulation, since transcytosis is a size-dependent two-way process. This would prevent the excessive accumulation of LDL in the intima layer. Therefore, additional modifications leading to an increase in the LDL particle size are needed to promote the massive subendothelial retention of lipoproteins [4]. Aggregation and fusion of LDL particles in the micro-environment of the arterial intima has a doubly harmful effect that favors lipoprotein retention. First, LDL aggregation increases its binding affinity to PGs due to the exposure of additional binding sites in apoB, such as site A (residues 3148–3158), which is solvent-exposed after phospholipase A2 degradation [5,6]. Second, the increase in size of aggregated/fused particles prevents their egress back from the arterial wall by transcytosis. Hence, the aggregation and fusion of LDL particles is considered the key early step in the development of atherogenesis. Reinforcing this view, Ruuth et al. have recently underlined the relevance of these processes demonstrating that the susceptibility to aggregation associates with future cardiovascular deaths [7].

LDL aggregation is triggered by various phenomena occurring in the arterial intima [4]. Oxidative processes, which are believed to be exacerbated in atherosclerotic lesion and are involved in the inflammatory response, can induce LDL aggregation. However, lipoperoxidation promotes the derivatization of positively charged residues in apoB necessary for the binding to PGs [8], which suggests a more relevant role for oxidized LDL in triggering inflammation than in lipoprotein retention. Proteolysis of apoB, whether secondary to oxidative processes or mediated by specific proteases, has also been shown to induce LDL aggregation [9,10]. But, probably the most relevant mechanism for LDL aggregation in the environment of the arterial wall is lipolysis, mainly mediated by sphingomyelinase (SMase) [11,12]. This enzyme is locally secreted by endothelial cells and macrophages and is hyper-expressed in areas of the atherosclerotic lesion. In vitro SMase-modified LDL particles resemble aggregated lipoproteins isolated from atherosclerotic lesions, including increased ceramide content [13–15]. Another phenomenon that would favor subendothelial LDL retention is self-aggregation. This is, in part, mediated by a type C phospholipolytic activity present in a minor electronegative subfraction of LDL (named electronegative LDL, LDL(-)). This enzymatic activity primarily degrades lysophosphatidylcholine (LPC) and sphingomyelin, triggering the aggregation of monomeric LDL particles [16,17].

Despite the relevance of LDL aggregation in atherogenesis and the increasing number of studies analyzing the physicochemical mechanisms leading to aggregation/fusion of LDL, no specific therapeutic strategies directed at inhibiting lipoprotein aggregation have been successfully developed. It is known that apolipoproteins containing amphipathic  $\alpha$ -helices, such as apolipoprotein A-I (apoA-I) or apolipoprotein III (an apolipoprotein from insects) [18,19], are able to prevent LDL aggregation induced by intense agitation or by phospholipase C-mediated lipolysis. In this context, Nguyen and colleagues reported that the apoA-I mimetic peptide 4F inhibits SMase-induced LDL aggregation, which opens the possibility of new therapeutic agents directed to prevent LDL aggregation [20]. Another mimetic peptide used for preventing atherosclerosis in animal models is D-[113–122]apoJ, derived from the sequence of apolipoprotein J (apoJ, also known as clusterin) [21]. ApoJ is an extracellular chaperone that forms part of the quality control system against protein unfolding and is present in blood partly bound to lipoproteins, including LDL [22–25]. Specifically, among LDL subfractions, apoJ is especially abundant in some minor aggregated LDL fractions, which should be interpreted as a protective mechanism against aggregation [26]. Our group previously found that apoJ protects LDL from SMase-mediated, proteolysis-mediated, and spontaneous aggregation [27]. Based on those findings, the aim of the present study was to analyze the ability of D-[113–122]apoJ peptide to inhibit the aggregation of LDL.

## 2. Materials and methods

### 2.1. Peptides

The amino acid sequence of D-[113–122]apoJ peptide is

Ac-LVGRQLEEF-NH<sub>2</sub>. This peptide forms a class G\* amphipathic helix in the presence of lipids [28]. The inactive control scrambled peptide (Sc-D-[113–122]apoJ) has the same overall amino acid composition as D-[113–122]apoJ but in a sequence that does not promote G\* amphipathic helix formation (Ac-LRGVQLLEFE-NH<sub>2</sub>). The use of D-peptides guarantees the resistance to proteolysis in the blood. Both peptides were obtained from Caslo (Kongens Lyngby, Denmark).

### 2.2. Lipoprotein isolation and characterization

The study was approved by the institutional ethics committee. Cholesterol and triglycerides were measured to ensure that all the samples were normolipemic. Total LDL was isolated from pooled plasma of healthy normolipemic volunteers by sequential ultracentrifugation using potassium bromide (KBr) gradients (density range 1.019–1.050 g/mL). All density solutions contained 1 mM ethylenediaminetetraacetic acid (EDTA) and 2  $\mu$ M butylated hydroxytoluene (BHT), and ultracentrifugation steps were performed at 4 °C to prevent lipoperoxidation. Total LDL contains a small amount of LDL(-), which displays a phospholipase C (PLC)-like activity [17], and thereby could interfere with our aggregation studies. For this reason, in SMase-induced aggregation studies, total LDL was sub-fractionated in native LDL (LDL(+)) and LDL(-) by anion-exchange chromatography, as described [29]; accordingly, in these experiments, we used LDL(+). In turn, for spontaneous aggregation studies we used total LDL (including LDL(+) and LDL(-)) because aggregated LDL(-) acts as a primer for lipoprotein aggregation. LDL composition of major lipids and apoB was measured by commercial methods adapted to a Cobas 6000/c501 autoanalyzer (Roche Diagnostics, Basel, Switzerland). Total cholesterol, triglycerides, and apolipoprotein (apo) B reagents were obtained from Roche Diagnostics (Basel, Switzerland). Total phospholipids, non-esterified fatty acids (NEFAs), and free cholesterol reagents were obtained from Wako Chemicals (Richmond, VA, USA). The relative content of sphingomyelin (SM), phosphatidylcholine (PC), LPC, and ceramide in LDLs after SMase lipolysis was assessed by thin layer chromatography (TLC), as described [30].

### 2.3. Induction of LDL aggregation

SMase-induced aggregation: Aggregation of LDL(+) was induced by SMase-induced lipolysis. Briefly, LDL(+) (0.5 mg/mL apoB) dialyzed in 20 mM Tris (pH 7.4) buffer, containing 150 mM NaCl, 2 mM CaCl<sub>2</sub>, 2 mM MgCl<sub>2</sub>, and 2  $\mu$ M BHT, was incubated at 37 °C for up to 24 h with SMase from *Bacillus cereus* sp. (Sigma Diagnostics, Livonia, MI, USA) with a final concentration of 5 mU/mL [31] in the presence or absence of D-[113–122]apoJ or scrambled peptide. In most experiments, a molar ratio of 1:1 of apoB/peptide was used. Enzymatic lipolysis was stopped by adding 10 mM of EDTA (final concentration). The degradation of SM was assessed by thin layer chromatography (TLC), as described [30].

Spontaneous aggregation: Alternatively to SMase-mediated lipolysis, spontaneous self-aggregation of total LDL was induced by incubation at 25 °C for up to 16 days without external aggregation stimuli [31].

### 2.4. Methods for monitoring aggregation

Turbidity: Samples' turbidity was determined by measuring absorbance at 450 nm of 100  $\mu$ L of LDLs (0.5 mg/mL apoB) in an AD340 microplate reader (Beckman Coulter, Brea, CA, USA).

Size exclusion chromatography (SEC): SEC was performed in a Superose 6 Increase 5/150 GL column in an AKTA-FPLC system (GE Healthcare, Chicago, IL, USA), using 50  $\mu$ L of LDL at 0.5 mg/mL apoB [31].

Non-denaturing gradient gel electrophoresis (GGE): The formation of aggregated particles was analyzed by non-denaturing polyacrylamide gradient (2–16%) gel electrophoresis after 6 h of electrophoresis at 100 V, as described [32].

Dynamic light scattering (DLS): Volume size distribution of LDL particles was determined by DLS at 633 nm in a Zetasizer NanoZS (Malvern Instruments Limited, Malvern, UK) at a concentration of

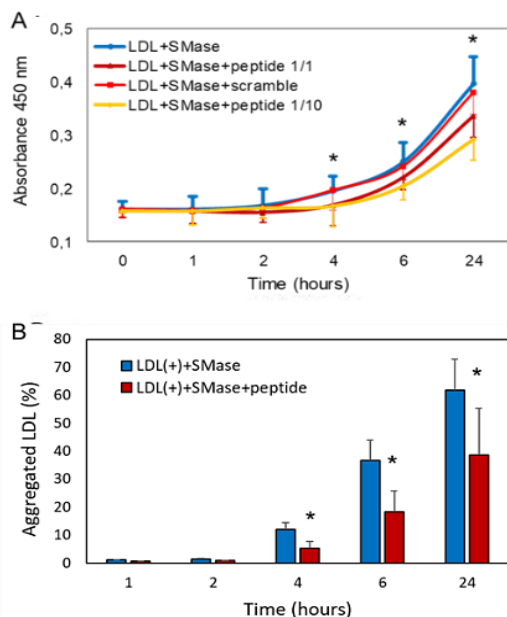


**Fig. 1.** Monitoring of SMase-mediated lipolysis of LDL(+). (A) LDL(+) (0.5 mg/mL) was incubated in the absence or presence of D-[113–122]apoJ peptide (apoB/peptide molar ratios of 1:1 and 1:10) or scramble peptide (1:1), and aggregation was induced by adding SMase (5 mU/mL). The increase in turbidity was measured at 450 nm for 24 h. Data are the mean  $\pm$  SD of 8 independent experiments. (B) The proportion of aggregated LDL particles after SMase lipolysis was determined by SEC in the absence or presence of D-[113–122]apoJ peptide at apoB/peptide molar ratio of 1:1, as described in Materials and methods. Data are the mean  $\pm$  SD of 6 independent experiments. \*  $P < 0.05$  between LDL(+) + SMase and LDL(+) + SMase + peptide.

0.5 mg/mL apoB. Particle size was derived from the function of distribution by intensity, whereas the relative proportion of each population was derived from the function of distribution by volume, using the software of the instrument.

Transmission electronic microscopy (TEM): TEM was performed as previously described [31]. Briefly, LDLs were absorbed and processed for negative staining with 2% potassium phosphotungstate, pH 7.0, on carbon-coated grids. Micrographs were obtained using a Jeol 120-kV JEM-1400 TEM with an Erlangshen ES1000W CCD camera (Gatan, Abingdon, UK).

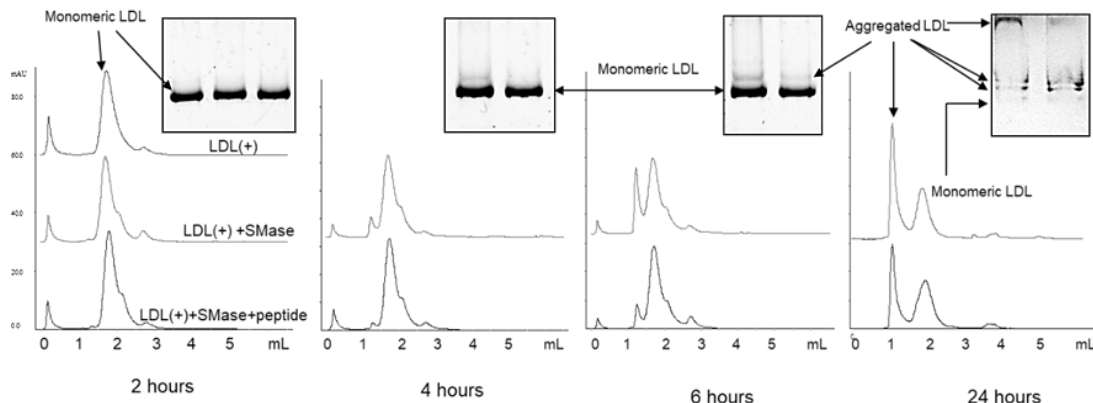


**Fig. 2.** Size exclusion chromatography (SEC) and native polyacrylamide gradient gel electrophoresis (GGE). Representative chromatograms of LDL(+) at 2, 4, 6, and 24 h of lipolysis with SMase alone or with D-[113–122]apoJ peptide at apoB/peptide molar ratio of 1:1. Inserts show bands of aggregated and monomeric LDL particles in GGE gels.

## 2.5. Alterations in apoB

Sodium dodecyl sulphate-polyacrylamide gel electrophoresis (SDS-PAGE): ApoB degradation was assessed by SDS-PAGE in 7.5% polyacrylamide gels stained with Coomassie Brilliant Blue. Spectroscopic analysis: Circular dichroism (CD) spectra were obtained using 50  $\mu$ g of apoB/L in a JASCO J-715 spectropolarimeter (Easton, MD 21601 USA) in the far-UV region (190–260 nm), as described [33]. A 0.2 cm quartz cuvette was used, and the temperature was maintained at 25  $^{\circ}$ C.

## 2.6. Alterations in lipid packaging

Laurdan (2-dimethylamino-6-lauroyl-naphthalene) generalized polarization (GP) fluorescence was used to assess the effect of D-[113–122]apoJ peptide on lipid packaging in the LDL surface. Fluorescence was measured in a Biotek Synergy HT fluorimeter (Biotek Instruments, Winooski, Vermont, USA), using an excitation wavelength at 380 nm and emission wavelengths at 420 and 480 nm, as described [34]. GP was calculated from the equation  $GP = (I_{420} - I_{480}) / (I_{420} + I_{480})$  [35].

## 2.7. Binding of D-[113–122]apoJ peptide to LDL

The ability of D-[113–122]apoJ peptide to bind to LDL with different levels of aggregation was tested in 96-well plates for fluorescent detection. One hundred  $\mu$ L of D-[113–122]apoJ peptide at 1 mg/mL was incubated for 12 h at 4  $^{\circ}$ C. The peptide not bound was washed out and the free binding sites in wells were blocked by adding a solution of 20 g/L albumin in PBS for 2 h at 37  $^{\circ}$ C. Then, LDLs at 0.5 g/L apoB were added in triplicate and incubated with gentle agitation for 12 h at 37  $^{\circ}$ C. Plates were washed four times with PBS, and the amount of bound LDL was assayed using an Amplex Red Cholesterol Assay Kit (Sigma Diagnostics, Livonia, MI, USA), according to the manufacturer's instructions.

To test the effect of aggregation, different LDLs with increasing levels of aggregation were used. For this purpose, total LDLs were left at room temperature to spontaneously aggregate. Finally, we used fresh LDL(+) (aggregation below 1%) and total LDL incubated for 7 days (10–15% of aggregated particles), 12 days (20–25% of aggregated particles), or 20 days (50–60% of aggregated particles) at room temperature. The level of aggregation was determined by SEC as previously described.

## 2.8. Statistical analysis

Results were expressed as mean  $\pm$  SD or as mean  $\pm$  SEM when indicated. Statistically significant differences were assessed by unpaired (Mann-Whitney) or paired (Wilcoxon) non-parametric tests, when appropriate.  $P < .05$  was considered statistically significant.



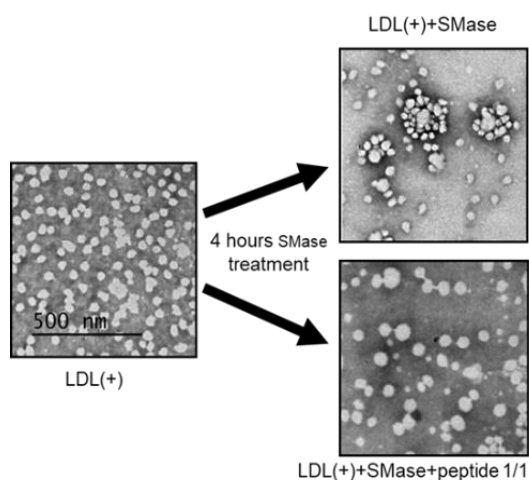


**Fig. 3.** Transmission electron microscopy (TEM). Micrographs were obtained in a Jeol 120 kV JEM-1400 microscope, and LDL(+) samples were incubated with SMase for 4 h, in the absence or presence of D-[113-122]apoJ peptide at apoB/peptide molar ratio of 1:1, as described in Materials and methods. Black bar, 500 nm.

### 3. Results

#### 3.1. Effect of D-[113-122]apoJ peptide on SMase-induced aggregation of LDL(+)

Monitoring of SMase-mediated lipolysis showed a progressive increase of absorbance at 450 nm indicating aggregation of LDL(+) particles (Fig. 1A). Aggregation was evident at 4 h of incubation and increased over time. The presence of D-[113-122]apoJ at an apoB/

peptide molar ratio of 1:1 delayed the increase in absorbance. Increasing the ratio apoB/peptide to 1:10 increased the inhibitory effect compared to 1:1. The scrambled peptide showed no inhibitory effect on LDL aggregation.

The blocking effect of D-[113-122]apoJ on SMase-induced LDL(+) aggregation was also analyzed by SEC (Fig. 1B). Fig. 2 shows representative chromatograms of LDL(+) at different stages of aggregation induced by SMase in the absence or presence of D-[113-122]apoJ. Native, non-aggregated LDL (LDL(+)) elutes as a single peak, whereas the incubation of LDL(+) with SMase results in the formation of an additional peak consisting of aggregated LDL particles of a larger size (Fig. 2). Integration of the peak areas of aggregated and non-aggregated LDLs showed that D-[113-122]apoJ, at a molar ratio of 1:1, inhibited the formation of aggregated particles by approximately 40–50% (Figs. 1B, 2). Similar findings were observed when GGE was used to monitor LDL aggregation (inserts in Fig. 2).

TEM was used to visualize aggregation. At first sight, a certain degree of size heterogeneity was observed in both images after SMase treatment (Fig. 3). The formation of both small and aggregated particles is a consequence of the action of SMase on LDL particles. Electron micrographs showed that, at 4 h of SMase treatment, the mean size of LDL(+) particles decreased. In addition, a trend to form aggregates was observed, even though the particles maintained their individuality. The presence of D-[113-122]apoJ prevented the decrease in particle size and, in part, the formation of aggregates.

These observations were confirmed by DLS analysis (Fig. 4). LDL(+) presented a sole peak of 30–34 nm formed by monomeric particles, whereas three peaks were detected in SMase-treated LDL(+). The first was formed by monomers with a size of 25–28 nm, and two populations of aggregated particles were observed, one with a 130–135 nm (peak 2) and the other with an out-of-range size (> 5000 nm, peak 3, not observed in the graph). The addition of D-[113-122]apoJ resulted in a normalization of the size of LDL monomers (30–34 nm), and the particles in the second peak of aggregated LDL were slightly larger (150–160 nm) than those observed in the absence of D-[113-122]apoJ.

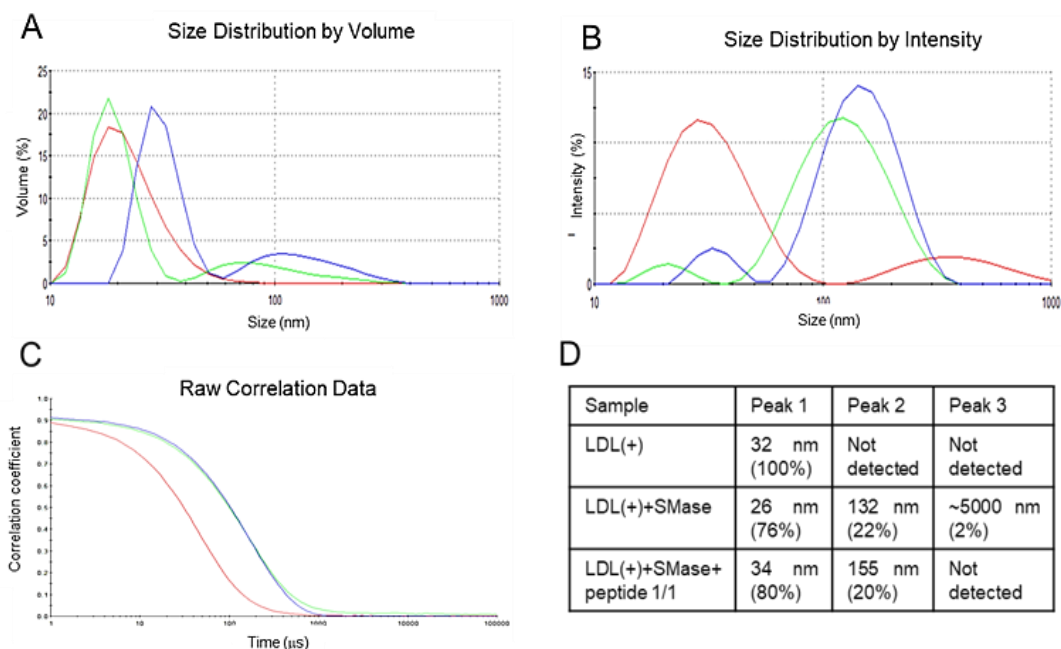


**Fig. 4.** Dynamic light scattering (DLS). Data are from LDL(+) samples incubated with SMase for 4 h, as described in Materials and methods. Panel (A) shows size distribution by volume, which has been used as a measurement of the amount of each population. Panel (B) shows size distribution by intensity, which has been used to determine the mean diameter size of the particles. Panel (C) shows the correlation function, which has been used to determine the extent of aggregation. A summary of the DLS data is found in Table D. Red line: LDL(+); blue line: LDL(+)+SMase; green line: LDL(+)+SMase+peptide 1:1.

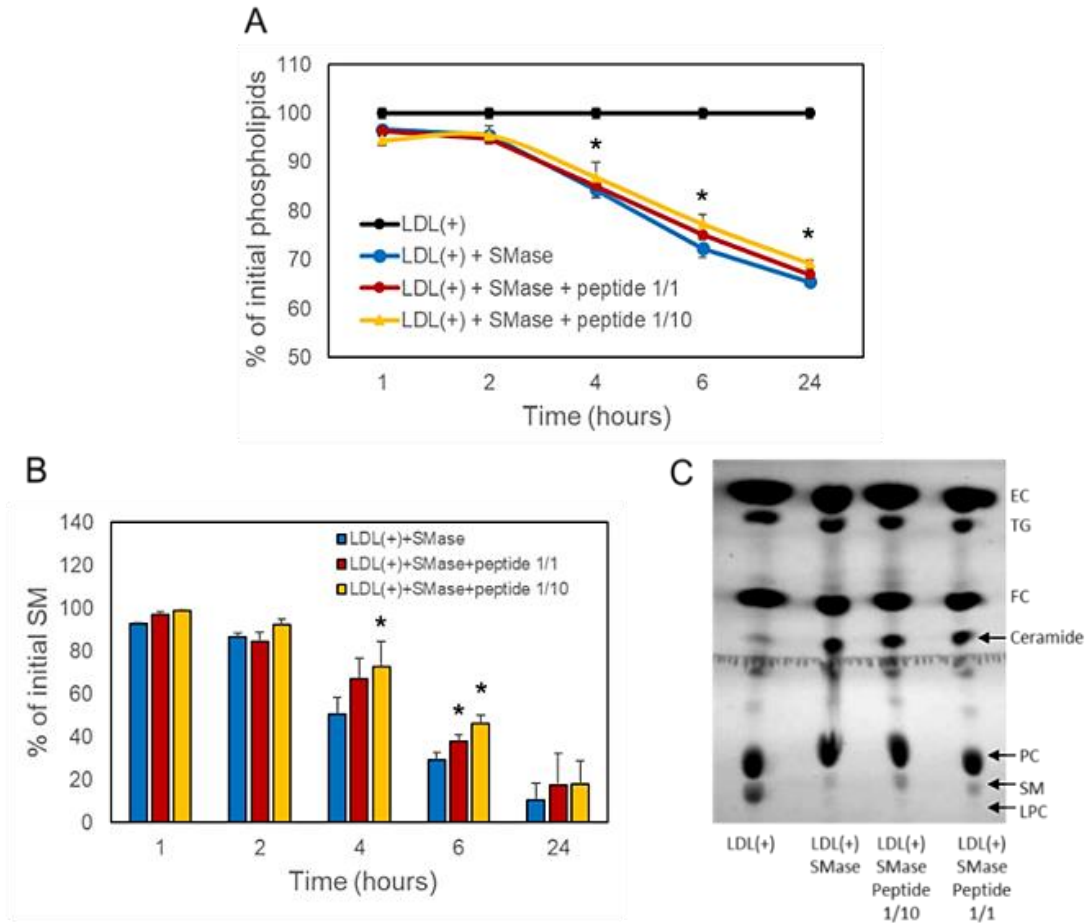


**Fig. 5.** Effect of SMase treatment on phospholipid content. LDL(+) (0.5 mg/mL) was incubated in the absence or presence of D-[113–122]apoJ peptide (apoB/peptide molar ratios of 1:1 and 1:10), and lipolysis was induced by adding SMase (5 mU/mL). (A) Total phospholipids were measured in a Cobas 6000/c501 autoanalyzer, as described in *Materials and methods*. Data are the mean  $\pm$  SD of 6 independent experiments. \*  $P < 0.05$  versus LDL(+). (B) The content of SM \*  $P < 0.05$  between LDL(+)+SMase and LDL(+)+SMase+peptide was determined by TLC, as described in *Materials and methods*. Data are the mean  $\pm$  SD of 6 independent experiments. \*  $P < 0.05$  versus LDL(+)+SMase. (C) Representative TLC plate of LDL(+) treated with SMase in the presence or absence of D-[113–122]apoJ peptide. EC: esterified cholesterol; TG: triglycerides; FC: free cholesterol; PC: phosphatidylcholine; SM: sphingomyelin; LPC: lysophosphatidylcholine.

Interestingly, the out-of-range peak was not formed when D-[113–122]apoJ was present.

### 3.2. Composition changes induced in LDL(+) by SMase-induced lipolysis

The content of free and esterified cholesterol, triglycerides, NEFA, and apoB in LDL(+) remained unchanged after SMase treatment (data not shown). In contrast, the amount of total phospholipids progressively decreased to 65–70% of the initial content after 24 h of incubation with SMase (Fig. 5A). These results are consistent with the percentage of SM that is usually reported in the phospholipid content in LDL, suggesting almost complete degradation of SM at 24 h. The addition of D-[113–122]apoJ had no statistical effect on the degradation of total phospholipids at 4, 6, and 24 h of SMase treatment, although, D-[113–122]apoJ peptide at 1:10 ratio showed a trend to inhibit phospholipid degradation. TLC analysis of LDLs after SMase-incubation showed that the decrease in phospholipids was progressive and due

specifically to SM degradation, which resulted in the increase in ceramide, whereas PC and LPC remained unchanged (Fig. 5C). Approximately 90% of SM was degraded after 24 h of incubation with SMase. A trend to the inhibition of SM degradation by D-[113–122]apoJ was observed at all the time points, but significant inhibition was observed only at the time points of 4 h (ratio apoB/apoJ 1/10) and 6 h (both ratios) (Fig. 5B).

To determine whether the inhibitory effect of the peptide was due to a direct action on the enzymatic activity of SMase, an Amplex Red SMase assay was conducted as described [16], using SM as a substrate in the presence or absence of peptides. No inhibition of SMase activity was observed when peptides were added to the assay, whereas the specific SMase inhibitor chlorpromazine blocked the SMase activity (data not shown).

Regarding the effect of SMase treatment on the protein moiety of LDL(+), SDS-PAGE analysis showed that apoB was not degraded during SMase-mediated lipolysis (Fig. 6A). In addition, the apoB content did

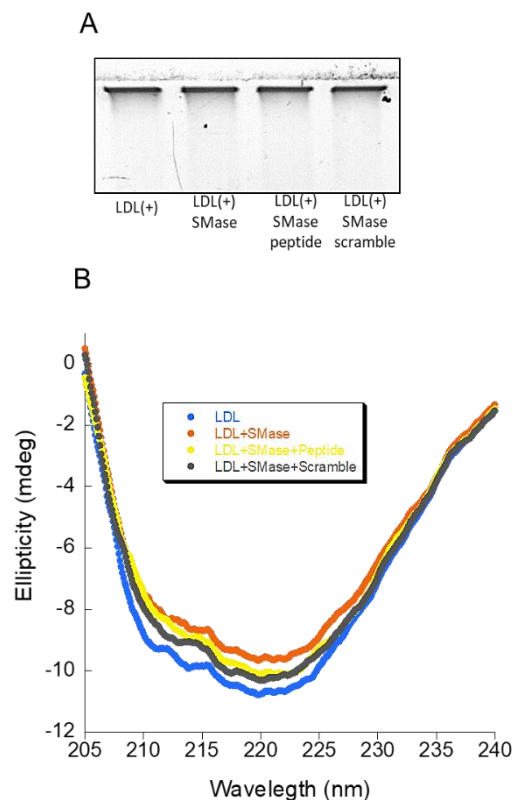


**Fig. 6.** Effect of SMase treatment on apoB. LDL(+) (0.5 mg/mL) was incubated in the absence or presence of D-[113–122]apoJ peptide (apoB/peptide molar ratios of 1:1 and 1:10), and lipolysis was induced by adding SMase (5 mU/mL). (A) SDS-PAGE of LDL(+) treated with SMase with or without D-[113–122]apoJ peptide was performed as described in *Materials and methods*. Samples were electrophoresed in 7.5% polyacrylamide gels for 1 h at 100 V and stained with Coomassie Brilliant Blue. Black arrow indicates the band corresponding to apoB-100. (B) CD spectra were acquired in a JASCO J-715 spectropolarimeter, as described in *Materials and methods*. Blue line: LDL(+); Red line: LDL(+) + SMase; Yellow line: LDL(+) + SMase + peptide 1:1; Black line: LDL(+) + SMase + peptide 1:10.

not change after SMase treatment (data not shown). This observation suggests that extensive changes in apoB conformation did not occur because the immunocolorimetric method used for its quantification is sensitive to conformational changes. CD analysis showed a moderate loss of signal after 6 h of SMase treatment (Fig. 6B), which was partially prevented by D-[113–122]apoJ peptide at 1:1 apoB/peptide ratio. This loss of signal is compatible with aggregation rather than with changes in the secondary structure, since the curve shape was very similar between LDL(+) and SMase-treated LDL(+). Of note, despite the presence of the enzyme and the peptide, all far-UV CD signals in Fig. 6 comes from apoB due to its huge mass excess over other proteins. Overall, these observations suggest that the relative proportion of secondary structures in apoB was not modified in our experimental conditions.

### 3.3. Spontaneous aggregation of total LDL

Spontaneous aggregation of total LDL in the presence of oxidation inhibitors (EDTA and BHT) is a process partly driven by the PLC-like activity intrinsic to the electronegative LDL fraction. The measurement of absorbance at 450 nm showed that the spontaneous aggregation of total LDL at room temperature increased over time and reached significant differences versus basal values after 4 days at room temperature (Fig. 7A). The addition of D-[113–122]apoJ peptide at a molar ratio of 1:1 (apoB/peptide) significantly inhibited the aggregation process compared with LDL alone at 12 days. When the peptide concentration was increased to an apoB/peptide ratio of 1:10, the inhibitory blocking effect was higher than with the ratio 1:1. SEC confirmed that the addition of peptide at a ratio of 1:1 inhibited the formation of aggregated LDL particles (Fig. 7B, C).

### 3.4. Composition changes induced in total LDL after spontaneous aggregation

The incubation of total LDL at 25 °C for up to 16 days promoted a modest but progressive increase in the NEFA content (Fig. 8). NEFAs probably come from partial degradation of esterified cholesterol, since free cholesterol also increased upon incubation. ApoB remained relatively stable up to 10 days, and then abruptly decreased, suggesting proteolysis and/or alterations in its conformation. When D-[113–122]apoJ peptide was added to LDL, either at an apoB/peptide ratio of 1:1 or 1:10, no effect was observed in the alterations of the lipid content, but its presence showed a trend to decrease apoB degradation, reaching statistically significant differences when the ratio 1:10 was used (Fig. 8).

### 3.5. In vitro binding of D-[113–122]apoJ peptide to LDL

To test the ability of D-[113–122]apoJ peptide for interaction with LDL at different levels of aggregation, experiments were conducted in 96-well plates coated with peptide. Our data show that D-[113–122]apoJ interacted poorly with native non-aggregated LDL, but such interaction increased strongly to 80% when the level of aggregation of LDL was moderate (10–12%) (Fig. 9). Surprisingly, with higher levels of aggregation, the binding progressively decreased as these levels increased. This observation suggests that D-[113–122]apoJ enhances its binding to LDL as hydrophobic surfaces become solvent-exposed during the first stages of the aggregation process.

### 3.6. Effect of D-[113–122]apoJ on LDL surface packaging

Laurdan GP fluorescence experiments showed that the order of lipids in the surface of native LDL was not altered by the presence of D-[113–122]apoJ, which is in accordance with the low binding of the peptide to native LDL (Fig. 10A). In contrast, treatment of LDL with SMase promoted a decrease in GP value, reflecting the decrease of lipid packaging during the aggregation process (Fig. 10A). This process was partially reverted by the addition of D-[113–122]apoJ in a concentration-dependent manner. Spontaneous aggregation of LDL resulted in a progressive decrease in GP, indicating a looser lipid packaging (Fig. 10B). The presence of D-[113–122]apoJ throughout this process retarded the loss of rigidity of the lipoprotein surface (Fig. 10B). Taken together, these observations suggest that, independent of the mechanism of aggregation, D-[113–122]apoJ could retard LDL aggregation by an increase of the lipid packaging order in the lipoprotein surface.



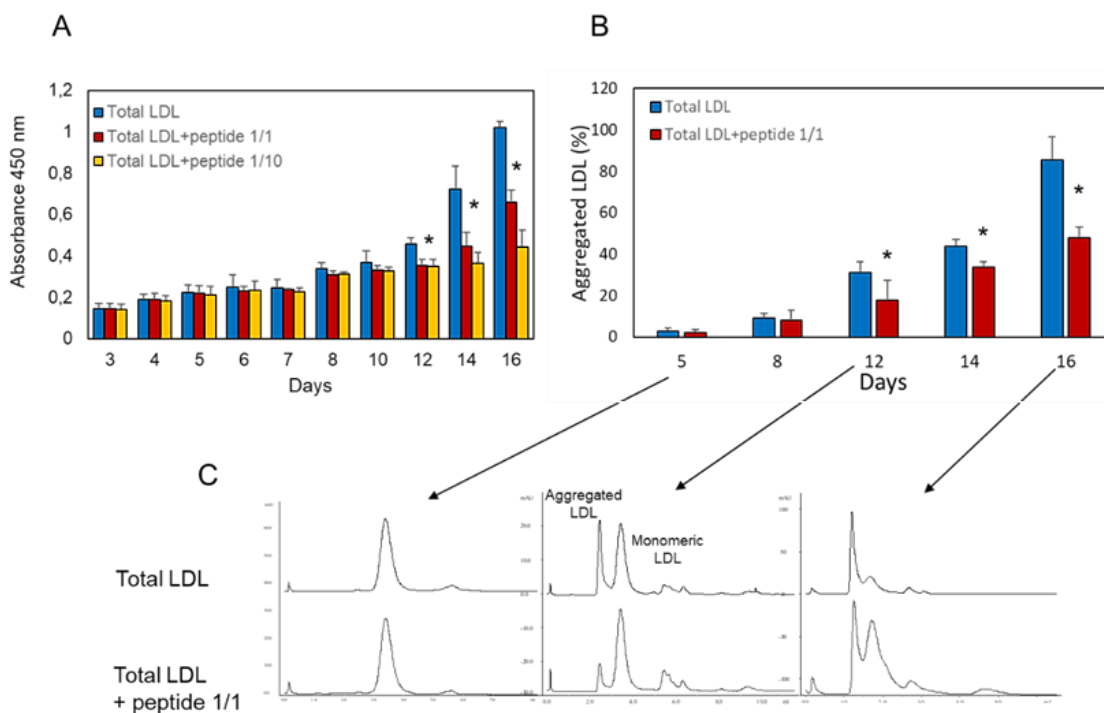


**Fig. 7.** Monitoring of spontaneous LDL aggregation. (A) Total LDL (0.5 mg/mL) was incubated at 25 °C in the absence or presence of D-[113–122]apoJ peptide (apoB/peptide molar ratios of 1:1 and 1:10), and aggregation occurred spontaneously. The increase in turbidity was measured at 450 nm up to 16 days. Data are the mean  $\pm$  SD of 6 independent experiments. \*  $P < 0.05$  between total LDL and total LDL + peptide at both ratios. (B) The proportion of aggregated LDL particles after spontaneous aggregation was determined by SEC in the absence or presence of D-[113–122]apoJ peptide at apoB/peptide molar ratio of 1:1, as described in [Materials and methods](#). Data are the mean  $\pm$  SD of 6 independent experiments. \*  $P < 0.05$  versus total LDL. (C) Representative SEC chromatograms. \*  $P < 0.05$  versus total LDL.

#### 4. Discussion

The use of apolipoprotein-derived mimetic peptides as therapeutic tools has aroused growing interest in recent years. In the field of cardiovascular disease, mimetic peptides derived from apoA-I are the most extensively studied, and different apoA-I mimetics have succeeded in preventing atherosclerosis in animal models [36]. This prevention was attributed to different mechanisms mimicking some functions of HDL, such as favoring the efflux of cholesterol or improving the anti-inflammatory and antioxidant capacity [37–39]. Such findings led to the design of new apoA-I mimetics and the development of several clinical trials [40–42]. However, such trials conducted in humans using different mimetics have failed to demonstrate a clinical benefit [43]. The reasons for these disappointing results in clinical trials are not clear. Perhaps, they could be related with the reported discordances between *in vitro* and *in vivo* properties of apoA-I mimetics [44]. Other factors could be related with the fact that targeting only HDL function could not be sufficient to prevent the onset of adverse cardiovascular outcomes since, in contrast to mice, in humans, LDL plays the main role in the development of atherosclerosis. The findings presented in this work add to these previous reports on using mimetic peptides derived from apolipoproteins, but in this case, instead of its effect improving the HDL function, the mimetic peptide derived from apoJ acted on a pro-atherogenic characteristic of LDL. Data presented in the current study show that D-[113–122]apoJ is able to prevent the aggregation of LDL. The effect was demonstrated by different experimental approaches, including turbidity, SEC, GGE, TEM, and DLS. This observation concurs with our previous finding that the whole molecule of apoJ also prevents LDL aggregation [27]. As previously demonstrated with apoJ, the inhibitory effect of the peptide is independent of the mechanism driving

aggregation, whether induced by SMase-mediated lipolysis or by spontaneous aggregation. Considering the relevance of LDL aggregation to trigger lipoprotein retention in the subendothelial environment during the early stages of atherosclerosis, this peptide could retard the onset or reduce the development of atheromatous lesions. In line with this, Navab et al. previously reported that subcutaneous administration of D-[113–122]apoJ prevented atherosclerosis development in apoE-KO mice [21]. These authors attributed their finding to the improvement of the anti-inflammatory properties of HDL by sequestering oxidized lipids that inhibit antioxidant enzymes in HDL. Our results point to an additional antiatherogenic mechanism of D-[113–122]apoJ, which would be mediated by the prevention of LDL aggregation and the subsequent subendothelial lipoprotein retention. It is likely that D-[113–122]apoJ may function through multiple mechanisms on different lipoproteins, the combination of these properties being responsible for atheroprotection.

In relation to our work, the study by Nguyen et al. is of special interest [20]. These authors reported a similar action of 4F, a mimetic of apoA-I, preventing LDL aggregation induced by SMase. However, despite the similarities, our peptide presents some differences compared to 4F. The most relevant is that D-[113–122]apoJ appears as more efficient than 4F when used at an equimolar ratio with apoB. In fact, 4F was effective only when it was used at supra-equimolar peptide/apoB ratios. As reported by Nguyen et al., we also observed that D-[113–122]apoJ partially inhibited the degradation of SM by SMase. However, in both the study of Nguyen et al. and in our work, it was demonstrated that this inhibition was not due to a direct effect of the peptides on the enzyme and, thereby, should be attributed to an indirect action rendering LDL less susceptible to SMase hydrolysis.

On the other hand, D-[113–122]apoJ also inhibited the spontaneous

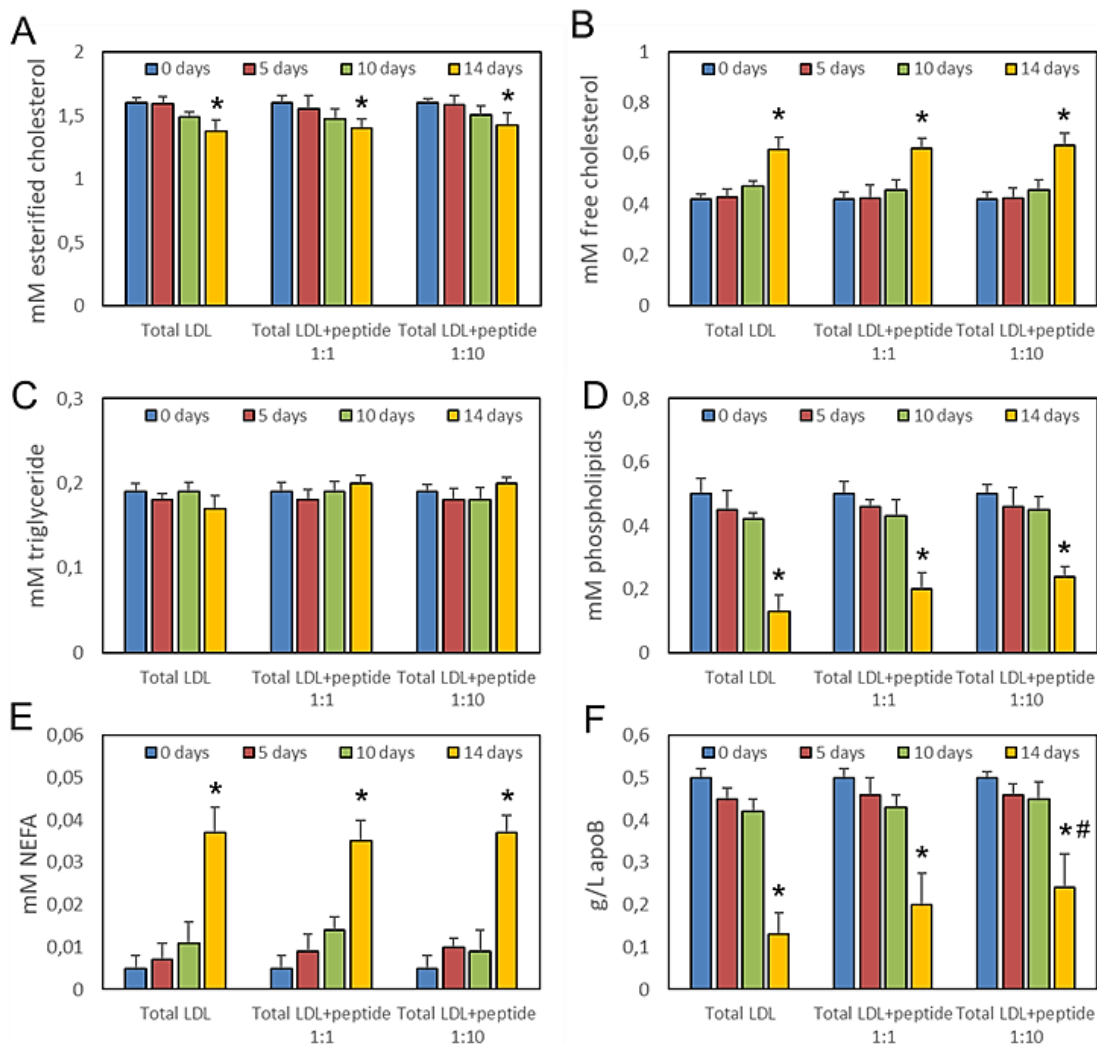


**Fig. 8.** Changes in LDL composition after spontaneous aggregation. (A) Total LDL (0.5 mg/mL) was incubated at 25 °C in the absence or presence of D-[113–122]apoJ peptide (apoB/peptide molar ratios of 1:1 and 1:10), and aggregation occurred spontaneously, as described in Materials and methods. All components were measured in a Cobas 6000/c501 autoanalyzer, as described in Materials and methods. Data are the mean  $\pm$  of 6 independent experiments. \*  $P < 0.05$  versus basal values (0 days); #  $P < 0.05$  versus total LDL alone.

aggregation of total LDL, suggesting that its action is independent of the mechanism driving aggregation. Spontaneous aggregation is partially due to a PLC-like activity present in the electronegative fraction of LDL [17]. This activity primarily degrades LPC [16], degrading the polar head group of the molecule and yielding phosphorylcholine, as SMase does with SM to yield ceramide. However, our data show that, during spontaneous aggregation, the main change in the composition of LDL was a slow but progressive increase in NEFA, and such an increase was not affected by the addition of D-[113–122]apoJ. Hence, the inhibition of this peptide seems to be independent of its effect on changes of the LDL composition. Therefore, D-[113–122]apoJ would prevent LDL aggregation by directly interacting with the surface of these particles.

Binding experiments showed that D-[113–122]apoJ binds poorly to native LDL. In this regard, this peptide differs from 4F, which was shown to interact strongly with lipids on the surface of native LDL

[20,45]. Interestingly, D-[113–122]apoJ increased its binding to LDL during the first stages of aggregation, but such interaction decreased as the aggregation level increased. A plausible mechanism for explaining this observation could be that, in the absence of hydrophobic surfaces (i.e., in native LDL), the peptide does not bind to LDL, but as hydrophobic areas become solvent-exposed during the early stages of aggregation, D-[113–122]apoJ is attracted by LDL. Later on, when aggregation is extensive and LDL particles have interacted among them through hydrophobic interactions, the binding of D-[113–122]apoJ to LDL decreases. LDL with a level of 10–15% of aggregated particles correspond approximately to 8 days of spontaneous aggregation (see Fig. 7). Although the composition of the LDL particles was not measured at this time point, it would be intermediate between 5 and 10 days of incubation (see Fig. 8). At this stage of aggregation, the changes in composition are minor without statistical differences versus

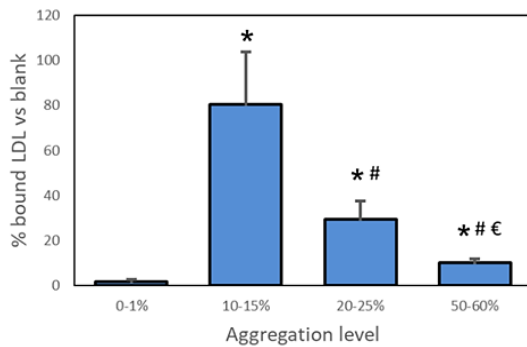


**Fig. 9.** Binding of D-[113-122]apoJ peptide to LDL. The binding of D-[113-122]apoJ peptide to LDLs with different levels of aggregation was tested in 96-well microtiter plates, as described in *Materials and methods*. Four LDL with increasing aggregation levels measured by SEC (0-1%, 10-15%, 20-25%, and 50-60% of aggregated LDL particles) were tested. Data are the mean  $\pm$  SD of 6 independent experiments. \*  $P < 0.05$  versus 0-1%; #  $P < 0.05$  versus 10-15%; €  $P < 0.05$  versus 20-25%.

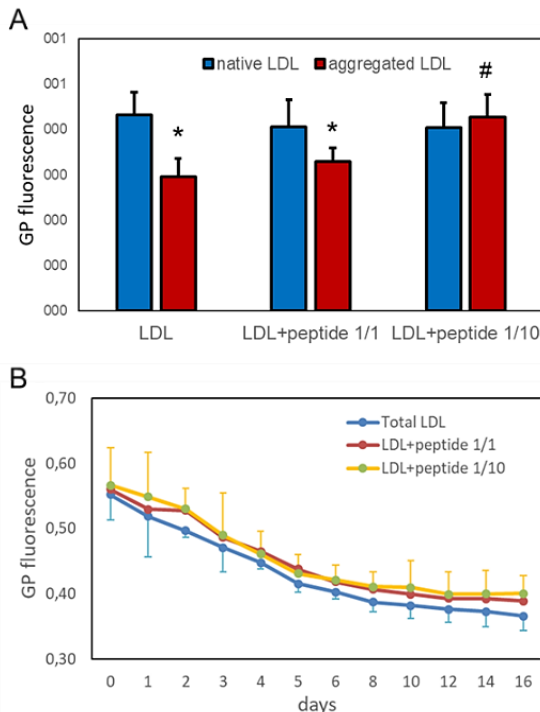


**Fig. 10.** Effects of D-[113-122]apoJ peptide on lipid packaging. Laurdan generalized polarization (GP) fluorescence was measured in a fluorimeter Biotek Synergy HT, using excitation wavelength at 380 nm and emission wavelengths at 420 and 480 nm, as described in *Materials and methods*. (A) GP values in native LDL(+) or aggregated LDL in the presence or absence of D-[113-122]apoJ peptide (ratios apoJ/apoB 1:1 and 1:10). Native LDL(+) contains < 0.5% of aggregated particles measured by SEC. Aggregated LDL was obtained by incubation with SMase (4 h of incubation in the conditions described in *Materials and methods*) and contained 15% of aggregated particles measured by GFC. Data are the mean  $\pm$  SD of 6 independent experiments. \*  $P < 0.05$  versus native LDL; #  $P < 0.05$  versus LDL without peptide. (B) Monitoring of GP values during spontaneous aggregation of LDL in the absence or presence of D-[113-122]apoJ peptide (ratios apoJ/apoB 1:1 and 1:10). Data are the mean  $\pm$  SD of 4 independent experiments.

non-aggregated particles. Therefore, it can be assumed that the increased binding of the peptide to LDL occurs in absence of major changes in the main components of LDL. We can speculate that during this early phase small hydrophobic patches appear in the lipoprotein surface attracting the peptides. As these hydrophobic patches become larger due to extensive modification, are the LDL particles themselves which cover the hydrophobic areas, decreasing the binding of the peptide. This distinctive behavior of D-[113-122]apoJ compared with that of 4F could be related to a different conformation. The 4F forms a class A amphipathic  $\alpha$ -helix known to strongly bind to the surface of lipoproteins [46]. In contrast, D-[113-122]apoJ is predicted to form a class G\* amphipathic  $\alpha$ -helix in the mature apoJ protein, and it adapts this structure in the presence of phospholipids, but in aqueous buffer shows a rather unordered conformation due to its small size [28]. It has been shown that, in hydrophobic environments, such as those formed during the aggregation of LDL, the  $\alpha$ -helical secondary structures of even small peptides can be stabilized through local inter-residue interactions. Therefore, processes favoring the emergence of hydrophobic regions in the LDL surface would favor the binding of D-[113-122]apoJ.

Another difference between 4F and D-[113-122]apoJ is that the former modifies apoB secondary structure [20], probably due to the binding of 4F to lipids on the surface of LDL particles, perturbing the distribution of lipids and, consequently, modulating apoB-100 conformation. The poor interaction of D-[113-122]apoJ with native LDL would explain the lack of changes in apoB secondary structure upon binding.

To gain insight into the interaction between D-[113-122]apoJ and the lipid moiety of LDL, we performed laurdan fluorescence experiments. This probe measures the compaction of the lipids in the surface of the lipoprotein [47]. This assay has been used to demonstrate that estradiol blocks the spontaneous aggregation of LDL stabilizing apoB folding [34]. Our data indicate that the peptide has no effect on the fluidity of the LDL surface in native LDL(+). However, when LDL is aggregated, either by SMase or spontaneously, the fluidity of its surface increases (decreased GP values). It is in this situation that D-[113-122]apoJ would bind to the hydrophobic areas generated, increasing the packaging of lipids (increased GP values) and preserving the native order of the LDL surface.

**Fig. 11** schematizes a putative mechanism of action of D-[113-122]apoJ. Degradation of LDL by SMase or spontaneous aggregation generates hydrophobic patches and unpacking of lipids in the surface of lipoproteins, favoring the interaction between these hydrophobic surfaces in LDL and leading to aggregation. In the presence of D-[113-122]apoJ, the peptide binds to these patches, avoiding the unpacking of surface lipids and the interaction of hydrophobic patches among LDL particles.

Of note, in the current study we have used a peptide with aminoacids in D configuration, instead of L-peptides. D-peptides are less susceptible to proteolytic degradation in the digestive tract or inside cells than L-peptides. D-peptides can therefore be taken orally and could be effective for a longer period of time. But its removal is slower, and this could result in some adverse side effects. The existence of these putative complications should be mandatorily assessed in further studies conducted in animal models and, later, in clinical trials.

In summary, the use of apolipoprotein-derived mimetic peptides as therapeutic tools has aroused growing interest. In the field of cardiovascular disease, mimetic peptides derived from apoA-I are the most extensively studied. Different apoA-I mimetics have succeeded in preventing atherosclerosis in several animal models but failed to achieve good results in clinical trials. Our findings show that an apoJ-derived peptide prevents LDL aggregation, which is the earliest event in the development of atherosclerotic lesions. Further studies in animal models are necessary to demonstrate that this anti-aggregative capacity could be translated to the in vivo situation.



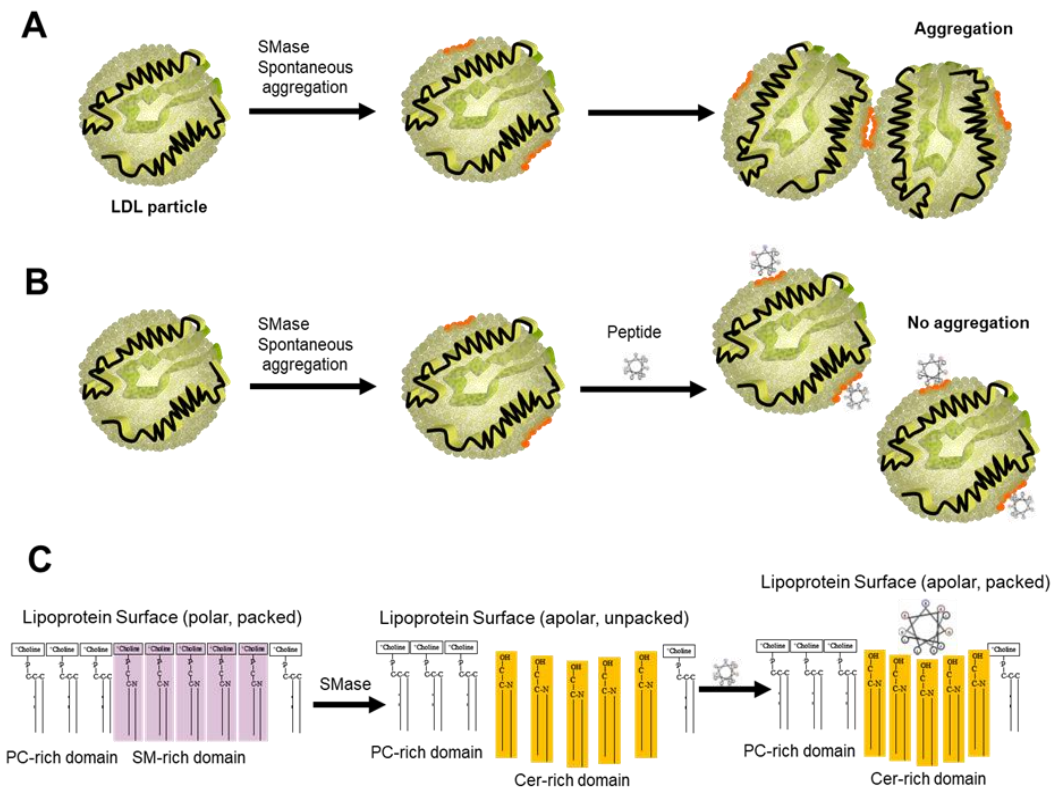


**Fig. 11.** Scheme of a putative mechanism of action of D-[113–122]apoJ. A) Degradation of LDL by SMase or driven by PLC-like, lead to spontaneous aggregation, generate hydrophobic patches in the surface of lipoproteins (in orange) and facilitate the interaction of modified LDL particles. B) In the presence of D-[113–122]apoJ, the peptide binds to these patches, avoiding the interaction of hydrophobic surfaces among LDL particles. C) At a molecular level, the degradation of the polar head group of SM (violet) generates domains enriched in ceramide (orange) and favors lipid unpacking. The presence of D-[113–122]apoJ reverts the unpacking of surface lipids and avoids aggregation.

#### Transparency document

The Transparency document associated with this article can be found, in the online version.

#### Acknowledgements/sources of funding

A.R.-U., A.R. M.P.-C., J.O.-L. and J.L.S.-Q. are supported by grants FIS PI13/00364 and PI16/00471 from the Instituto de Salud Carlos III, Spanish Ministry of Health (co-financed by the European Regional Development Fund). AR is supported by a grant from the Acció Instrumental d'incorporació de científics i tecnòlegs (PERIS SLT002/16/00101), Departament de Salut, Generalitat de Catalunya, S.V. is supported by grant SAF2017-89613R from the Ministerio de Economía y Empresa (co-financed by the European Regional Development Fund). CIBERDEM (CB07/08/0016) is an Instituto de Salud Carlos III Project. A.R.-U., J.O.-L., and J.L.S.-Q. are members of the Quality Research Group 2017-SGR-1149 from Generalitat de Catalunya. A.R.-U. and J.L.S.-Q. are members and of the Group of Vascular Biology of the Spanish Society of Atherosclerosis.

#### Declaration of competing interest

The authors declare that they have no conflicts of interest.

#### References

- [1] K.J. Williams, I. Tabas, Lipoprotein retention—and clues for atheroma regression, *Arterioscler. Thromb. Vasc. Biol.* 25 (2005) 1536–1540.
- [2] G. Camejo, E. Hurt-Camejo, O. Wiklund, G. Bondjers, Association of apo B lipoproteins with arterial proteoglycans: pathological significance and molecular basis, *Atherosclerosis* 139 (1998) 205–222.
- [3] J. Boren, I. Lee, W. Zhu, K. Arnold, S. Taylor, T.L. Innerarity, Identification of the low density lipoprotein receptor-binding site in apolipoprotein B100 and the modulation of its binding activity by the carboxyl terminus in familial defective apo-B100, *J. Clin. Invest.* 101 (1998) 1084–1093.
- [4] M.O. Pentikainen, K. Oorni, M. Ala-Korpela, P.T. Kovanen, Modified LDL - trigger of atherosclerosis and inflammation in the arterial intima, *J. Intern. Med.* 247 (2000) 359–370.
- [5] C. Flood, M. Gustafsson, R.E. Pitas, L. Arnaboldi, R.L. Walzem, J. Boren, Molecular mechanism for changes in proteoglycan binding on compositional changes of the core and the surface of low-density lipoprotein-containing human apolipoprotein B100, *Arterioscler. Thromb. Vasc. Biol.* 24 (2004) 564–570.
- [6] C. Flood, M. Gustafsson, P.E. Richardson, S.C. Harvey, J.P. Segrest, J. Boren, Identification of the proteoglycan binding site in apolipoprotein B48, *J. Biol. Chem.* 277 (2002) 32228–32233.
- [7] M. Ruuth, S.D. Nguyen, T. Vihaveara, M. Hilvo, T.D. Laajala, P.K. Kondadi, A. Gistera, H. Lahteenmaki, T. Kittila, J. Huusko, M. Uusitupa, U. Schwab, M.J. Savolainen, J. Sinisalo, M.L. Lokki, M.S. Nieminen, A. Jula, M. Perola, S. Yla-Herttula, L. Rudel, A. Oorni, M. Baumann, A. Baruch, R. Laaksonen, D.F.J. Ketelhuth, T. Aittokallio, M. Jauhainen, R. Kakela, J. Boren, K.J. Williams, P.T. Kovanen, K. Oorni, Susceptibility of low-density lipoprotein particles to aggregate depends on particle lipidome, is modifiable, and associates with future cardiovascular deaths, *Eur. Heart J.* 39 (2018) 2562–2573.
- [8] K. Oorni, M.O. Pentikainen, A. Annala, P.T. Kovanen, Oxidation of low density lipoprotein particles decreases their ability to bind to human aortic proteoglycans. Dependence on oxidative modification of the lysine residues, *J. Biol. Chem.* 272 (1997) 21303–21311.



- [9] M.O. Pentikainen, M.T. Hyvonen, K. Oorni, T. Hevonoja, A. Korhonen, E.M. Lehtonen-Smeds, M. Ala-Korpela, P.T. Kovanen, Altered phospholipid- $\text{apoB}$ -100 interactions and generation of extra membrane material in proteolysis-induced fusion of LDL particles, *J. Lipid Res.* 42 (2001) 916–922.
- [10] R. Pihlari, E. Hurt-Camejo, K. Oorni, P.T. Kovanen, Proteolysis of LDL particles sensitizes them to phospholipolysis by secretory phospholipase A2 group V and secretory sphingomyelinase - a novel mechanism of enhanced LDL retention, *J. Lipid Res.* 51 (2010) 1801–1809.
- [11] K. Oorni, P. Posio, M. Ala-Korpela, M. Jauhiainen, P.T. Kovanen, Sphingomyelinase induces aggregation and fusion of small very low-density lipoprotein and intermediate-density lipoprotein particles and increases their retention to human arterial proteoglycans, *Arterioscler. Thromb. Vasc. Biol.* 25 (2005) 1678–1683.
- [12] S.L. Schissel, J. Tweedie-Hardman, J.H. Rapp, G. Graham, K.J. Williams, I. Tabas, Rabbit aorta and human atherosclerotic lesions hydrolyze the sphingomyelin of retained low-density lipoprotein. Proposed role for arterial-wall sphingomyelinase in subendothelial retention and aggregation of atherogenic lipoproteins, *J. Clin. Invest.* 98 (1996) 1455–1464.
- [13] K. Oorni, M.O. Pentikainen, M. Ala-Korpela, P.T. Kovanen, Aggregation, fusion, and vesicle formation of modified low density lipoprotein particles: molecular mechanisms and effects on matrix interactions, *J. Lipid Res.* 41 (2000) 1703–1714.
- [14] K. Oorni, J.K. Hakala, A. Annala, M. Ala-Korpela, P.T. Kovanen, Sphingomyelinase induces aggregation and fusion, but phospholipase A2 only aggregation, of low density lipoprotein (LDL) particles. Two distinct mechanisms leading to increased binding strength of LDL to human aortic proteoglycans, *J. Biol. Chem.* 273 (1998) 29127–29134.
- [15] S. Lehti, S.D. Nguyen, I. Belevich, H. Vihinen, H.M. Heikkilä, R. Solymani, R. Kakeala, J. Saksi, M. Jauhiainen, G.A. Grabowski, O. Kummus, S. Horkko, M. Baumann, P.J. Lindsberg, E. Jokitalo, P.T. Kovanen, K. Oorni, Extracellular lipids accumulate in human carotid arteries as distinct three-dimensional structures and have proinflammatory properties, *Am. J. Pathol.* 188 (2018) 525–538.
- [16] C. Bancelis, S. Benitez, S. Villegas, O. Jorba, J. Ordonez-Llanos, J.L. Sanchez-Quesada, Novel phospholipolytic activities associated with electronegative low-density lipoprotein are involved in increased self-aggregation, *Biochemistry* 47 (2008) 8186–8194.
- [17] C. Bancelis, S. Villegas, F.J. Blanco, S. Benitez, I. Gallego, L. Beloki, M. Perez-Cuellar, J. Ordonez-Llanos, J.L. Sanchez-Quesada, Aggregated electronegative low density lipoprotein in human plasma shows a high tendency toward phospholipolysis and particle fusion, *J. Biol. Chem.* 285 (2010) 32425–32435.
- [18] J.C. Khoo, E. Miller, P. McLoughlin, D. Steinberg, Prevention of low density lipoprotein aggregation by high density lipoprotein or apolipoprotein A-I, *J. Lipid Res.* 31 (1990) 645–652.
- [19] H. Liu, D.G. Scraba, R.O. Ryan, Prevention of phospholipase-C induced aggregation of low density lipoprotein by amphipathic apolipoproteins, *FEBS Lett.* 316 (1993) 27–33.
- [20] S.D. Nguyen, M. Javanainen, S. Rissanen, H. Zhao, J. Huusko, A.M. Kivela, S. Yla-Herttuala, M. Navab, A.M. Fogelman, I. Vattulainen, P.T. Kovanen, K. Oorni, Apolipoprotein A-I mimetic peptide 4F blocks sphingomyelinase-induced LDL aggregation, *J. Lipid Res.* 56 (2015) 1206–1221.
- [21] M. Navab, G.M. Anantharamaiah, S.T. Reddy, B.J. Van Lenten, A.C. Wagner, S. Hama, G. Hough, E. Bachihi, D.W. Garber, V.K. Mishra, M.N. Palgunachari, A.M. Fogelman, An oral apoJ peptide renders HDL antiinflammatory in mice and monkeys and dramatically reduces atherosclerosis in apolipoprotein E-null mice, *Arterioscler. Thromb. Vasc. Biol.* 25 (2005) 1932–1937.
- [22] S. Park, K.W. Mathis, I.K. Lee, The physiological roles of apolipoprotein J/clusterin in metabolic and cardiovascular diseases, *Rev. Endocr. Metab. Disord.* 15 (2014) 45–53.
- [23] M.R. Wilson, S.B. Easterbrook-Smith, Clusterin is a secreted mammalian chaperone, *Trends Biochem. Sci.* 25 (2000) 95–98.
- [24] M. Calero, T. Tokuda, A. Rostagno, A. Kumar, B. Zlokovic, B. Frangione, J. Ghiso, Functional and structural properties of lipid-associated apolipoprotein J (clusterin), *Biochem. J.* 344 (Pt 2) (1999) 375–383.
- [25] M. Martinez-Bujidos, A. Rull, B. Gonzalez-Cura, M. Perez-Cuellar, L. Montoliu-Gaya, S. Villegas, J. Ordonez-Llanos, J.L. Sanchez-Quesada, Clusterin/apolipoprotein J binds to aggregated LDL in human plasma and plays a protective role against LDL aggregation, *FASEB J* 29 (2015) 1688–1700.
- [26] A. Rull, J. Ordonez-Llanos, J.L. Sanchez-Quesada, The role of LDL-bound apoJ in the development of atherosclerosis, *Clinical Lipidology* 10 (2015) 321–328.
- [27] M. Martinez-Bujidos, A. Rull, B. Gonzalez-Cura, M. Perez-Cuellar, L. Montoliu-Gaya, S. Villegas, J. Ordonez-Llanos, J.L. Sanchez-Quesada, Clusterin/apolipoprotein J binds to aggregated LDL in human plasma and plays a protective role against LDL aggregation, *FASEB J* 29 (2015) 1688–1700.
- [28] V.K. Mishra, M.N. Palgunachari, J.S. Hudson, R. Shin, T.D. Keenum, N.R. Krishna, G.M. Anantharamaiah, Structure and lipid interactions of an anti-inflammatory and anti-atherogenic 10-residue class G(\*) apolipoprotein J peptide using solution NMR, *Biochim. Biophys. Acta* 1808 (2011) 498–507.
- [29] J.L. Sanchez-Quesada, M. Camacho, R. Anton, S. Benitez, L. Vila, J. Ordonez-Llanos, Electronegative LDL of FH subjects: chemical characterization and induction of chemokine release from human endothelial cells, *Atherosclerosis* 166 (2003) 261–270.
- [30] M. Estruch, J.L. Sanchez-Quesada, L. Beloki, J. Ordonez-Llanos, S. Benitez, The induction of cytokine release in monocytes by electronegative low-density lipoprotein (LDL) is related to its higher ceramide content than native LDL, *Int. J. Mol. Sci.* 14 (2013) 2601–2616.
- [31] M. Martinez-Bujidos, A. Rull, B. Gonzalez-Cura, M. Perez-Cuellar, L. Montoliu-Gaya, S. Villegas, J. Ordonez-Llanos, J.L. Sanchez-Quesada, Clusterin/apolipoprotein J binds to aggregated LDL in human plasma and plays a protective role against LDL aggregation, *FASEB J* 29 (2015) 1688–1700.
- [32] J.L. Sanchez-Quesada, S. Benitez, C. Otal, M. Franco, F. Blanco-Vaca, J. Ordonez-Llanos, Density distribution of electronegative LDL in normolipemic and hyperlipemic subjects, *J. Lipid Res.* 43 (2002) 699–705.
- [33] S. Benitez, V. Villegas, C. Bancelis, O. Jorba, F. Gonzalez-Sastre, J. Ordonez-Llanos, J.L. Sanchez-Quesada, Impaired binding affinity of electronegative low-density lipoprotein (LDL) to the LDL receptor is related to nonesterified fatty acids and lysophosphatidylcholine content, *Biochemistry* 43 (2004) 15863–15872.
- [34] R. Brunelli, G. Balogh, G. Costa, M. De Spirito, G. Greco, G. Mei, E. Nicolai, L. Vigh, F. Ursini, T. Parasassi, Estradiol binding prevents ApoB-100 misfolding in electronegative LDL(-), *Biochemistry* 49 (2010) 7297–7302.
- [35] T. Parasassi, G. Bittolo-Bon, R. Brunelli, G. Cazzolato, E.K. Krasnowska, G. Mei, A. Sevanian, F. Ursini, Loss of apoB-100 secondary structure and conformation in hydroperoxide rich electronegative LDL(-), *Free Radic Biol Med* 31 (2001) 82–89.
- [36] R.M. Stoekenbroek, E.S. Stroes, G.K. Hovingh, ApoA-I mimetics, *Handb. Exp. Pharmacol.* 224 (2015) 631–648.
- [37] M.J. Amar, W. D'Souza, S. Turner, S. Demosky, D. Sviridov, J. Stonik, J. Luchoomun, J. Voogt, M. Hellerstein, D. Sviridov, A.T. Remaley, 5A apolipoprotein mimetic peptide promotes cholesterol efflux and reduces atherosclerosis in mice, *J. Pharmacol. Exp. Ther.* 334 (2010) 634–641.
- [38] J.K. Bielicki, H. Zhang, Y. Cortez, Y. Zheng, V. Narayanaswami, A. Patel, J. Johansson, S. Azhar, A new HDL mimetic peptide that stimulates cellular cholesterol efflux with high efficiency greatly reduces atherosclerosis in mice, *J. Lipid Res.* 51 (2010) 1496–1503.
- [39] F. Tabet, A.T. Remaley, A.I. Segaliny, J. Millet, L. Yan, S. Nakhla, P.J. Barter, K.A. Rye, G. Lambert, The 5A apolipoprotein A-I mimetic peptide displays anti-inflammatory and antioxidant properties in vivo and in vitro, *Arterioscler. Thromb. Vasc. Biol.* 30 (2010) 246–252.
- [40] C.E. Watson, N. Weissbach, L. Kjemis, S. Ayalamayajula, Y. Zhang, I. Chang, M. Navab, S. Hama, G. Hough, S.T. Reddy, D. Soffer, D.J. Rader, A.M. Fogelman, A. Schechter, Treatment of patients with cardiovascular disease with L-4F, an apoA1 mimetic, did not improve select biomarkers of HDL function, *J. Lipid Res.* 52 (2011) 361–373.
- [41] J. Andrews, A. Janssan, T. Nguyen, A.D. Pisanelli, D.J. Scherer, J.J. Kastelein, B. Merkely, S.E. Nissen, K. Ray, G.G. Schwartz, S.G. Worthley, C. Keyserling, J.L. Dasseux, J. Butters, J. Girardi, R. Miller, S.J. Nicholls, Effect of serial infusions of reconstituted high-density lipoprotein (CER-001) on coronary atherosclerosis: rationale and design of the CARAT study, *Cardiovasc Diagn Ther* 7 (2017) 45–51.
- [42] J.C. Tardif, C.M. Ballantyne, P. Barter, J.L. Dasseux, Z.A. Fayad, M.C. Guertin, J.J. Kastelein, C. Keyserling, H. Klepp, W. Koenig, P.L. L'Allier, J. Lesperance, T.F. Lüscher, J.F. Paolini, A. Tawakol, D.L. Waters, Can HDL Infusions Significantly Quicken Atherosclerosis REgression (CHI-SQUARE) Investigators. Effects of the high-density lipoprotein mimetic agent CER-001 on coronary atherosclerosis in patients with acute coronary syndromes: a randomized trial, *Eur. Heart J.* 35 (46) (2014 Dec 7) 3277–3286.
- [43] I. Karalis, J.W. Jukema, HDL mimetics infusion and regression of atherosclerosis: is it still considered a valid therapeutic option? *Curr. Cardiol. Rep.* 20 (2018) 66.
- [44] M. Ditiatkovski, J. Palsson, J. Chin-Dusting, A.T. Remaley, D. Sviridov, Apolipoprotein A-I mimetic peptides: discordance between in vitro and in vivo properties-brief report, *Arterioscler. Thromb. Vasc. Biol.* 37 (2017) 1301–1306.
- [45] G. Datta, M. Chaddha, S. Hama, M. Navab, A.M. Fogelman, D.W. Garber, V.K. Mishra, R.M. Epanand, R.F. Epanand, S. Lund-Katz, M.C. Phillips, J.P. Segrest, G.M. Anantharamaiah, Effects of increasing hydrophobicity on the physical-chemical and biological properties of a class A amphipathic helical peptide, *J. Lipid Res.* 42 (2001) 1096–1104.
- [46] D.W. Garber, G. Datta, M. Chaddha, M.N. Palgunachari, S.Y. Hama, M. Navab, A.M. Fogelman, J.P. Segrest, G.M. Anantharamaiah, A new synthetic class A amphipathic peptide analogue protects mice from diet-induced atherosclerosis, *J. Lipid Res.* 42 (2001) 545–552.
- [47] L.A. Bagatoli, T. Parasassi, G.D. Fidelfio, E. Gratton, A model for the interaction of 6-lauroyl-2-(N,N-dimethylamino)naphthalene with lipid environments: implications for spectral properties, *Photochem. Photobiol.* 70 (1999) 557–564.





## PUBLICATION 2

Subcutaneous Administration of Apolipoprotein J-Derived Mimetic Peptide D-[113-122]apoJ Improves LDL and HDL Function and Prevents Atherosclerosis in LDLR-KO Mice



Article

# Subcutaneous Administration of Apolipoprotein J-Derived Mimetic Peptide D-[113–122]apoJ Improves LDL and HDL Function and Prevents Atherosclerosis in LDLR-KO Mice

Andrea Rivas-Urbina <sup>1,2,†</sup> , Anna Rull <sup>1,3,†</sup> , Joile Aldana-Ramos <sup>1</sup>, David Santos <sup>4,5</sup> , Nuria Puig <sup>1</sup>, Nuria Farre-Cabrerizo <sup>4</sup>, Sonia Benitez <sup>1</sup>, Antonio Perez <sup>5,6</sup> , David de Gonzalo-Calvo <sup>7,8</sup> , Joan Carles Escola-Gil <sup>4,5</sup> , Josep Julve <sup>4,5</sup> , Jordi Ordoñez-Llanos <sup>1,2</sup>  and Jose Luis Sanchez-Quesada <sup>1,5,\*</sup> 

<sup>1</sup> Cardiovascular Biochemistry Group, Research Institute of the Hospital de Sant Pau (IIB Sant Pau), 08041 Barcelona, Spain; arivas@santpau.cat (A.R.-U.); anna.rull@iispv.cat (A.R.); joile.aldana@gmail.com (J.A.-R.); npuigg@santpau.cat (N.P.); sbenitez@santpau.cat (S.B.); jordonez@santpau.cat (J.O.-L.)

<sup>2</sup> Biochemistry and Molecular Biology Department, Universitat Autònoma de Barcelona, 08193 Cerdanyola, Spain

<sup>3</sup> Hospital Universitari Joan XXIII, IISPV, Universitat Rovira i Virgili, 43005 Tarragona, Spain

<sup>4</sup> Molecular Basis of Cardiovascular Risk, Research Institute of the Hospital de Sant Pau (IIB Sant Pau), 08041 Barcelona, Spain; dsantos@santpau.cat (D.S.); farre.nuria88@gmail.com (N.F.-C.); jescola@santpau.cat (J.C.E.-G.); jjulve@santpau.cat (J.J.)

<sup>5</sup> CIBER of Diabetes and Metabolic Diseases (CIBERDEM), Institute of Health Carlos III, 28029 Madrid, Spain; aperez@santpau.cat

<sup>6</sup> Endocrinology Department, Hospital de la Santa Creu i Sant Pau, 08041 Barcelona, Spain

<sup>7</sup> Translational Research in Respiratory Medicine, University Hospital Arnau de Vilanova and Santa Maria, IRBLleida, 25198 Lleida, Spain; David.degonzalo@gmail.com

<sup>8</sup> CIBER of Respiratory Diseases (CIBERES), Institute of Health Carlos III, 28029 Madrid, Spain

\* Correspondence: jsanchezq@santpau.cat; Tel.: +34-35537588

† Both authors contributed equally to this work.

Received: 2 April 2020; Accepted: 21 May 2020; Published: 29 May 2020



**Abstract:** Mimetic peptides are potential therapeutic agents for atherosclerosis. D-[113–122]apolipoprotein (apo) J (D-[113–122]apoJ) is a 10-residue peptide that is predicted to form a class G<sup>\*</sup> amphipathic helix 6 from apoJ; it shows anti-inflammatory and anti-atherogenic properties. In the present study, we analyzed the effect of D-[113–122]apoJ in low-density lipoprotein receptor knockout mice (LDLR-KO) on the development of atherosclerosis and lipoprotein function. Fifteen-week-old female LDLR-KO mice fed an atherogenic Western-type diet were treated for eight weeks with D-[113–122]apoJ peptide, a scrambled peptide, or vehicle. Peptides were administered subcutaneously three days per week (200 µg in 100 µL of saline). After euthanasia, blood and hearts were collected and the aortic arch was analyzed for the presence of atherosclerotic lesions. Lipoproteins were isolated and their composition and functionality were studied. The extent of atherosclerotic lesions was 43% lower with D-[113–122]apoJ treatment than with the vehicle or scramble. The lipid profile was similar between groups, but the high-density lipoprotein (HDL) of D-[113–122]apoJ-treated mice had a higher antioxidant capacity and increased ability to promote cholesterol efflux than the control group. In addition, low-density lipoprotein (LDL) from D-[113–122]apoJ-treated mice was more resistant to induced aggregation and presented lower electronegativity than in mice treated with D-[113–122]apoJ. Our results demonstrate that the D-[113–122]apoJ peptide prevents the extent of atherosclerotic lesions, which could be partially explained by the improvement of lipoprotein functionality.

**Keywords:** mimetic peptide; atherosclerosis; lipoprotein function; apolipoprotein J; LDL; HDL; mice

---

## 1. Introduction

Cardiovascular disease (CVD) is the leading cause of mortality worldwide; coronary artery disease of atherosclerotic origin is the most common expression of CVD. Plasma lipid levels are a major cause for the development of atherosclerotic lesions and, accordingly, lipid-lowering drugs are the main therapeutic strategy for decreasing cardiovascular risk [1]. However, even with normal lipid levels and in the absence of other classical CVD risk factors, such as hypertension, diabetes, obesity or smoking habits, cardiovascular events can occur. This is known as residual cardiovascular risk, and part of this risk is of lipid origin [2]. This is because the development of atherosclerosis does not come only from high lipid levels but it is also determined by the quality and functionality of lipoproteins. Low-density lipoproteins (LDL) are the main source of the cholesterol that accumulates in the arterial wall. The aggregation of these lipoprotein particles in the subendothelial space is the necessary first step to promote their entrapment in the artery wall and their chemical modification by different mechanisms, including oxidation, lipolysis, and proteolysis [3]. Oxidative modification of lipids in lipoproteins is a key event that triggers the inflammatory process that perpetuates atherosclerosis [4]. Regarding high-density lipoproteins (HDL), these particles play a protective role against atherosclerotic development through several mechanisms that include, among others, the reverse transport of the cholesterol accumulated in arterial lesions and the inhibition of the oxidative modification of LDL [5]. Indeed, increased susceptibility of LDL to oxidation or to aggregation [6], as well as a loss of the protective properties of HDL, has been related to accelerated atherosclerosis [7].

Accordingly, therapies targeting the function and qualitative properties of lipoproteins could help to decrease the residual cardiovascular risk, which persists even after statin treatment [8]. Interest in using peptides has been aroused for a few years. These short peptides are directly derived from the sequence of apolipoproteins (apo) or have another amino acid sequence that mimics their conformation of amphipathic helices [9]. Most studies have analyzed the effects of peptides derived from apolipoprotein A-I (apoA-I) and apolipoprotein E (apoE) [10,11], although other apolipoprotein mimetic peptides, such as apolipoprotein C-II (apoC-II) [12] or apolipoprotein J (apoJ) [13], have also been used. The main mechanisms of action of apoA-I and apoE mimetics are theoretically different, since apoE mimetics mediate hepatic clearance of atherogenic apoB-containing lipoproteins from the circulation via interaction with lipoprotein receptors, whereas apoA-I mimetics mainly stimulate the reverse cholesterol transport pathway [11]. Additionally, apoE mimetics enhance cholesterol efflux from cholesterol-loaded macrophages [14]. However, both groups of mimetics have also shown anti-inflammatory and antioxidant properties, avoiding the oxidation of LDL by sequestering lipoperoxides [11]. In both cases, the administration of these peptides has been successful for atherosclerosis prevention in animal models [15–17]. However, clinical trials conducted in humans with HDL mimetics have failed to demonstrate a clinical benefit [18]. One possibility that could explain the lack of positive results is the fact that targeting only HDL function could not be enough to prevent the development of atherosclerosis in humans, since, in contrast to mice, LDL is the main transporter of cholesterol in humans. So far there are no data from clinical trials carried out with apoE mimetics.

Despite the relevance of LDL aggregation in the earliest stages of atherogenesis, no specific therapeutic strategies targeting this process have been successfully developed. Compelling evidence supports the potential therapeutic use of mimetic peptides as potential agents to prevent LDL aggregation. Indeed, 4F, a mimetic of apoA-I, was reported to inhibit LDL aggregation *in vitro* [19]. Another peptide that has been shown to inhibit LDL aggregation *in vitro* is D-[113–122]apoJ, a mimetic derived from the sequence of apoJ [20]. This peptide is a 10-residue peptide spanning the predicted class G\* amphipathic helix 6 from apoJ and has been successfully used to retard atherosclerosis in apoE-knockout mice, which was attributed to its capacity to improve the anti-inflammatory properties

of HDL [13]. Our group previously described that both the whole molecule of apoJ [21] and the peptide D-[113–122]apoJ [22] inhibit SMase-induced and spontaneous LDL aggregation *in vitro*. Based on these observations, the aim of the present study was to analyze the effect of the D-[113–122]apoJ peptide on lipoprotein function and the development of atherosclerosis. For this purpose, we used LDLR-KO mice fed an atherogenic diet, a model that, in contrast to other murine models of accelerated atherosclerosis, generates abundant lipoprotein particles similar in size and density to human LDL [23]. This allowed us to test not only the effect of treatment on HDL function but also on LDL susceptibility to aggregation and their relationship with atherosclerosis.

## 2. Materials and Methods

### 2.1. Animal Study Design

LDLR-KO mice from the C57BL/6 background were purchased from Jackson Laboratories (#002207). Mice were housed in a controlled temperature environment (22 °C), exposed to a 12-h light/dark cycle, and food and water were provided *ad libitum*. For this study, we used 15-week-old female mice fed a Western diet (WD) (TD.88137, Harlan Teklad, Madison, WI, USA, containing 21% fat and 0.2% cholesterol) for eight weeks. The reason for using females is that the development of atherosclerosis is higher in female than in male mice [24]. Animals were randomly assigned to one of three groups and treated for eight weeks with the D-[113–122]apoJ peptide ( $n = 12$ ), scrambled peptide ( $n = 8$ ) or vehicle (control,  $n = 8$ ). Peptides (10 µg/g body weight) were administered subcutaneously three days per week (200 µg in 100 µL of saline). Weight control and food intake were monitored for all experimental groups (Supplementary Figure S1). Animals were sacrificed after eight weeks of treatment. After euthanasia, fasting blood, heart, and liver were collected. Figure S2 depicts a flow chart of the experimental design. All animal procedures were conducted in accordance with published regulations and were approved by the Institutional Animal Care Committee of the Institut de Recerca of the Hospital de la Santa Creu i Sant Pau (ref. 9375).

### 2.2. Peptides

The amino acid sequence of the D-[113–122]apoJ peptide is Ac-LVGRQLEEFL-NH<sub>2</sub>. This peptide forms a class G\* amphipathic helix in the presence of lipids [20]. The inactive control scrambled peptide (Sc-D-[113–122]apoJ) has the same overall amino acid composition as D-[113–122]apoJ but in a sequence that prevents G\* amphipathic helix formation (Ac-LRGVQLLEFE-NH<sub>2</sub>). Both peptides were obtained from Caslo (Kongens Lyngby, Denmark). The use of D-peptides guarantees the resistance to proteolysis in the blood since these are less susceptible to proteolytic degradation in the digestive tract or inside cells [25]. Navab et al. reported that D-[113–122]apoJ was poorly associated with lipoproteins and mostly remained in the fraction of lipoprotein-deficient plasma during the first hours in blood. Then, the peptide progressively tended to associate with lipoprotein fractions, showing a prolonged residence-time since D-[113–122]apoJ was cleared from plasma much more slowly than peptides derived from apoA-I [13].

### 2.3. Lipid Analysis

Plasma lipid profile and lipoprotein composition of major lipids were measured by commercial methods adapted to a Cobas 6000/c501 autoanalyzer (Roche Diagnostics, Basel, Switzerland). Total cholesterol, triglycerides, aspartate transaminase (AST), and alanine transaminase (ALT) reagents were obtained from Roche Diagnostics. Total phospholipids, non-esterified fatty acids (NEFAs), and free cholesterol reagents were obtained from Wako Chemicals (Richmond, VA, USA). Cholesterol, triglycerides, and phospholipid content in livers was determined by commercial methods adapted to a Cobas 6000/c501 autoanalyzer (Roche Diagnostics, Basel, Switzerland) after solvent extraction [26]. Briefly, liver lipids were extracted with isopropyl alcohol-hexane (2:3, *v/v*). The lipid layer was evaporated and resuspended in 0.5% (*w/v*) sodium cholate (Serva, Heidelberg, Germany).



#### 2.4. Lipoprotein Isolation and Characterization

VLDL (density <1.019 g/mL), LDL (density 1.019–1.063 g/mL), and HDL (density 1.063–1.210 g/mL) were isolated from mice plasma by sequential ultracentrifugation, using potassium bromide for density adjustment, at  $100,000\times g$  for 24 h with an analytical fixed-angle rotor (50.3, Beckman Coulter, Fullerton, CA, USA) [27]. Lipoprotein composition of major lipids was measured by commercial methods adapted to a Cobas 6000/c501 autoanalyzer, as described above. The protein content of each lipoprotein was assessed by the Pierce™ BCA Protein Assay (Thermo Fisher Scientific, Rockford, IL, USA).

#### 2.5. Susceptibility to Oxidation of Lipoproteins

Mice LDL and HDL susceptibility to copper-induced lipid oxidation and mice HDL capacity to inhibit the oxidative modification of human LDL were measured by monitoring the formation of conjugated dienes at 234 nm, for 7 h at 37 °C in a BioTek Synergy HT spectrophotometer (BioTek Synergy, Winooski, VT, USA) [28]. Briefly, LDL was dialyzed in phosphate-buffered saline by gel filtration chromatography on PD-10 columns (GE Healthcare, Chicago, IL, USA) and HDL was dialyzed by Dialysis Cassettes G2 (Thermo Fisher Scientific, Rockford, IL, USA). Oxidation was started by adding 2.5  $\mu\text{mol/L}$   $\text{CuSO}_4$  in wells containing mice LDL, mice HDL alone or mice HDL in the presence of human LDL (0.1 mmol/L cholesterol in all cases). The maximum slope during the propagation phase of the kinetics was the parameter used to estimate the susceptibility of lipoproteins to oxidation. The antioxidant capacity of HDL was expressed as the ability to decrease the slope of the oxidation kinetics of human LDL alone after the subtraction of the kinetics of mice HDL alone, as previously described [29].

#### 2.6. Susceptibility to LDL Aggregation

Aggregation of mice LDL was induced by SMase lipolysis. Mice LDL (0.6 mmol/L cholesterol) dialyzed in phosphate-buffered saline was incubated at 37 °C for 2 h with SMase from *Bacillus cereus* sp. (Sigma Diagnostics, Livonia, MI, USA) with a final concentration of 50 mU/mL in the presence of 2 mM  $\text{CaCl}_2$  and 2 mM  $\text{MgCl}_2$ . Size-exclusion chromatography (SEC) was performed for monitoring aggregation using a Superose 6 Increase 5/150 GL column in an AKTA-FPLC system (GE Healthcare), as described [21]. Two hundred  $\mu\text{L}$  of LDL was injected in the column, eluted at a flow rate of 0.3 mL/min, and peaks were detected at 280 nm. This chromatography discriminates two peaks of LDL, eluting first aggregated LDL (2.5 mL) and later monomeric LDL (3.1 mL).

#### 2.7. Electronegativity of LDL

The electric charge of LDL was determined by anion exchange chromatography. Chromatography was conducted in an ÄKTA-FPLC system (GE Healthcare), using a MonoQ 5/50 GL column (GE Healthcare). LDL isolated from mice (0.4 mmol/L cholesterol) was dialyzed against buffer A (Tris 10 mmol/L, EDTA 1 mmol/L, pH 7.4) and 100  $\mu\text{L}$  was injected in the column at a flow rate of 2 mL/min. Two fractions of LDL (native or LDL(+) and modified or LDL(-)) were separated with a stepwise NaCl gradient using buffer A and buffer B (same composition as buffer A containing 1 M NaCl). This gradient was similar to that previously described [30], except that both LDL fractions in mice eluted at a higher ionic strength than human LDL. Accordingly, LDL(+) eluted at 35% buffer B while LDL(-) eluted at 70% buffer B. The percentage of these fractions was calculated from the 280 nm peak area integration.

#### 2.8. Cholesterol Efflux Capacity of HDL

In vitro cellular cholesterol efflux induced by HDL was determined using [ $^3\text{H}$ ]cholesterol-labeled J774A.1 mouse macrophages (ATCC® TIB67™, Manassas, VA, USA), as previously described [31]. Briefly,  $1.5 \times 10^5$  cells/well were seeded in 6-well plates and allowed to grow for three days in RPMI 1640 medium containing 2 mM L-Glutamine (Pan Biotech, Aidenbach, Germany) complemented with

10% fetal bovine serum (FBS) (Pan Biotech) and 100 U/mL penicillin/streptomycin (Dominique Dutscher, Brumath, France). After that, cells were labeled for 60 h in the presence of one  $\mu\text{Ci}$ /well of [ $1\alpha,2\alpha(n)$ - $^3\text{H}$ ]cholesterol (GE Healthcare, Little Chalfont, UK) and 5% FBS. The cells were then equilibrated with 0.2% bovine serum albumin (BSA) in medium overnight and incubated for 4 h with mice HDL (25  $\mu\text{g}/\text{mL}$  protein), previously isolated by ultracentrifugation and dialyzed in phosphate-buffered saline, as described above. Radioactivity was measured in both the medium and the cells, and the percentage of cholesterol efflux was calculated.

## 2.9. Evaluation of Atherosclerotic Lesions

The proximal aorta in each mouse was isolated, embedded in optimal cutting temperature (OCT) (VWR, Fontenay-sous-Bois, France), and immediately flash frozen. The proximal aorta was serial sectioned, and eight sections were stained for lipids with Oil red O. Atherosclerotic lesion severity was expressed as the area of positive Oil red O staining in four sections separated by 80  $\mu\text{m}$ . The first section was taken 80  $\mu\text{m}$  distal to the point placed between the end of the aortic sinus and the beginning of the aorta. The lesion area (surface area stained with Oil red O) was quantified using AxioVision V 4.8.1.0 image analysis software (Zeiss, Oberkochen, Germany).

## 2.10. Quantitative RT-PCR Analyses

Total liver RNA was obtained using TRIzol LS reagent (Invitrogen, Carlsbad, CA, USA) and was purified with an EZ-10 DNAaway RNA Miniprep Kit (Bio Basic, Markham, ON, Canada). cDNA was generated using EasyScript First-Strand cDNA Synthesis SuperMix (Transgen Biotech, Beijing, China) and quantitative real-time PCR amplification was performed using the GoTaq(R) Probe qPCR Master Mix (Promega, Madison, WI, USA). Specific TaqMan probes (Applied Biosystems, Foster City, CA, USA) were used for *Tnfa* (Mm99999068\_m1), *Ccl2* (Mcp1, Mm0441242\_m1), *Cd36* (Mm00432403\_m1), and *Cd68* (Mm03047343\_m1); *Gapdh* (Mm99999915\_g1) was used as the control housekeeping gene. Reactions were run on a CFX96TM Real-Time System (Bio-Rad, Hercules, CA, USA) according to the manufacturer's instructions. The relative mRNA expression levels were calculated using the  $\Delta\Delta C_t$  formula.

## 2.11. Statistical Methods

GraphPad Prism 6.0 software (GraphPad, San Diego, CA, USA) and the statistical software package R version 3.5.2 ([www.r-project.org](http://www.r-project.org)) were used to perform statistical analyses. Student's *t*-test was used to compare the differences between two groups. Two-way ANOVA with Tukey's multiple comparisons post-test was used to compare more than two groups. To analyze the association between atherosclerosis and parameters of lipoprotein function, Spearman's rho correlation was used, considering all variables as non-parametric. Linear regression analyses were performed to explore potential confounding. Data are expressed as the standardized beta coefficient ( $\beta$ ). A *p*-value < 0.05 was considered statistically significant.

## 3. Results

### 3.1. Subcutaneous Administration of $\text{D}$ -[113–122]apoJ Reduces Atherosclerosis

After the atherogenic diet,  $\text{D}$ -[113–122]apoJ-treated mice developed less extensive aortic atherosclerosis than control and scramble-treated mice. Figure 1a shows the mean size of atherosclerotic lesions in four consecutive sections of the proximal aorta. The area of proximal atherosclerosis in  $\text{D}$ -[113–122]apoJ-treated mice was 40%–45% lower ( $55,305 \pm 19,155 \mu\text{m}^2/\text{section}$ ) than in control ( $92,549 \pm 18,880 \mu\text{m}^2/\text{section}$ ) or scramble ( $97,144 \pm 36,140 \mu\text{m}^2/\text{section}$ ) mice. Representative examples of the lesions observed in each group are shown in Figure 1b (Control), Figure 1c (Scramble), and Figure 1d ( $\text{D}$ -[113–122]apoJ peptide). These images also showed that mice treated with the apoJ



peptide developed less advanced atherosclerotic lesions and more restricted aortic valve attachments compared with the larger lesions that extended to the free aortic wall in both Control and Scramble mice.

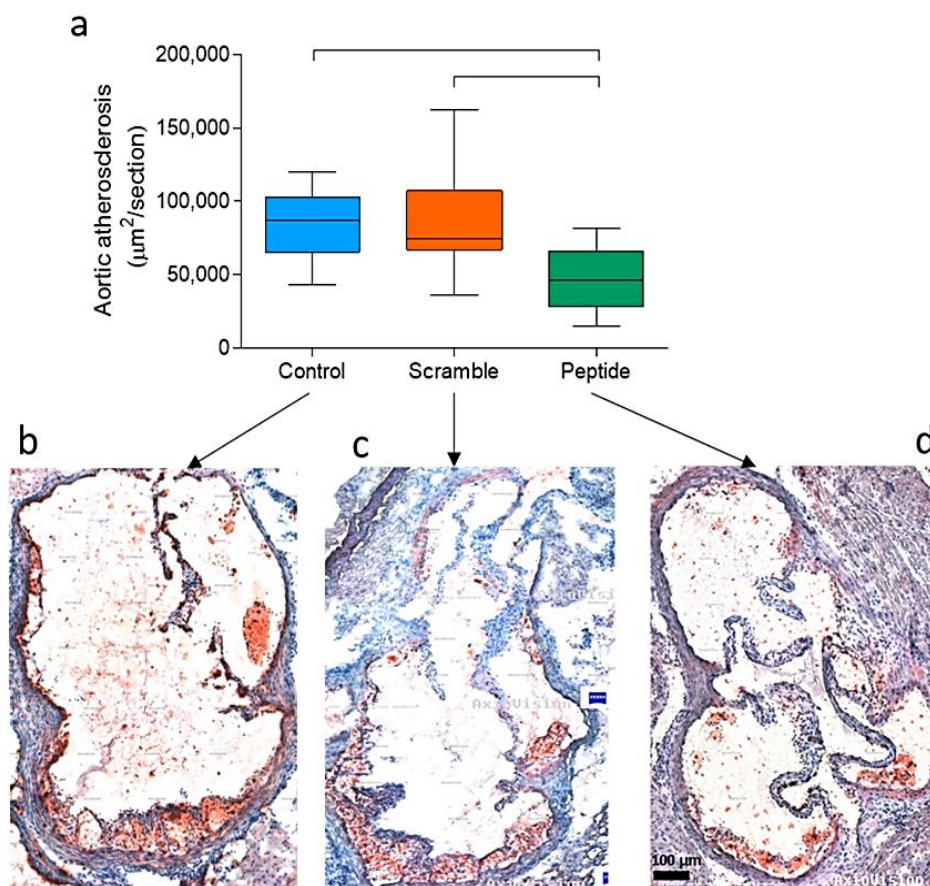


**Figure 1.** Evaluation of atherosclerotic lesions. Fifteen-week-old female low-density lipoprotein receptor knockout mice (LDLR-KO) mice fed an atherogenic Western-type diet were treated for eight weeks with the  $\text{D}$ -[113–122]apoJ peptide ( $n = 12$ ), scrambled peptide ( $n = 8$ ) or vehicle (control,  $n = 8$ ). Peptides were administered subcutaneously three days every week (200  $\mu\text{g}$  in 100  $\mu\text{L}$  of saline), as described in the Methods. After euthanasia, hearts were collected, embedded in optimal cutting temperature (OCT) compound, and the aortic arch was sectioned every 20  $\mu\text{m}$ . Lesion areas were stained with Oil red O, and the surface size was quantified using AxioVision image analysis software. (a) Lesion size in four consecutive sections of the proximal aorta. Data are shown as box-plot graphs. Bars indicate  $p < 0.05$  vs. control or scramble mice. (b–d) are representative lesions of mice treated with vehicle, scramble or  $\text{D}$ -[113–122]apoJ peptide, respectively.

### 3.2. $\text{D}$ -[113–122]apoJ Did Not Alter the Lipid Profile

Table 1 shows the main biochemical parameters of LDLR-KO mice after eight weeks on a Western diet. This atherogenic diet promoted strong hyperlipidemia with very high levels of total plasma cholesterol, triglycerides, and phospholipids in LDLR-KO mice. Most of the cholesterol was associated with VLDL and LDL, and approximately only 7–8% of cholesterol was transported by HDL when lipoproteins were isolated by ultracentrifugation. However, no statistical difference in the parameters of the lipid profile was observed between groups, with very similar levels of triglycerides, phospholipids, and cholesterol (Table 1). This was confirmed when the lipoprotein profile was determined by size

exclusion chromatography (Figure 2). The chromatographic profiles overlapped in the three groups based on the absorbance at 280 nm or the cholesterol in the collected fractions.

**Table 1.** Lipid profile and hepatic parameters of low-density lipoprotein receptor knockout mice (LDLR-KO) after eight weeks on a western diet.

	Controls	Scramble	D-[113–122]apoJ
Total cholesterol (mM)	52.5 ± 8.2	50.7 ± 7.7	51.9 ± 7.6
VLDL-c (mM)	39.3 ± 8.2	36.5 ± 7.5	34.9 ± 8.0
LDL-c (mM)	9.6 ± 2.0	10.4 ± 3.8	13.6 ± 4.0
HDL-c (mM)	3.5 ± 1.5	3.3 ± 0.9	3.5 ± 1.8
Triglycerides (mM)	9.6 ± 2.2	7.8 ± 3.1	7.9 ± 3.5
Phospholipids (mM)	10.8 ± 0.5	10.6 ± 1.5	10.2 ± 1.8
AST (U/L)	107.4 ± 71.4	110.3 ± 70.9	86.8 ± 47.6
ALT (U/L)	29.3 ± 20.2	38.4 ± 25.5	22.1 ± 11.0
Liver weight (g)	1.48 ± 0.23	1.34 ± 0.32	1.33 ± 0.22
Liver cholesterol (μmol/g liver)	9.50 ± 4.67	11.57 ± 4.25	10.84 ± 3.63
Liver triglycerides (μmol/g liver)	12.42 ± 3.98	15.43 ± 3.05	11.51 ± 3.89
Liver phospholipids (μmol/g liver)	4.62 ± 1.97	4.30 ± 1.75	4.64 ± 1.43

Data are expressed as mean ± SD, *n* = 8 (controls and scramble), *n* = 12 (peptide). VLDL: very-low-density lipoprotein, LDL: low-density lipoprotein, HDL: high-density lipoprotein, AST: aspartate transaminase, ALT: alanine transaminase, SD: standard deviation.

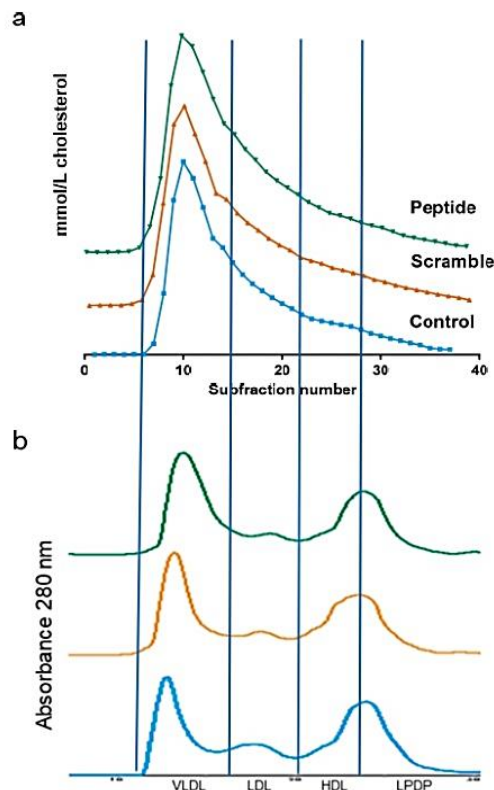


**Figure 2.** Representative lipoprotein profile determined by size exclusion chromatography, as described in the Methods. Briefly, 400 μL of plasma was injected in a Superose 6 column and eluted with an isocratic buffer at 0.5 mL/min. Fractions (100 μL) were collected and tested for the cholesterol content. (a) Cholesterol profile. (b) Ultraviolet (UV) 280 nm profile. Vertical lines indicate the volumes at which VLDL, LDL, HDL, and lipoprotein-deficient plasma (LPDP) eluted.

Regarding liver parameters, no evidence of hepatic injury was observed in any of the groups, and the liver weights were similar among groups (Table 1). Accordingly, the content of cholesterol or triglycerides in livers was also similar in all groups (Table 1).

Regarding the composition of isolated lipoproteins, no statistically significant difference was detected between groups with respect to LDL. The VLDL of the control group presented an increased triglyceride content compared with scramble or peptide groups (Figure 3). We also observed an increased content of free cholesterol in HDL of mice treated with the peptide compared to control and scramble groups.

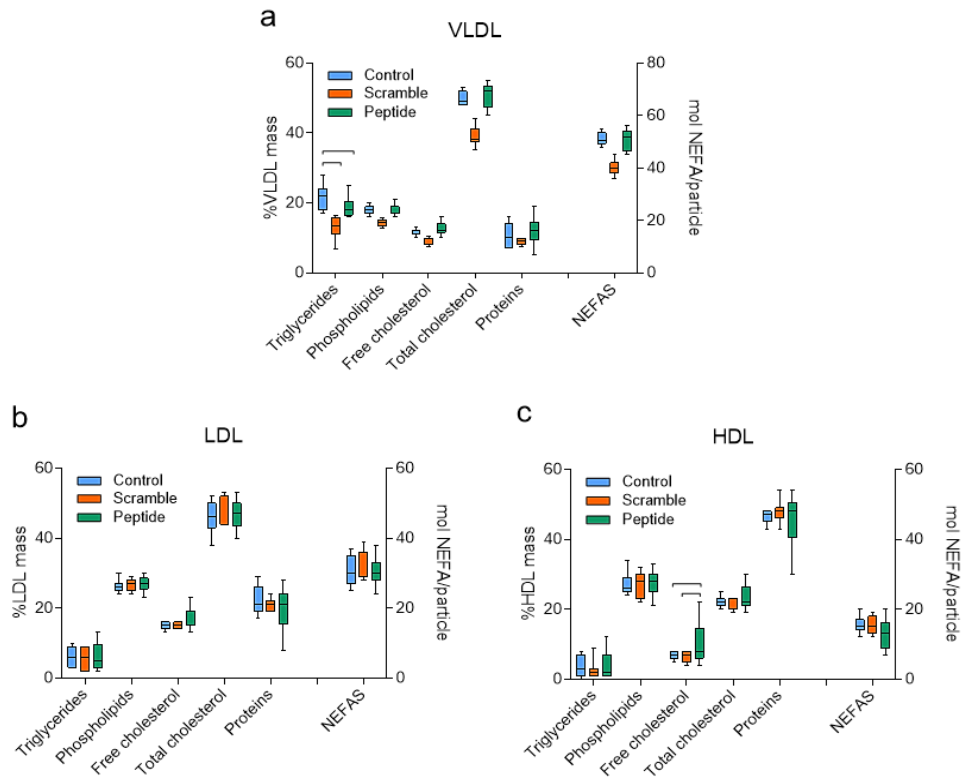


**Figure 3.** Lipoprotein composition. (a) VLDL, (b) LDL, (c) HDL. Each graph shows the relative mass of each major component (triglycerides, phospholipids, free cholesterol, total cholesterol, and proteins) and the amount in moles per lipoprotein particle of the non-esterified fatty acids (NEFAS). Data are shown as box-plot graphs,  $n = 8$  (controls and scramble),  $n = 12$  (peptide). Bars indicate  $p < 0.05$  vs. other groups.

### 3.3. $D$ -[113–122]apoJ Favorably Influences the Oxidative Properties of Lipoproteins

The oxidizability of LDL was determined by monitoring the kinetics of LDL oxidation induced by  $\text{CuSO}_4$ , measuring the conjugated diene formation at 234 nm. Data are expressed as the mean increase in absorbance per minute, instead of the classical lag phase time because, unlike human LDL, murine LDL does not follow the characteristic sigmoidal curve but rather presents a continuous increase in absorbance. This assay showed that all groups had similar LDL susceptibility to oxidation (Figure 4a,b). HDL susceptibility to oxidation was measured from the maximum slope of the oxidation kinetics. In contrast to LDL, HDL susceptibility to oxidation was significantly lower in mice treated with  $D$ -[113–122]apoJ than in control or scramble mice (Figure 4c,d). Moreover, HDL from  $D$ -[113–122]apoJ-mice presented a higher capacity to retard the oxidation of human LDL than HDL from the other two groups (Figure 4e,f), as can be deduced from the decreased increase in absorbance



at a maximum slope of the propagation phase. These data indicate that although the oxidative properties of LDL were similar among groups, the antioxidative action of HDL was potentiated in D-[113–122]apoJ-treated mice.

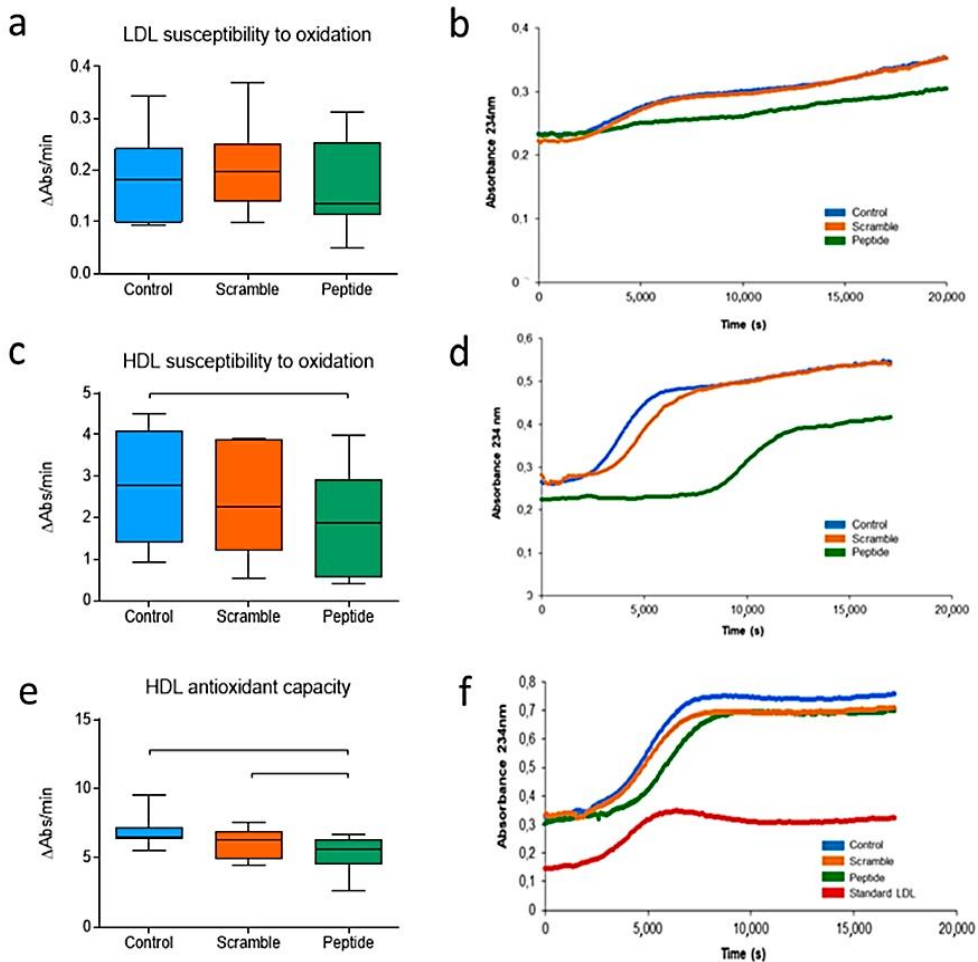


**Figure 4.** Oxidation-related parameters. Oxidation of lipoproteins dialyzed in PBS was induced by adding 5  $\mu$ M  $\text{CuSO}_4$  and was monitored at 234 nm. (a) LDL susceptibility to oxidation. Data are expressed as the increase in the absorbance per minute. (b) Representative kinetics of LDL oxidation. (c) HDL susceptibility to oxidation. Data are expressed as the increase in absorbance per minute during the phase of maximal slope, mean  $\pm$  SEM. (d) Representative kinetics of HDL oxidation. (e) Protective effect of HDL on LDL oxidation. Data are expressed as the increase in absorbance per minute during the maximal slope phase. (f) Representative kinetics of human LDL + murine HDL oxidation. Data in (a,c,e) are shown as box-plot graphs,  $n = 7$  in control and scramble groups,  $n = 10$  in the peptide group. Bars indicate  $p < 0.05$  vs. other groups.

To test if the observed effects of the D-[113–122]apoJ peptide on lipoprotein oxidation were due to a direct action of the peptide on the surface of lipoproteins, we performed oxidation kinetics using human LDL, HDL or LDL + HDL under the same conditions described above, adding increasing amounts of D-[113–122]apoJ (peptide/apoB or peptide/apoA-I molar ratios of 1/10, 1/1, and 10/1). No direct effect of the peptide was observed (Supplementary Figure S3). This suggests that the ability of D-[113–122]apoJ to increase the antioxidant capacity of HDL could be due to secondary alterations in HDL metabolism rather than to a primary effect of the peptide.

### 3.4. D-[113–122]apoJ Decreases the Susceptibility of LDL to Aggregation

The aggregation of LDL was induced by incubation with SMase and was measured by size-exclusion chromatography, as indicated in the Methods. The basal proportion of aggregated LDL particles (without SMase treatment) was similar in all groups. LDL SMase-induced aggregation assay showed that LDL isolated from mice treated with the D-[113–122]apoJ peptide was less prone to aggregate than LDLs isolated from the control or scramble groups (Figure 5a). Figure 5b shows a representative size-exclusion chromatogram after the induction of LDL aggregation by SMase.

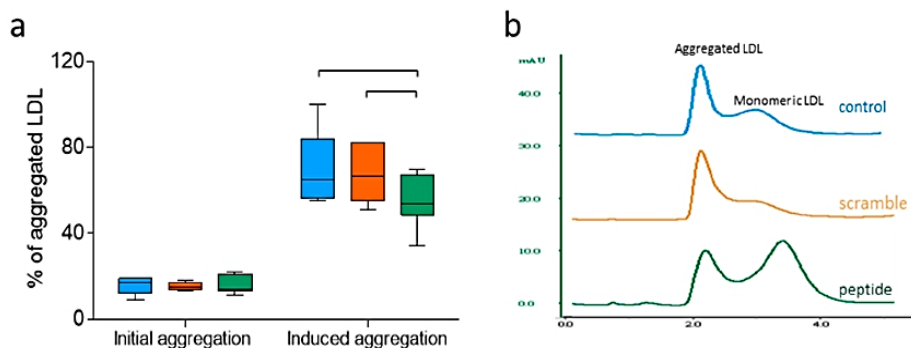


**Figure 5.** LDL susceptibility to aggregation. Susceptibility to aggregation experiments were conducted as indicated in the Methods. The degree of aggregation was estimated by size exclusion chromatography in a Superose 6 column, and the percentage of aggregated LDL particles was determined by quantifying the area of the eluted peaks corresponding to aggregated and non-aggregated LDL subfractions. (a) Percentage of aggregated LDL. Data are shown as box-plot graphs,  $n = 7$  in control and scramble groups,  $n = 10$  in the peptide group. Bars indicate  $p < 0.05$  vs. other groups. (b) Representative chromatograms of LDLs from each group after aggregation.

### 3.5. Electronegativity of LDL Decreased upon D-[113–122]apoJ Treatment

The electronegativity of LDL was determined by anion-exchange chromatography separating LDL subfractions according to their electric negative charge, as indicated in the Methods. LDL from D-[113–122]apoJ-treated mice had a lower proportion of the most electronegative subfraction (LDL(-)) than control or scramble-treated mice (Figure 6). This observation was not due to a direct effect of D-[113–122]apoJ on the LDL particle since *in vitro* addition of the peptide to human LDL did not increase the electric charge of LDL (data not shown).

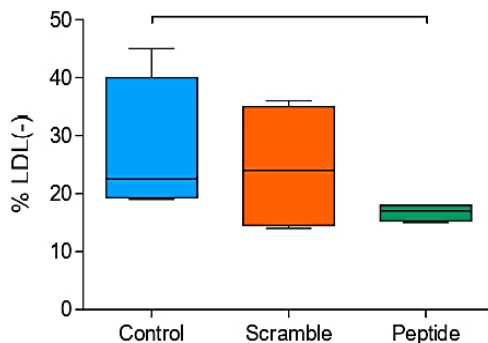


**Figure 6.** Electric charge of LDL. LDL dialyzed in buffer A was chromatographed in a MonoQ anion-exchange column, as described in the Methods. Data are expressed as the proportion of the electronegative LDL fraction. Data are shown as box-plot graphs,  $n = 4$  in each group. Bars indicate  $p < 0.05$  vs. other groups.

### 3.6. D-[113–122]apoJ Improves the Cholesterol Efflux Capacity of HDL

The ability of HDL to enhance cholesterol efflux from [3H]cholesterol-labeled J774A.1 mouse macrophages was measured in vitro, as described in the Methods. HDL from mice treated with D-[113–122]apoJ exhibited a higher efflux capacity compared to scramble or control groups (Figure 7).

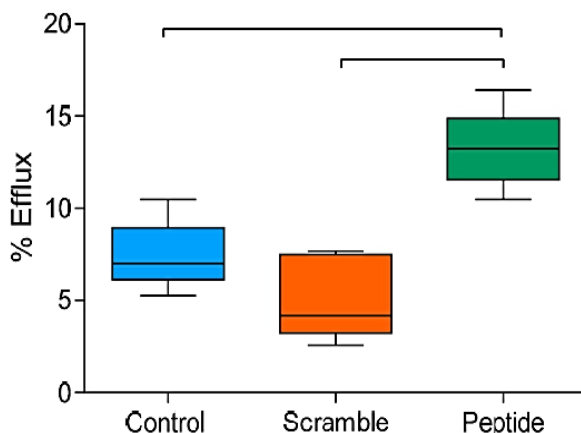


**Figure 7.** In vitro cholesterol efflux capacity of HDL. HDL (25 µg/mL) was incubated for 4 h with 3H-cholesterol-loaded J774A.1 mouse macrophages, as described in the Methods. Cholesterol efflux is expressed as the proportion of [3H]-cholesterol detected in the culture medium relative to total [3H]-cholesterol in cells and medium. Data are expressed as shown in box-plot graphs, n = 4 in the control and scramble group, with 6 mice in the peptide group. Bars indicate p < 0.05 vs. other groups.

### 3.7. D-[113–122]apoJ Reduces the Hepatic Expression of Inflammation-Related Genes

The administration of D-[113–122]apoJ had no effect on liver size or lipid content (Table 1). However, the expression of the inflammatory mediators *Tnfa* and *Ccl2* was lower than in the other mice groups (Figure 8). Additionally, the expressions of *Cd36* and *Cd68* scavenger receptors were significantly lower in mice treated with the D-[113–122]apoJ peptide than in control or scramble-treated mice. As a whole, these findings suggest an anti-inflammatory effect of the subcutaneous administration of D-[113–122]apoJ at the hepatic level.

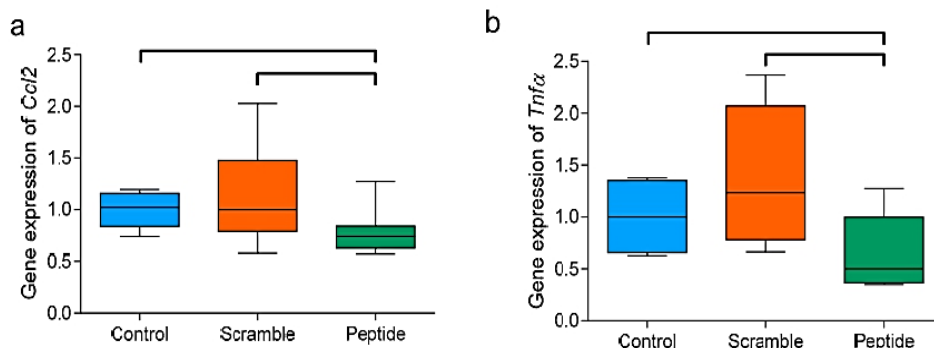


**Figure 8.** Cont.

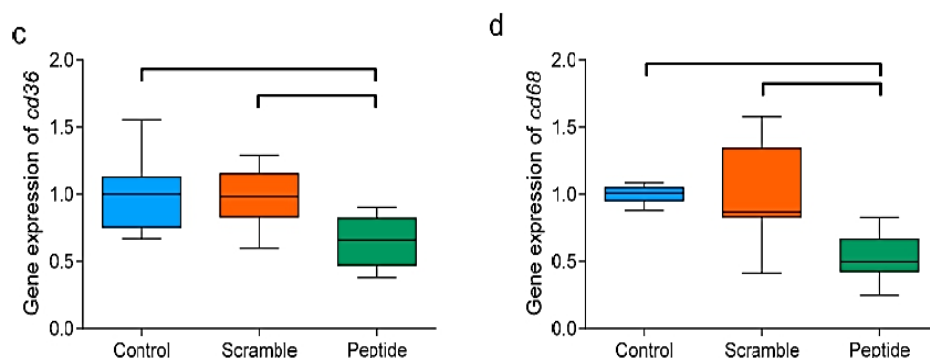


**Figure 8.** Hepatic expression of inflammation-related genes. (a) *Ccl2*, (b) *Tnfa*, (c) *Cd36*, and (d) *Cd68*. Total liver RNA was obtained as described in the Methods, and the expression of target genes was analyzed by RT-PCR. Data are expressed as shown in the box-plot graphs,  $n = 6$  in each group. Bars indicate  $p < 0.05$  vs. other groups.

### 3.8. Improvements in HDL Oxidation and LDL Electronegativity Are Associated with Atherosclerosis Burden

Spearman's rho correlation was used to analyze the statistical correlations between the atherosclerosis burden and the different parameters of lipoprotein function. Figure 9 shows correlations of atherosclerosis with the main parameters of lipoprotein function. We found statistically significant correlations between the area of atherosclerotic lesions and two parameters of lipoprotein function, the susceptibility to oxidation of HDL and the electronegativity of LDL. These observations suggest that both parameters could be related to the development of atherosclerosis, and that the improvement promoted by the subcutaneous administration of the D-[113–122]apoJ peptide in these functions could be involved in the reduction of atherosclerotic lesions. Linear regression analysis confirmed that HDL susceptibility to oxidation was independently associated with atherosclerosis after adjusting for confounding (Table S2). Regarding LDL electronegativity, the association with atherosclerosis was not as strong, with a loss of significance with some variables. Probably, the relatively weak association between LDL electronegativity and atherosclerosis was due to the small sample size ( $n = 4$  in each group), but a clear trend of statistical significance was observed.

Besides the correlations observed with atherosclerosis burden (Figure 9), other correlations among lipoprotein function parameters were detected (Table S1). HDL susceptibility to oxidation was associated with the antioxidant capacity of HDL and also with LDL susceptibility to oxidation. This observation probably reflects the presence of an increased oxidative stress in blood of mice, which was improved by the administration of the peptide. In addition, the electronegative charge of LDL correlated negatively with LDL susceptibility to aggregation.

Alternatively, to analyze if the effect of the treatment was associated with some of the variables, we also conducted a linear regression analysis using the treatment as a covariate and sequentially adding the rest of the variables (Table S3). A slight attenuation was observed for both HDL susceptibility to oxidation and LDL electronegativity. This analysis concurs with the results shown in Tables S1 and S2 and strengthens the putative role of the improvement of HDL susceptibility to oxidation and LDL electronegativity, mediating the effect of the peptide.

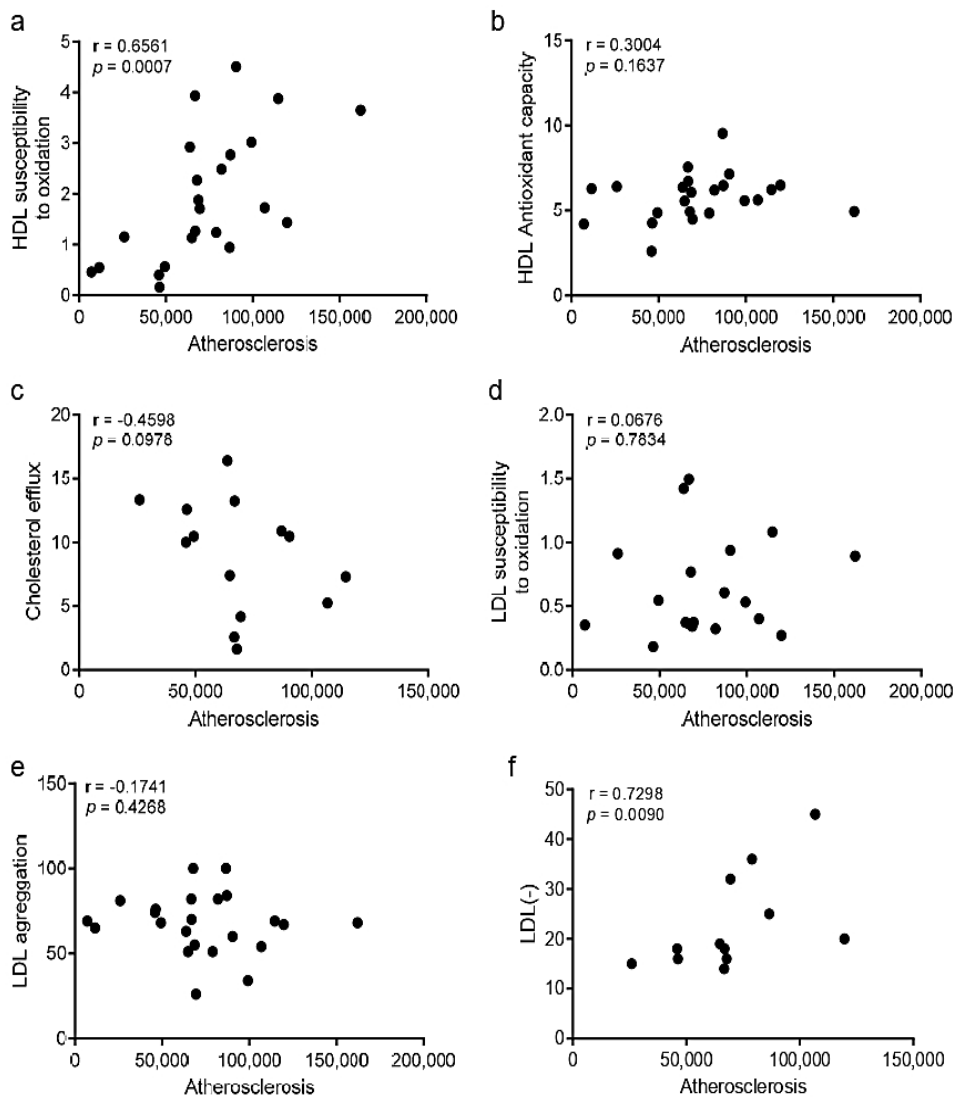


**Figure 9.** Univariate correlations between atherosclerosis development and lipoprotein function parameters. (a) HDL susceptibility to oxidation, (b) HDL antioxidant capacity, (c) cholesterol efflux induced by HDL, (d) LDL susceptibility to oxidation, (e) LDL susceptibility to aggregation, and (f) electronegative charge of LDL. Data were analyzed using Spearman's rho correlation.

### 3.9. The Atherosclerosis Burden Correlates with Hepatic Inflammation

Spearman's rho correlation was also used to analyze the statistical correlations between the atherosclerosis burden and parameters of hepatic inflammation (Figure 10). We found statistically significant correlations between the area of atherosclerotic lesions and the hepatic expression of *Ccl2*, *Tnfa*, and *Cd68*, and a positive trend with *Cd36*. These observations suggest that the development of atherosclerosis is related to the degree of inflammation at a hepatic level.



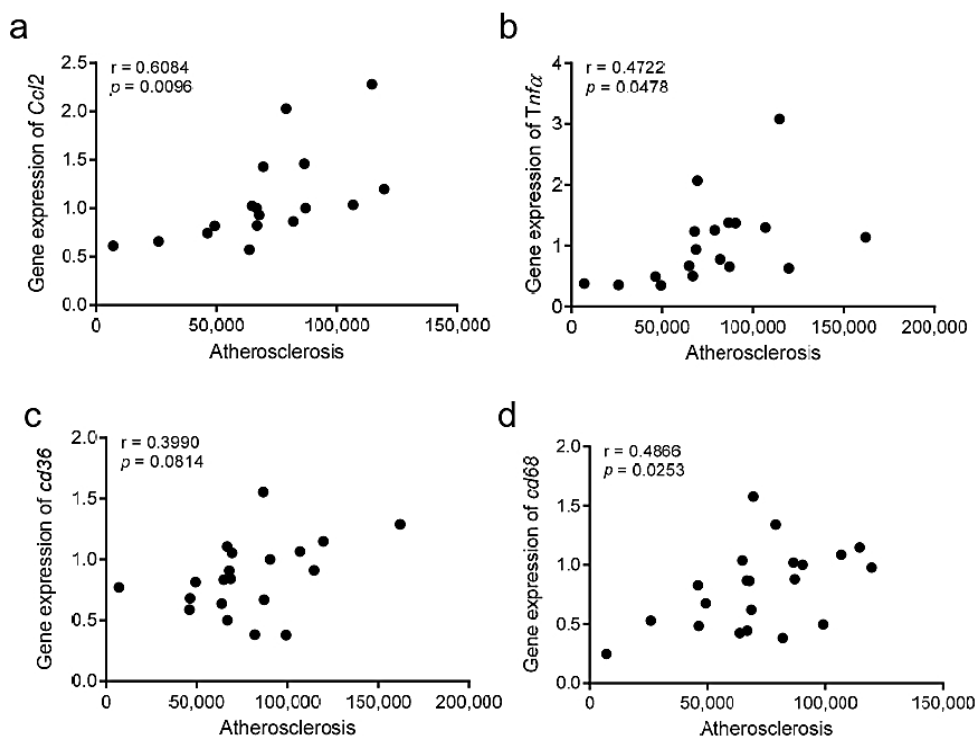


**Figure 10.** Univariate correlations between atherosclerosis development and hepatic inflammation parameters. (a) *Ccl2*, (b) *Tnf $\alpha$* , (c) *Cd36*, (d) *Cd68*. Data were analyzed using Spearman's rho correlation.

#### 4. Discussion

Our data show that subcutaneous administration of the peptide D-[113–122]apoJ for eight weeks retards the development of atherosclerosis in LDLR-KO mice fed atherogenic diet. Since the 1980s, short synthetic peptides with sequences that mimic those found in natural apolipoproteins have been studied and used to prevent atherosclerosis [9,32]. Several mimetics of apoA-I and apoE have succeeded in preventing atherosclerosis in animal models [10,11,33]; however, human clinical trials involving ApoA-I apolipoprotein mimetic peptides have failed to prove a clinical benefit [18,32]. This could be due to the marked differences in the lipoprotein metabolism between humans and mice. Thus, while LDL plays a preponderant role in cholesterol transport in humans, in mice, most of the cholesterol is transported in blood by HDL. Furthermore, LDL cholesterol plasma levels are not the only risk factor, and besides its plasma concentration, qualitative characteristics of LDL determine its atherogenicity [34,35]. The same occurs with HDL plasma levels, since it has been shown that only increasing its concentration does not decrease cardiovascular risk if its antiatherogenic qualitative properties are not improved [36,37].

We hypothesized that one peptide acting simultaneously on the function of both HDL and LDL could retard the onset or reduce the development of atheromatous lesions. Based on previous studies, we hypothesized that the peptide D-[113–122]apoJ could accomplish protective actions by improving both HDL and LDL function. On one hand, the D-[113–122]apoJ mimetic peptide has in vitro protective effects on human LDL aggregation, a crucial LDL event for the development of atherosclerosis [22]. On the other hand, this peptide was proven to retard atherosclerosis in apoE KO mice by improving the anti-inflammatory properties and the cholesterol efflux capacity of HDL [13]. The novelty of the present study is the analysis of the effect of D-[113–122]apoJ in the LDLR-KO mice which showed higher LDL levels and enhanced atherosclerosis when fed a western-type diet.

In accordance with this hypothesis, data presented in the current study show that the D-[113–122]apoJ peptide induced a reduction of 40% of atherosclerotic lesion areas under severe hyperlipidemic conditions, which is related to a qualitative increase of the antiatherogenic actions of HDL, as well as the improvement of the atherogenic properties of LDL. This action was not caused by quantitative changes in the lipoprotein profile since D-[113–122]apoJ did not exert any effect on the plasma concentration of lipoproteins. Our data show that D-[113–122]apoJ had only minor effects on the main components of lipoproteins; however, a relevant change was an increase in the content of free cholesterol in D-[113–122]apoJ-treated mice. A higher content of free cholesterol on the surface of lipoproteins is known to reduce their oxidizability by increasing the lipid packaging [38,39]; this could therefore contribute to the improved antioxidant properties observed in HDL from D-[113–122]apoJ-treated mice. Another positive effect of D-[113–122]apoJ administration on HDL was a rise in its capacity to promote the efflux of cholesterol from macrophages. Both observations agree with the previous findings by Navab et al., who previously reported that oral administration of D-[113–122]apoJ prevented atherosclerosis development in apoE-KO mice [13]. According to our findings, these authors also reported an improvement of the anti-inflammatory properties and the cholesterol efflux capacity of HDL from treated mice. However, in comparison with the work by Navab et al., our study presents some novelties. First, in our case, LDLR-KO mice were fed an atherogenic diet, whereas in the study of Navab et al., apoE-KO mice were fed a chow diet. Consequently, the levels of plasma cholesterol were much higher in our model and presumably, the development of lesions should be higher. Despite the high levels of cholesterol, the administration of the peptide in our model was able to reduce the extent of atherosclerotic lesions.

Another important difference between our study and the work of Navab and collaborators is the fact that LDLR-KO mice presented high LDL levels whereas in apoE-KO mice, most of apoB-containing particles were in the size and density ranges of VLDL. Thus, our study allowed us to evaluate the effect of D-[113–122]apoJ on the atherogenic properties of murine LDL. Although we did not observe an effect of peptide administration on LDL composition or susceptibility to oxidation, other atherogenic characteristics of LDL were improved. First, we found that D-[113–122]apoJ treatment prevented the aggregation of LDL induced in vitro by SMase, suggesting LDL particles would be less prone to aggregation in vivo, and thereby could have a protective role against the subsequent subendothelial lipoprotein retention. Second, the electronegativity of LDL particles was lower in mice treated with D-[113–122]apoJ than in the control or scramble groups. Although the atherogenic and inflammatory properties of electronegative LDL fractions in mice are not as well established as in humans [40], an increased proportion has been reported in rodents suffering accelerated atherosclerosis [41,42]. The finding of a negative significant correlation between LDL electronegativity and aggregability is paradoxical since studies conducted in humans show that the electronegative fraction of LDL (LDL(-)) is prone to aggregation [40]. However, this aspect has not been previously studied in mice, and the putative association between electronegativity and aggregability of human LDL could be different in murine LDL.

The role of the liver as a crucial driver of inflammation in cardiovascular disease [43] guided us to determine the expression of genes known to be involved in inflammation. Because mRNA levels of *Tnfa*, *Ccl2*, and *Cd68* are commonly elevated in hepatic inflammation, they were selected to assess the potential anti-inflammatory response by ApoJ mimetic peptide in this organ. The hepatic expression of inflammatory mediators was decreased in those mice treated with the D-[113–122]apoJ peptide, as indicated by the reduced expression of *Tnfa* and *Ccl2* (also known as *mcp1*) genes. In line with these observations, the decreased expression of *Cd68* in D-[113–122]apoJ-treated mice indicates lower infiltration of macrophages in the liver. On the other hand, the expression of the scavenger receptor CD36 was significantly lower in those mice treated with D-[113–122]apoJ, which indicates that the increased liver *Cd36* expression associated with enhanced hepatic fatty acid uptake and triglyceride accumulation, as a consequence of a high-fat diet [44], is prevented by the administration of the

D-[113–122]apoJ peptide. Overall, these changes in gene expression indicate that the administration of D-[113–122]apoJ improves some abnormalities induced by an atherogenic diet in liver inflammation.

Our results strongly indicate that D-[113–122]apoJ acts through several mechanisms on the function of different lipoproteins and also at the hepatic level, and the combination of these effects would be responsible for atheroprotection. Univariate correlation and linear regression analyses suggest that the main determinants of the decrease of atherosclerosis development by D-[113–122]apoJ administration were the HDL susceptibility to oxidation and LDL electronegativity. However, the specific mechanisms by which the peptide exerts this protective action are not well understood. Regarding LDL, we previously reported that D-[113–122]apoJ protects LDL from *in vitro* aggregation induced by different mechanisms, including spontaneous and SMase-induced aggregation [22]. We proposed that this effect was mediated by the binding of the peptide to hydrophobic patches in the lipoprotein surface generated during the aggregation process, avoiding the interaction of different LDL particles. Therefore, this direct effect could be the cause of decreased susceptibility to aggregation observed *ex vivo*. However, the reason for decreased negative electric charge of LDL is unclear. It could be due to the increased antioxidant capacity of HDL preventing the formation of oxidized LDL. Another mechanism that could be related to the reduction of LDL electronegativity is the decrease of liver inflammation, which could reflect a reduction in the systemic inflammation status. It is known that inflammation favors different mechanisms of lipoprotein modification such as oxidative stress, or increased expression at the arterial wall level of lipases and proteases [45]. On the other hand, Navab et al. demonstrated that D-[113–122]apoJ reduces the content of lipoperoxides in lipoproteins from monkeys treated with this peptide, this property being shared by other amphipathic peptides [13]. Thus, this lipoperoxide-sequestering activity of D-[113–122]apoJ could be key to explain the decreased susceptibility to oxidation of HDL, as well as its increased antioxidative properties. At the same time, decreased oxidation of HDL results in maintaining the activities of several enzymes and apolipoproteins involved in the reverse cholesterol transport, such as apoA-I, lecithin:cholesterol acyltransferase, cholesteryl ester transfer protein, paraoxonase or platelet-activating factor acetylhydrolase. Of note, the correlation analysis showed that the parameters mainly related to the reduction in atherosclerosis development were the susceptibility to the oxidation of HDL and the electronegativity of LDL, which gives special relevance to maintain the physiological properties of both lipoproteins. In addition, the development of atherosclerosis was also related to markers of liver inflammation. However, the correlation analysis should be considered with caution since the number of analyzed samples is small to draw more consistent conclusions, and other factors related or not with lipoprotein function or hepatic inflammation could be involved in the anti-atherogenic action of D-[113–122]apoJ.

## 5. Conclusions

In summary, our data show that D-[113–122]apoJ administration decreases the extent of atherosclerotic lesions in close association with simultaneous improvements in the functionality of both HDL and LDL, and with lower inflammation at the hepatic level. These effects were observed under strong hypercholesterolemic conditions, suggesting that D-[113–122]apoJ administration could be a useful therapy against diet-induced atherosclerosis.

**Supplementary Materials:** The following are available online at <http://www.mdpi.com/2218-273X/10/6/829/s1>, Figure S1: Experimental design flow chart, Figure S2: Weight-related parameters, Figure S3: *In vitro* oxidation analysis with human LDL and HDL in presence of D-[113–122]apoJ peptide, and Table S1: Univariate correlations of atherosclerosis development and lipoprotein function parameters, Table S2: Linear regression model relating atherosclerosis development with HDL susceptibility to oxidation and LDL electronegativity, Table S3: Association between atherosclerosis and treatment group after adjusting for the main variables of lipid profile and lipoprotein function.



**Author Contributions:** Conceptualization, A.R., J.L.S.-Q.; methodology, A.R.-U., J.A.-R., D.S., N.P., N.F.-C.; formal analysis, A.R.-U., D.d.G.-C., J.C.E.-G., J.J.; investigation, A.R.-U., A.R., S.B., J.C.E.-G., J.J., J.L.S.-Q.; resources, A.P., J.O.-L.; data curation, A.R.-U., A.R., S.B., D.d.G.-C., J.C.E.-G., J.J., J.L.S.-Q.; writing—original draft preparation, A.R.-U., J.L.S.-Q.; writing—review and editing, A.R., S.B., J.C.E.-G., J.J.; supervision, J.O.-L., J.L.S.-Q.; funding acquisition, J.C.E.-G., J.J., A.P., J.L.S.-Q. All authors have read and agreed to the published version of the manuscript.

**Funding:** This research was funded by Instituto de Salud Carlos III (co-financed by the European Regional Development Fund FEDER “Una manera de hacer Europa”), grant numbers PI13/00364, PI16/00471, PI17-00232, PI16-00139, CB07/06/2008, and CB07/08/0016. A.R.-U. was funded by Instituto de Salud Carlos III predoctoral contract FI17/00031. A.R. was funded by Instituto de Salud Carlos III postdoctoral Sra Borrell contract CD12-00439 and by postdoctoral contract Miguel Servet CP19/00146. J.J. was funded by Instituto de Salud Carlos III postdoctoral contract Miguel Servet CPII18/00004. A.R.-U., D.S., N.P., N.F.-C., S.B., J.C.E.-G., J.J. and J.L.S.-Q. are members of the Quality Research Group 2017-SGR-1149 from Generalitat de Catalunya. A.R., N.P., S.B., J.C.E.-G., J.J., and J.L.S.-Q. are members of the Group of Vascular Biology from the Spanish Atherosclerosis Society. A.P., J.C.E.-G., J.J., and J.L.S.-Q. are members of CIBERDEM from the Instituto de Salud Carlos III, D.G.-C. is a member of CIBERES from Carlos III Health Institute.

**Conflicts of Interest:** The authors declare no conflict of interest.

## References

1. Mach, F.; Baigent, C.; Catapano, A.L.; Koskinas, K.C.; Casula, M.; Badimon, L.; Chapman, M.J.; De Backer, G.G.; Delgado, V.; Ference, B.A.; et al. 2019 ESC/EAS Guidelines for the management of dyslipidaemias: Lipid modification to reduce cardiovascular risk. *Eur. Heart J.* **2020**, *41*, 111–188. [[CrossRef](#)]
2. Fruchart, J.C.; Davignon, J.; Hermans, M.P.; Al-Rubeaan, K.; Amarenco, P.; Assmann, G.; Barter, P.; Betteridge, J.; Bruckert, E.; Cuevas, A.; et al. Residual macrovascular risk in 2013: What have we learned? *Cardiovasc. Diabetol.* **2014**, *13*, 26. [[CrossRef](#)] [[PubMed](#)]
3. Tabas, I.; Williams, K.J.; Boren, J. Subendothelial lipoprotein retention as the initiating process in atherosclerosis: Update and therapeutic implications. *Circulation* **2007**, *116*, 1832–1844. [[CrossRef](#)]
4. Witztum, J.L.; Steinberg, D. The oxidative modification hypothesis of atherosclerosis: Does it hold for humans? *Trends Cardiovasc. Med.* **2001**, *11*, 93–102. [[CrossRef](#)]
5. Rosenson, R.S.; Brewer, H.B., Jr.; Ansell, B.J.; Barter, P.; Chapman, M.J.; Heinecke, J.W.; Kontush, A.; Tall, A.R.; Webb, N.R. Dysfunctional HDL and atherosclerotic cardiovascular disease. *Nat. Rev. Cardiol.* **2016**, *13*, 48–60. [[CrossRef](#)]
6. Ruuth, M.; Nguyen, S.D.; Vihervaara, T.; Hilvo, M.; Laajala, T.D.; Kondadi, P.K.; Gistera, A.; Lahteenmaki, H.; Kittila, T.; Huusko, J.; et al. Susceptibility of low-density lipoprotein particles to aggregate depends on particle lipidome, is modifiable, and associates with future cardiovascular deaths. *Eur. Heart J.* **2018**, *39*, 2562–2573. [[CrossRef](#)]
7. Khera, A.V.; Demler, O.V.; Adelman, S.J.; Collins, H.L.; Glynn, R.J.; Ridker, P.M.; Rader, D.J.; Mora, S. Cholesterol Efflux Capacity, High-Density Lipoprotein Particle Number, and Incident Cardiovascular Events: An Analysis from the JUPITER Trial (Justification for the Use of Statins in Prevention: An Intervention Trial Evaluating Rosuvastatin). *Circulation* **2017**, *135*, 2494–2504. [[CrossRef](#)]
8. Gallone, G.; Baldetti, L.; Pagnesi, M.; Latib, A.; Colombo, A.; Libby, P.; Giannini, F. Medical Therapy for Long-Term Prevention of Atherothrombosis Following an Acute Coronary Syndrome: JACC State-of-the-Art Review. *J. Am. Coll. Cardiol.* **2018**, *72*, 2886–2903. [[CrossRef](#)]
9. Recio, C.; Maione, F.; Iqbal, A.J.; Mascolo, N.; De Feo, V. The Potential Therapeutic Application of Peptides and Peptidomimetics in Cardiovascular Disease. *Front. Pharmacol.* **2016**, *7*, 526. [[CrossRef](#)]
10. Uehara, Y.; Chiesa, G.; Saku, K. High-Density Lipoprotein-Targeted Therapy and Apolipoprotein A-I Mimetic Peptides. *Circ. J.* **2015**, *79*, 2523–2528. [[CrossRef](#)]
11. White, C.R.; Garber, D.W.; Anantharamaiah, G.M. Anti-inflammatory and cholesterol-reducing properties of apolipoprotein mimetics: A review. *J. Lipid Res.* **2014**, *55*, 2007–2021. [[CrossRef](#)]
12. Wolska, A.; Lo, L.; Sviridov, D.O.; Pourmoussa, M.; Pryor, M.; Ghosh, S.S.; Kakkar, R.; Davidson, M.; Wilson, S.; Pastor, R.W.; et al. A dual apolipoprotein C-II mimetic-apolipoprotein C-III antagonist peptide lowers plasma triglycerides. *Sci. Transl. Med.* **2020**, *12*, eaaw7905. [[CrossRef](#)] [[PubMed](#)]

13. Navab, M.; Anantharamaiah, G.M.; Reddy, S.T.; Van Lenten, B.J.; Wagner, A.C.; Hama, S.; Hough, G.; Bachini, E.; Garber, D.W.; Mishra, V.K.; et al. An oral apoJ peptide renders HDL antiinflammatory in mice and monkeys and dramatically reduces atherosclerosis in apolipoprotein E-null mice. *Arterioscler. Thromb. Vasc. Biol.* **2005**, *25*, 1932–1937. [[CrossRef](#)]
14. Getz, G.S.; Reardon, C.A. Apoprotein E and Reverse Cholesterol Transport. *Int. J. Mol. Sci.* **2018**, *19*, 3479. [[CrossRef](#)]
15. Tabet, F.; Remaley, A.T.; Segaliny, A.I.; Millet, J.; Yan, L.; Nakhla, S.; Barter, P.J.; Rye, K.A.; Lambert, G. The 5A apolipoprotein A-I mimetic peptide displays antiinflammatory and antioxidant properties in vivo and in vitro. *Arterioscler. Thromb. Vasc. Biol.* **2010**, *30*, 246–252. [[CrossRef](#)] [[PubMed](#)]
16. Bielicki, J.K.; Zhang, H.; Cortez, Y.; Zheng, Y.; Narayanaswami, V.; Patel, A.; Johansson, J.; Azhar, S. A new HDL mimetic peptide that stimulates cellular cholesterol efflux with high efficiency greatly reduces atherosclerosis in mice. *J. Lipid Res.* **2010**, *51*, 1496–1503. [[CrossRef](#)] [[PubMed](#)]
17. Xu, Y.; Liu, H.; Liu, M.; Li, F.; Liu, L.; Du, F.; Fan, D.; Yu, H. A human apolipoprotein E mimetic peptide reduces atherosclerosis in aged apolipoprotein E null mice. *Am. J. Transl. Res.* **2016**, *8*, 3482–3492.
18. Karalis, I.; Jukema, J.W. HDL Mimetics Infusion and Regression of Atherosclerosis: Is It Still Considered a Valid Therapeutic Option? *Curr. Cardiol. Rep.* **2018**, *20*, 66. [[CrossRef](#)]
19. Nguyen, S.D.; Javanainen, M.; Rissanen, S.; Zhao, H.; Huusko, J.; Kivela, A.M.; Yla-Herttuala, S.; Navab, M.; Fogelman, A.M.; Vattulainen, I.; et al. Apolipoprotein A-I mimetic peptide 4F blocks sphingomyelinase-induced LDL aggregation. *J. Lipid Res.* **2015**, *56*, 1206–1221. [[CrossRef](#)]
20. Mishra, V.K.; Palgunachari, M.N.; Hudson, J.S.; Shin, R.; Keenum, T.D.; Krishna, N.R.; Anantharamaiah, G.M. Structure and lipid interactions of an anti-inflammatory and anti-atherogenic 10-residue class G(\*) apolipoprotein J peptide using solution NMR. *Biochim. Biophys. Acta* **2011**, *1808*, 498–507. [[CrossRef](#)]
21. Martinez-Bujidos, M.; Rull, A.; Gonzalez-Cura, B.; Perez-Cuellar, M.; Montoliu-Gaya, L.; Villegas, S.; Ordonez-Llanos, J.; Sanchez-Quesada, J.L. Clusterin/apolipoprotein J binds to aggregated LDL in human plasma and plays a protective role against LDL aggregation. *FASEB J.* **2015**, *29*, 1688–1700. [[CrossRef](#)]
22. Rivas-Urbina, A.; Rull, A.; Montoliu-Gaya, L.; Perez-Cuellar, M.; Ordonez-Llanos, J.; Villegas, S.; Sanchez-Quesada, J.L. Low-density lipoprotein aggregation is inhibited by apolipoprotein J-derived mimetic peptide d-[113–122]apoJ. *Biochim. Biophys. Acta Mol. Cell Biol. Lipids* **2020**, *1865*, 158541. [[CrossRef](#)]
23. Oppi, S.; Luscher, T.F.; Stein, S. Mouse Models for Atherosclerosis Research-Which Is My Line? *Front. Cardiovasc. Med.* **2019**, *6*, 46. [[CrossRef](#)]
24. Mansukhani, N.A.; Wang, Z.; Shively, V.P.; Kelly, M.E.; Vercammen, J.M.; Kibbe, M.R. Sex Differences in the LDL Receptor Knockout Mouse Model of Atherosclerosis. *Artery Res.* **2017**, *20*, 8–11. [[CrossRef](#)]
25. Melchionna, M.; Styan, K.E.; Marchesan, S. The Unexpected Advantages of Using D-Amino Acids for Peptide Self-Assembly into Nanostructured Hydrogels for Medicine. *Curr. Top. Med. Chem.* **2016**, *16*, 2009–2018. [[CrossRef](#)]
26. Folch, J.; Lees, M.; Sloane Stanley, G.H. A simple method for the isolation and purification of total lipides from animal tissues. *J. Biol. Chem.* **1957**, *226*, 497–509.
27. Havel, R.J.; Eder, H.A.; Bragdon, J.H. The distribution and chemical composition of ultracentrifugally separated lipoproteins in human serum. *J. Clin. Investig.* **1955**, *34*, 1345–1353. [[CrossRef](#)]
28. de Juan-Franco, E.; Perez, A.; Ribas, V.; Sanchez-Hernandez, J.A.; Blanco-Vaca, F.; Ordonez-Llanos, J.; Sanchez-Quesada, J.L. Standardization of a method to evaluate the antioxidant capacity of high-density lipoproteins. *Int. J. Biomed Sci.* **2009**, *5*, 402–410.
29. Ribas, V.; Sanchez-Quesada, J.L.; Anton, R.; Camacho, M.; Julve, J.; Escola-Gil, J.C.; Vila, L.; Ordonez-Llanos, J.; Blanco-Vaca, F. Human apolipoprotein A-II enrichment displaces paraoxonase from HDL and impairs its antioxidant properties: A new mechanism linking HDL protein composition and antiatherogenic potential. *Circ. Res.* **2004**, *95*, 789–797. [[CrossRef](#)]
30. Benitez, S.; Sanchez-Quesada, J.L.; Lucero, L.; Arcelus, R.; Ribas, V.; Jorba, O.; Castellvi, A.; Alonso, E.; Blanco-Vaca, F.; Ordonez-Llanos, J. Changes in low-density lipoprotein electronegativity and oxidizability after aerobic exercise are related to the increase in associated non-esterified fatty acids. *Atherosclerosis* **2002**, *160*, 223–232. [[CrossRef](#)]
31. Yu, Y.; Si, Y.; Song, G.; Luo, T.; Wang, J.; Qin, S. Ethanolic extract of propolis promotes reverse cholesterol transport and the expression of ATP-binding cassette transporter A1 and G1 in mice. *Lipids* **2011**, *46*, 805–811. [[CrossRef](#)] [[PubMed](#)]

32. Leman, L.J.; Maryanoff, B.E.; Ghadiri, M.R. Molecules that mimic apolipoprotein A-I: Potential agents for treating atherosclerosis. *J. Med. Chem.* **2014**, *57*, 2169–2196. [[CrossRef](#)] [[PubMed](#)]
33. Stoekenbroek, R.M.; Stroes, E.S.; Hovingh, G.K. ApoA-I mimetics. *Handb. Exp. Pharmacol.* **2015**, *224*, 631–648. [[CrossRef](#)] [[PubMed](#)]
34. Rivas-Urbina, A.; Rull, A.; Ordonez-Llanos, J.; Sanchez-Quesada, J.L. Electronegative LDL: An Active Player in Atherogenesis or a By-Product of Atherosclerosis? *Curr. Med. Chem.* **2019**, *26*, 1665–1679. [[CrossRef](#)] [[PubMed](#)]
35. Diffenderfer, M.R.; Schaefer, E.J. The composition and metabolism of large and small LDL. *Curr. Opin. Lipidol.* **2014**, *25*, 221–226. [[CrossRef](#)] [[PubMed](#)]
36. Nicholls, S.J.; Bubb, K. The mystery of evacetrapib—why are CETP inhibitors failing? *Expert Rev. Cardiovasc. Ther.* **2020**, *18*, 127–130. [[CrossRef](#)]
37. Tall, A.R. Plasma high density lipoproteins: Therapeutic targeting and links to atherogenic inflammation. *Atherosclerosis* **2018**, *276*, 39–43. [[CrossRef](#)]
38. Tribble, D.L. Lipoprotein oxidation in dyslipidemia: Insights into general mechanisms affecting lipoprotein oxidative behavior. *Curr. Opin. Lipidol.* **1995**, *6*, 196–208. [[CrossRef](#)]
39. Zerrad-Saadi, A.; Therond, P.; Chantepie, S.; Couturier, M.; Rye, K.A.; Chapman, M.J.; Kontush, A. HDL3-mediated inactivation of LDL-associated phospholipid hydroperoxides is determined by the redox status of apolipoprotein A-I and HDL particle surface lipid rigidity: Relevance to inflammation and atherogenesis. *Arterioscler. Thromb. Vasc. Biol.* **2009**, *29*, 2169–2175. [[CrossRef](#)] [[PubMed](#)]
40. Estruch, M.; Sanchez-Quesada, J.L.; Ordonez Llanos, J.; Benitez, S. Electronegative LDL: A circulating modified LDL with a role in inflammation. *Mediat. Inflamm.* **2013**, *2013*, 181324. [[CrossRef](#)]
41. Chen, W.Y.; Chen, F.Y.; Lee, A.S.; Ting, K.H.; Chang, C.M.; Hsu, J.F.; Lee, W.S.; Sheu, J.R.; Chen, C.H.; Shen, M.Y. Sesamol reduces the atherogenicity of electronegative L5 LDL in vivo and in vitro. *J. Nat. Prod.* **2015**, *78*, 225–233. [[CrossRef](#)] [[PubMed](#)]
42. Lai, Y.S.; Yang, T.C.; Chang, P.Y.; Chang, S.F.; Ho, S.L.; Chen, H.L.; Lu, S.C. Electronegative LDL is linked to high-fat, high-cholesterol diet-induced nonalcoholic steatohepatitis in hamsters. *J. Nutr. Biochem.* **2016**, *30*, 44–52. [[CrossRef](#)] [[PubMed](#)]
43. Stahl, E.P.; Dhindsa, D.S.; Lee, S.K.; Sandesara, P.B.; Chalasani, N.P.; Sperling, L.S. Nonalcoholic Fatty Liver Disease and the Heart: JACC State-of-the-Art Review. *J. Am. Coll. Cardiol.* **2019**, *73*, 948–963. [[CrossRef](#)]
44. Koonen, D.P.; Jacobs, R.L.; Febbraio, M.; Young, M.E.; Soltys, C.L.; Ong, H.; Vance, D.E.; Dyck, J.R. Increased hepatic CD36 expression contributes to dyslipidemia associated with diet-induced obesity. *Diabetes* **2007**, *56*, 2863–2871. [[CrossRef](#)] [[PubMed](#)]
45. Back, M.; Yurdagul, A., Jr.; Tabas, I.; Oorni, K.; Kovanen, P.T. Inflammation and its resolution in atherosclerosis: Mediators and therapeutic opportunities. *Nat. Rev. Cardiol.* **2019**, *16*, 389–406. [[CrossRef](#)]



# Subcutaneous Administration of Apolipoprotein J-derived Mimetic Peptide D-[113–122]apoJ Improves LDL and HDL Function and Prevents Atherosclerosis in LDLR-KO Mice

Andrea Rivas-Urbina, Anna Rull, Joile Aldana-Ramos, David Santos, Nuria Puig, Nuria Farre-Cabrerizo, Sonia Benitez, Antonio Perez, David de Gonzalo-Calvo, Joan Carles Escola-Gil, Josep Julve, Jordi Ordoñez-Llanos and Jose Luis Sanchez-Quesada

## Supplementary materials

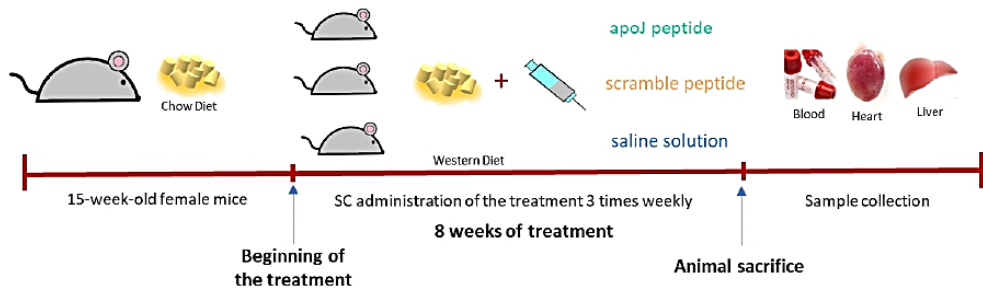


Figure S1. Experimental design flow chart.

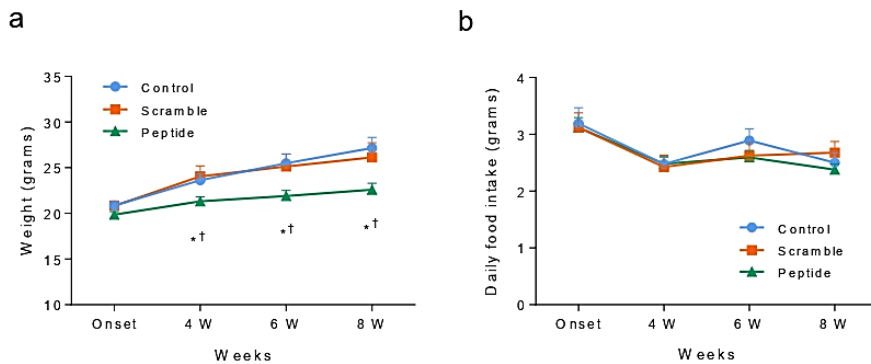
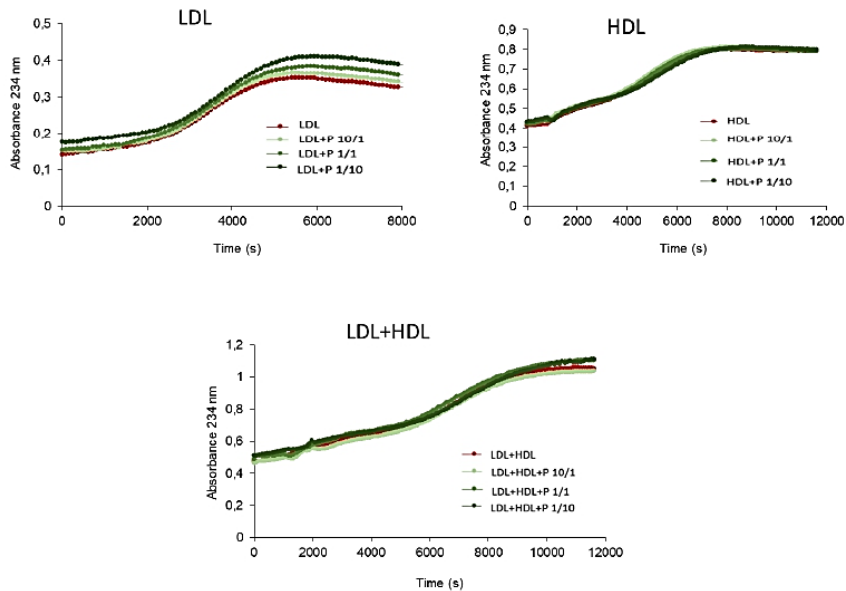


Figure S2. Weight-related parameters. (a) Increment of weight after 8 weeks on western diet. (b) Daily food intake. Data are the mean  $\pm$  SEM of 8 mice from the control and scramble group, and 12 mice from the peptide group. \*  $p < 0.05$  vs control mice. †  $p < 0.05$  vs scramble mice.



**Figure S3.** In vitro oxidation analysis of human LDL and HDL in presence of D-[113–122]apoJ peptide. Oxidation of lipoproteins was induced by adding 5  $\mu$ M CuSO<sub>4</sub> and monitored at 234 nm, as described in Methods. Molar ratios of 10:1, 1:1 and 1:10 apoB:peptide or apoA-I:peptide were used.

**Table S1.** Univariate correlations of atherosclerosis development and lipoprotein function parameters. Data were analyzed using the Spearman’s rho correlation analysis. Significant correlations are shown in yellow.

		Atherosclerosis	HDL_susceptibility _to_oxidation	HDL_Antioxidant capacity	Cholesterol efflux	LDL_susceptibility _to_oxidation	LDL_aggregation	LDL(-)
Spearman rho correlation	Atherosclerosis	Correlation coefficient	1,000	,656**	,300	-,460	,068	-,174
		Sig. (bilateral)		,005	,164	,098	,783	,427
		N	24	24	24	14	24	12
	HDL_susceptibility _to_oxidation	Correlation coefficient		1,000	,452*	-,242	,660**	-,080
		Sig. (bilateral)			,031	,404	,002	,716
		N		24	24	14	24	24
	HDL_Antioxidant capacity	Correlation coefficient			1,000	,185	,386	,271
		Sig. (bilateral)				,527	,102	,212
	N			24	14	24	24	
Cholesterol_efflux	Correlation coefficient				1,000	-,096	,042	
	Sig. (bilateral)					,754	,887	
	N				14	14	14	
LDL_susceptibility _to_oxidation	Correlation coefficient					1,000	,136	
	Sig. (bilateral)						,578	
	N					24	24	
LDL_aggregation	Correlation coefficient						1,000	
	Sig. (bilateral)							
	N						24	
LDL(-)	Correlation coefficient							1,000
	Sig. (bilateral)							
	N							12

\*\* P < 0,01 (bilateral).

\* P < 0,05 (bilateral).



**Table S2.** Linear regression model relating atherosclerosis development with HDL susceptibility to oxidation and LDL electronegativity. Data are expressed as standardized beta ( $\beta$ ).

HDL Susceptibility to Oxidation			LDL(-)		
Association between atherosclerosis and HDL susceptibility to oxidation after adjusting for each of the following variables ( $\beta$ ):	$\beta$	<i>p</i> -Value	Association between atherosclerosis and LDL electronegativity after adjusting for each of the following variables ( $\beta$ ):	$\beta$	<i>p</i> -Value
HDL Antioxidant capacity	0.618	0.004	HDL susceptibility to oxidation	0.577	0.011
Cholesterol efflux	0.562	0.036	HDL Antioxidant capacity	0.569	0.061
LDL susceptibility to oxidation	1.033	<0.001	Cholesterol efflux	0.486	0.210
LDL aggregation	0.611	0.002	LDL susceptibility to oxidation	0.681	0.088
LDL(-)	0.640	0.006	LDL aggregation	0.719	0.054
Cholesterol	0.634	0.005	Cholesterol	0.668	0.024
Triglycerides	0.628	0.002	Triglycerides	0.653	0.053
Phospholipids	0.620	0.002	Phospholipids	0.645	0.057
VLDL-c	0.637	0.002	VLDL-c	0.704	0.033
LDL-c	0.561	0.008	LDL-c	0.485	0.146
HDL-c	0.618	0.003	HDL-c	0.627	0.044

$\beta$  estimates of HDL susceptibility to oxidation and LDL electronegativity when adjusted for each variable. Each row is a model containing that variable and the main variable in the heading.

**Table S3.** Association between atherosclerosis and treatment group after adjusting for the main variables of lipid profile and lipoprotein function. Data are expressed as standardized beta ( $\beta$ ).

	$\beta$	<i>p</i> -Value
Treatment group	0.455	0.029
Association between atherosclerosis and treatment group after adjusting for each of the following variables ( $\beta$ ):		
HDL susceptibility to oxidation	0.320	0.070
HDL Antioxidant capacity	0.444	0.057
Cholesterol efflux	0.368	0.249
LDL susceptibility to oxidation	0.452	0.058
LDL aggregation	0.460	0.030
LDL(-)	0.257	0.415
Cholesterol	0.464	0.023
Triglycerides	0.553	0.018
Phospholipids	0.481	0.030
VLDL-c	0.492	0.023
LDL-c	0.368	0.105
HDL-c	0.526	0.014

$\beta$  estimates for the treatment when adjusted for each variable in the row.

- GLOBAL DISCUSSION



## **Novel therapeutic targets against CVD**

Cardiovascular disease is the leading cause of mortality worldwide, and in the vast majority of individuals who suffer from it, the origin is the development of arteriosclerotic lesions. Atherosclerosis is a multifactorial disease in which numerous pathophysiological processes overlap, one of the most relevant being the modification of LDL by different independent physicochemical mechanisms. LDL particles can suffer multiple modifications, being its aggregation one of the most important. Aggregation and fusion of LDL in the arterial intima favor its retention in the subendothelial space because of the increase in the size of these particles and its enhanced binding affinity to PGs present in the arterial wall [181]. Both phenomena result in the entrapment of LDL particles in the intima due to the impossibility of leaving this space. The relevance of this type of modification is that it occurs during the early stages of development of the lesion, at a time when this process is still reversible. Being able to intervene during the initial phases of the formation of the atherosclerotic lesion would be an interesting strategy in order to prevent health complications derived from the appearance of advanced lesions. However, the current therapeutic arsenal against cardiovascular disease is mainly limited to prevent the main risk factors (lipid-lowering, antihypertensive, hypoglycemic drugs) or mitigating the effects of the injuries that have led to vascular accidents (anticoagulant, anti-inflammatory drugs). Thus, research on alternative therapeutics is needed.

One of these alternatives has focused on HDL/apoA-I mimicking molecules, intending mainly to improve reverse cholesterol transport. The first synthesized apoA-I mimetic peptide was the 18A and several modifications have been made to generate peptides that more closely mimic the apoA-I function, such as 4F, 6F, FX-5A and FAMP peptides [182]. Most of these peptides efficiently promote cholesterol efflux [157,

183] and possess anti-inflammatory and antioxidant effects in *in vitro* studies and experimental models [184]. Additionally, infusible HDL mimetic therapies have been described. Recently, three of them (apoA-I Milano, CSL-112 and CER-001) have reached clinical trials in humans. These mimetics increase cholesterol efflux capacity. However, they have failed to translate in a favorable effect on regression of coronary atherosclerosis, except CSL-112 since the results of the clinical trial are not yet known [185].

Additionally, apoE and apoC-II derived peptides have been synthesized. The Ac-hE18A-NH<sub>2</sub> peptide was the first apoE mimetic and it is the only one that has reach clinical trials in humans [186]. This peptide improves the hepatic removal of apoB-containing lipoproteins. There have been used other apoE-related peptides that reduce plasma cholesterol, such as mR18L and hEp peptides. Also, some of them promote cholesterol efflux [153]. Regarding apoC-II peptides, the 18A-CII was the first apoC-II produced peptide, which is a strong activator of LPL [187]. Recently, the D6PV peptide has been described. This peptide also activates LPL and significantly lowers plasma TG levels in mouse models [153]. Still, no clinical trials of apoC-II mimetic peptides have been reported [188].

### **LDL susceptibility to aggregation as a therapeutic target**

Another novel alternative is considering the aggregation process of LDL as a therapeutic target, which could be very efficient considering that this is one of the initial events of injury development. Ruuth *et al.* previously demonstrated that LDL particles of patients who had suffered coronary death aggregated faster than those who had no cardiovascular events. Also, this study described an association between the existence of aggregation-prone LDLs with future coronary artery disease deaths independent of conventional CAD risk factors [189]. In line with this, Heffron *et al.* showed that patients with atherosclerotic occlusive peripheral arterial

disease had LDLs that aggregated faster than LDLs obtained from healthy controls. Moreover, these patients also had a significantly elevated risk of major adverse cardiovascular events [190].

In this case, the studies conducted to prevent the aggregation of LDL during these early stages of atherosclerosis are much scarcer than those focused on the regression of advanced lesions. Despite that the aggregation of LDL in the subendothelial space is the triggering event in atherogenesis few studies have proposed the intervention in this process. Nguyen and coworkers showed that the apoA-I mimetic peptide 4F is able to inhibit the SMase-induced LDL aggregation and it also decreases the binding of SMase-treated LDL to human aortic proteoglycans [191]. More recently, Ruuth *et al.* demonstrated that consumption of plant stanol esters reduces the aggregation susceptibility of LDL particles by modifying LDL lipid composition. Also, it decreases the binding of LDL to proteoglycans by lowering LDL levels in circulation [192].

#### **Effect of D-[113–122]apoJ on the LDL susceptibility to aggregation *in vitro***

The rationale for using the D-[113–122]apoJ mimetic peptide was based on previous studies from our group conducted with the whole apoJ molecule. We have previously demonstrated that apoJ bound to LDL is increased in the aggregated forms of this lipoprotein present in blood and, its addition *in vitro* prevents LDL aggregation [147]. We considered these findings as indicative of a putative protective action. Earlier, Navab *et al.* reported that oral administration of the same peptide prevented atherosclerosis development in apoE-KO mice [171], being important the improvement of the anti-inflammatory properties of HDL and the stimulation of the reverse cholesterol transport. Based on these studies and considering the fact that the use of apolipoprotein-derived mimetic peptides

has become more and more relevant in recent years, we studied the effects of the D-[113–122]apoJ mimetic peptide on LDL aggregation.

Peptides can be synthesized using D or L amino acids. In our studies, we used peptides formed by D-amino acids. D-peptides are less vulnerable to proteolytic degradation in the digestive tract or inside cells than L-peptides. D-peptides can consequently be taken orally and be effective for a longer period [193]. In contrast, the L-peptides are more easily absorbed and could have a faster effect. There is currently some discussion as to which of the two types of peptides might be more efficient from a pharmacological point of view.

We first demonstrated by different *in vitro* experimental approaches (turbidity, SEC, GGE, TEM, and DLS) that D-[113–122]apoJ mimetic peptide, at equimolar ratio with apoB, is able to prevent the aggregation of LDL independently of the mechanism by which this aggregation is achieved, either by SMase-mediated lipolysis or by spontaneous aggregation. The beneficial effects of D-[113–122]apoJ mimetic peptide described by Navab *et al.* and the effects found in our study, demonstrate that this peptide acts through various mechanisms on different lipoproteins. Not only an improvement of HDL function, as described by Navab *et al.* define the atheroprotective property of D-[113–122]apoJ mimetic peptide but the effect of this peptide on LDL susceptibility to aggregation appears as a putative alternative/complementary mechanism.

When LDL(+) aggregation was induced by SMase, the D-[113–122]apoJ mimetic peptide inhibited the degradation of SM. This inhibition was not due to a direct effect on the enzyme but to an indirect action that makes LDL more resistant to SMase hydrolysis. Similar results were obtained by Nguyen *et al.* preventing SMase-induced LDL aggregation with 4F, an apoA-I-derived mimetic peptide [191]. When spontaneous LDL

aggregation occurs, D-[113–122]apoJ peptide also inhibits aggregation by directly interacting with the LDL particle surface since the changes in the lipoprotein composition is not affected by the presence of the D-[113–122]apoJ peptide.

Our results also demonstrated that this peptide poorly binds to native LDL, but this binding is strong during the first stages of LDL aggregation. However, such contact decreases when the levels of aggregation are elevated. It seems that D-[113–122]apoJ peptide interacts with LDL when its hydrophobic areas become solvent-exposed during the initial stages of aggregation. As the aggregation progresses, the LDL particles themselves cover the extensive hydrophobic areas, decreasing the binding of the peptide. This behavior could be explained because D-[113–122]apoJ adapts its structure forming a class G\* amphipathic  $\alpha$ -helix conformation in the presence of phospholipids [172]. Following this line, we also demonstrated by the Laurdan assay that D-[113–122]apoJ peptide increases the packaging of lipids on LDL surface and preserves its order.

### **Effect of D-[113–122]apoJ on the LDL susceptibility to aggregation *in vivo***

Once we demonstrated this anti-aggregative capacity of D-[113–122]apoJ peptide *in vitro*, we tested this peptide on an animal model of accelerated atherosclerosis, specifically on the LDLR-KO mice, to find out if this ability would occur in an *in vivo* situation. As LDL aggregation is an important process during atherosclerosis development, we considered that the D-[113–122]apoJ peptide could retard the progression of atherosclerotic lesions. Furthermore, since the qualitative characteristics of LDL and HDL determine its atherogenicity or anti-atherogenicity, respectively [47, 105, 194, 195], we hypothesized that this peptide could reach protective roles



by improving lipoprotein function, and a possible new therapy could be developed based on these effects.

Genetic defects in the LDL receptor produce hypercholesterolemia in humans with familial hypercholesterolemia (FH). Patients with this condition in homozygosis, have vastly elevated levels of IDL and LDL, and they develop atherosclerosis at an early age [196]. There are two hypercholesterolemic mouse models which similarly reproduce this HF condition, and they have been widely used as animal models of atherogenesis, the apo-E deficient mouse and the LDL receptor-deficient [30]. Previous studies have demonstrated that LDLR-KO mice under CD show mildly increased plasma cholesterol levels from an accumulation of LDL and develop no or only minimal atherosclerotic lesions in the proximal aortic root [27]. We choose the LDLR-KO mice over the apoE-KO mice because the LDLR-KO mouse specifically shows an increase in the level of both VLDL and LDL particles, in contrast with apoE-KO, which mainly increases VLDL particles and has low levels of LDL-like particles. Although LDL was not the only target lipoprotein in this study, we wanted to analyze the susceptibility to aggregation of these particles. LDL from LDLR-KO is similar in size and density to human LDL [197]. To accelerate the onset of atherosclerosis we fed the animals with a high-fat diet or WD, thus, the development of arteriosclerotic lesions and high LDL plasma concentrations were guaranteed.

As mentioned before, Navab *et al.* demonstrated that the oral administration of D-[113–122]apoJ peptide for 24 weeks reduced atherosclerosis in apoE-KO mice by 70.2% in the aortic root sinus lesion area. It was associated with a significant increase in HDL-cholesterol levels and an increase in HDL paraoxonase activity. Also, this peptide significantly improved the ability of apoE-KO mice plasma to promote cholesterol efflux from macrophages [171]. Data shown in our study

demonstrated a reduction of 40% of aortic root atherosclerotic lesion areas under hyperlipidemic conditions as a consequence of qualitative improvements of both the antiatherogenic HDL abilities and the LDL atherogenic properties. These results agreed with those found by Navab *et al.* when the same peptide was administered to apoE-KO mice. However, we fed the LDLR-KO mice an atherogenic diet, while in the study of Navab *et al.*, the apoE-KO mice were fed a chow diet. As a result, the plasma cholesterol concentrations were much higher in our model, and probably, the development of lesions should be higher as well. Despite these higher levels of cholesterol the D-[113–122]apoJ peptide was able to reduce the extent of atherosclerotic lesions.

The administration of [113–122]apoJ peptide did not change the usual mice plasma lipoprotein concentration, consequently, their lipoprotein profile was unaffected. Regarding lipoprotein composition, our data showed an increased concentration of free cholesterol in the HDL of D-[113–122]apoJ-treated mice. Higher content of free cholesterol on the surface of the lipoproteins reduces their oxidizability by enhancing the lipid packaging [198, 199], which could be an important factor for the preservation of the antioxidant properties seen in the HDL from these treated mice. Both, HDL susceptibility to oxidation and HDL antioxidant capacity from D-[113–122]apoJ-treated mice group, were improved. This observation agrees with the study by Navab *et al.*, which proved that D-[113–122]apoJ diminishes the content of lipoperoxides in lipoproteins from monkeys treated with this peptide [171]. In this way, this lipoperoxide-sequestering action of D-[113–122]apoJ could be important to explain the decreased susceptibility to oxidation of HDL, as well as its increased antioxidative properties. Moreover, it was shown a rise in the HDL capacity from D-[113–122]apoJ-treated mice to promote the efflux of cholesterol from macrophages.

The use of the LDLR-KO mice model allowed us to evaluate the peptide effects on murine LDL, which is scarce in most mice models. Our results show that neither the LDL composition nor the LDL susceptibility to oxidation from D-[113–122]apoJ-treated mice changes after treatment. In contrast, the use of the peptide enhanced other LDL atherogenic characteristics or reduced atherogenic characteristics. D-[113–122]apoJ treatment prevented the LDL aggregation induced *in vitro* by SMase, which might indicate that the LDL particles present in the blood of treated mice are less susceptible to the *in vivo* aggregation process. Consequently, it could be extrapolated that LDL would be possibly protected from the aggregation in the subendothelial environment, thus preventing lipoprotein retention. Another atherogenic characteristic of LDL is its electronegativity, which has been extensively studied in humans [200] but in mice is not so well described. Even though, some studies reported an increased proportion of these particles in rodents undergoing accelerated atherosclerosis [201, 202]. In accordance with these studies, we found that the electronegativity of the LDL particles was lower in those mice treated with than control or scramble groups. However, the reason for this decreased negative electric charge of LDL is still unclear. It might be due to the improved antioxidant capacity of HDL preventing the formation of oxidized LDL. Another possible mechanism is the decrease of liver inflammation, which could indicate a reduction in the systemic inflammation status, which in turn would imply fewer lipoprotein modifications by oxidative stress, or increased expression at the arterial wall level of lipases and proteases. All these D-[113–122]apoJ peptide effects on LDL of treated mice could also have contributed to the reduced atherosclerotic lesions observed in these mice.

Inflammation is an important process in the development of atherosclerosis and the liver plays a key role in CVD [203]. Accordingly, we determine the possible anti-inflammatory effect of the D-[113–122]apoJ peptide through

the hepatic expression of genes that are implicated in inflammation. We selected *Tnf*, *Ccl2*, and *Cd68* genes, whose mRNA levels are usually elevated in hepatic inflammation [204]. *Tnf* and *Ccl2*, two inflammatory mediators, showed a reduced hepatic expression in those mice treated with the D-[113–122]apoJ peptide. Also, a decreased gene expression of *Cd68* in these mice was observed, which suggests lower infiltration of macrophages in the liver. Moreover, the expression of the scavenger receptor CD36 was significantly lower in treated mice. It means that the increased liver Cd36 expression related to improved hepatic fatty acid uptake and triglyceride accumulation, as a result of a high-fat diet [205], is prevented by the administration of the D-[113–122]apoJ peptide. Overall, the use of D-[113–122]apoJ improves some alterations induced by an atherogenic diet in liver inflammation.

As we hypothesized before, our results strongly indicate that D-[113–122]apoJ peptide acts through several different mechanisms on lipoprotein function and also at the hepatic level, and the combination of these effects could be responsible for atheroprotection. One observation in our study which is important to highlight is that the correlation analysis revealed that the parameters related to the reduction in atherosclerosis development were the susceptibility to the oxidation of HDL and the electronegativity of LDL. This finding demonstrates the special significance to preserve the physiological properties of both lipoproteins.

However, the specific mechanisms by which the peptide shows this protective action are not completely understood. Our first publication describes that D-[113–122]apoJ protects LDL from induced in vitro aggregation through the binding of the peptide to hydrophobic patches in the lipoprotein surface generated during the aggregation process [206]. Consequently, it may be the cause of decreased susceptibility to aggregation observed ex vivo. Nevertheless, the reason for other

lipoprotein-related protective effects induced by D-[113–122]apoJ is unclear. For example, the decreased negative electric charge of LDL might be due to the improved antioxidant capacity of HDL preventing the formation of oxidized LDL, but how the peptide renders HDL molecules with increased antioxidant potential is unknown. However, the fact that other amphipathic peptides, such as 4F and 5F display similar effects on HDL oxidizability suggest a common mechanism. This mechanism could be related to the capacity of amphipathic peptides to sequester lipoperoxides facilitating their deactivation by enzymes carried by HDL, such as PON1, PAF-AH, CETP, LCAT, or glutathione reductase [169, 170].

Regarding the improvement of the expression of inflammatory mediators induced by D-[113–122]apoJ in the liver, the mechanisms involved are unclear and further studies are necessary to unravel this effect. However, in agreement with our data, other studies using mimetic peptides from apoA-I have found similar results [207-211]. These coincidences could also be related to having an amphipathic helix structure. The decrease in liver inflammation not only could have a protective effect reducing systemic inflammation but also could affect lipoprotein function. Thus, it could have an effect on the electronegativity of LDL since an increase in inflammatory mediators causes a greater expression of lipases and proteases, which in turn results in the modification of lipoproteins.

In conclusion, our data indicate that D-[113–122]apoJ mimetic peptide could be a potential therapy against atherosclerosis, by acting on different atherogenic mechanisms, including lipoprotein and hepatic function. However, further analyses are warranted to achieve a better understanding of the effects displayed by D-[113–122]apoJ on other aspects of the lipid metabolism, as well as to determine its safety.

- **CONCLUSIONS**



From the results presented in this thesis, we can conclude:

1. D-[113–122]apoJ peptide retards the spontaneous and SMase-induced *in vitro* LDL aggregation process at a molar ratio of 1:1 (apoB/peptide).
2. The D-[113–122]apoJ binding to the LDL occurs during the early stages of aggregation, however, this ability is reduced as aggregation progresses.
3. The presence of D-[113–122]apoJ peptide enhances the rigidity of the LDL surface. Consequently, the LDL aggregation is prevented by an increase of the lipid packaging order in the lipoprotein surface.
4. Subcutaneous administration of D-[113–122]apoJ reduces aortic atherosclerosis in LDLR-KO mice fed with atherogenic diet independently of alterations on lipoprotein profile.
5. D-[113–122]apoJ peptide favorably influences the oxidative properties of lipoproteins, specifically, the HDL susceptibility to oxidation is improved as well as the HDL capacity to retard the oxidation of human LDL.
6. D-[113–122]apoJ treatment prevents the aggregation of LDL induced *in vitro* by SMase.
7. D-[113–122]apoJ treatment decreases the LDL electronegativity.



8. The cholesterol efflux capacity of HDL is improved by D-[113–122]apoJ peptide.
9. D-[113–122]apoJ reduces the hepatic expression of inflammation-related genes and significantly correlates with aortic lesions.
10. The susceptibility to oxidation of HDL and the electronegativity of LDL significantly correlate with the area of atherosclerotic lesions in those mice treated with D-[113–122]apoJ peptide.

## ■ REFERENCES



- [1] P. Libby, A.H. Lichtman, G.K. Hansson, Immune effector mechanisms implicated in atherosclerosis: from mice to humans, *Immunity* 38(6) (2013) 1092-104.
- [2] B. Emini Veseli, P. Perrotta, G.R.A. De Meyer, L. Roth, C. Van der Donckt, W. Martinet, G.R.Y. De Meyer, Animal models of atherosclerosis, *Eur J Pharmacol* 816 (2017) 3-13.
- [3] A.J. Lusis, Atherosclerosis, *Nature* 407(6801) (2000) 233-41.
- [4] G.R. Geovanini, P. Libby, Atherosclerosis and inflammation: overview and updates, *Clin Sci (Lond)* 132(12) (2018) 1243-1252.
- [5] P. Libby, Inflammation in atherosclerosis, *Nature* 420(6917) (2002) 868-74.
- [6] J.P. Strong, G.T. Malcom, C.A. McMahan, R.E. Tracy, W.P. Newman, 3rd, E.E. Herderick, J.F. Cornhill, Prevalence and extent of atherosclerosis in adolescents and young adults: implications for prevention from the Pathobiological Determinants of Atherosclerosis in Youth Study, *JAMA* 281(8) (1999) 727-35.
- [7] Natural history of aortic and coronary atherosclerotic lesions in youth. Findings from the PDAY Study. Pathobiological Determinants of Atherosclerosis in Youth (PDAY) Research Group, *Arterioscler Thromb* 13(9) (1993) 1291-8.
- [8] H.C. Stary, *Atlas of Atherosclerosis - Progression and Regression*, The Parthenon Publishing Group Inc, New York, 2003.
- [9] B.A. Ference, H.N. Ginsberg, I. Graham, K.K. Ray, C.J. Packard, E. Bruckert, R.A. Hegele, R.M. Krauss, F.J. Raal, H. Schunkert, G.F. Watts, J. Borén, S. Fazio, J.D. Horton, L. Masana, S.J. Nicholls, B.G. Nordestgaard, B. van de Sluis, M.R. Taskinen, L. Tokgözoğlu, U. Landmesser, U. Laufs, O. Wiklund, J.K. Stock, M.J. Chapman, A.L. Catapano, Low-density lipoproteins cause atherosclerotic cardiovascular disease. 1. Evidence from genetic, epidemiologic, and clinical studies. A consensus statement from the European Atherosclerosis Society Consensus Panel, *Eur Heart J* 38(32) (2017) 2459-2472.
- [10] J. Borén, M.J. Chapman, R.M. Krauss, C.J. Packard, J.F. Bentzon, C.J. Binder, M.J. Daemen, L.L. Demer, R.A. Hegele, S.J. Nicholls, B.G. Nordestgaard, G.F. Watts, E. Bruckert, S. Fazio, B.A. Ference, I. Graham, J.D. Horton, U. Landmesser, U. Laufs, L. Masana, G. Pasterkamp, F.J. Raal, K.K. Ray, H. Schunkert, M.R. Taskinen, B. van de Sluis, O. Wiklund, L. Tokgozoglul, A.L. Catapano, H.N. Ginsberg, Low-density lipoproteins cause atherosclerotic cardiovascular disease: pathophysiological, genetic, and therapeutic insights: a consensus statement from the European

Atherosclerosis Society Consensus Panel, *Eur Heart J* 41(24) (2020) 2313-2330.

[11] M. Bäck, A. Yurdagul, Jr., I. Tabas, K. Öörni, P.T. Kovanen, Inflammation and its resolution in atherosclerosis: mediators and therapeutic opportunities, *Nat Rev Cardiol* 16(7) (2019) 389-406.

[12] W. Insull, Jr., The pathology of atherosclerosis: plaque development and plaque responses to medical treatment, *Am J Med* 122(1 Suppl) (2009) S3-S14.

[13] A.P. Burke, F.D. Kolodgie, A. Farb, D.K. Weber, G.T. Malcom, J. Smialek, R. Virmani, Healed plaque ruptures and sudden coronary death: evidence that subclinical rupture has a role in plaque progression, *Circulation* 103(7) (2001) 934-40.

[14] D.A. Eggen, L.A. Solberg, Variation of atherosclerosis with age, *Lab Invest* 18(5) (1968) 571-9.

[15] R. Virmani, F.D. Kolodgie, A.P. Burke, A. Farb, S.M. Schwartz, Lessons from sudden coronary death: a comprehensive morphological classification scheme for atherosclerotic lesions, *Arterioscler Thromb Vasc Biol* 20(5) (2000) 1262-75.

[16] P.K. Cheruvu, A.V. Finn, C. Gardner, J. Caplan, J. Goldstein, G.W. Stone, R. Virmani, J.E. Muller, Frequency and distribution of thin-cap fibroatheroma and ruptured plaques in human coronary arteries: a pathologic study, *J Am Coll Cardiol* 50(10) (2007) 940-9.

[17] P.R. Moreno, K.R. Purushothaman, E. Zias, J. Sanz, V. Fuster, Neovascularization in human atherosclerosis, *Curr Mol Med* 6(5) (2006) 457-77.

[18] B.A. Ference, D.L. Bhatt, A.L. Catapano, C.J. Packard, I. Graham, S. Kaptoge, T.B. Ference, Q. Guo, U. Laufs, C.T. Ruff, A. Cupido, G.K. Hovingh, J. Danesh, M.V. Holmes, G.D. Smith, K.K. Ray, S.J. Nicholls, M.S. Sabatine, Association of Genetic Variants Related to Combined Exposure to Lower Low-Density Lipoproteins and Lower Systolic Blood Pressure With Lifetime Risk of Cardiovascular Disease, *Jama* 322(14) (2019) 1381-1391.

[19] A.R. Bond, C.L. Jackson, The fat-fed apolipoprotein E knockout mouse brachiocephalic artery in the study of atherosclerotic plaque rupture, *J Biomed Biotechnol* 2011 (2011) 379069.

[20] G.S. Getz, C.A. Reardon, Animal models of atherosclerosis, *Arterioscler Thromb Vasc Biol* 32(5) (2012) 1104-15.

[21] K.S. Meir, E. Leitersdorf, Atherosclerosis in the apolipoprotein-E-deficient mouse: a decade of progress, *Arterioscler Thromb Vasc Biol* 24(6) (2004) 1006-14.

- [22] J.A. Piedrahita, S.H. Zhang, J.R. Hagaman, P.M. Oliver, N. Maeda, Generation of mice carrying a mutant apolipoprotein E gene inactivated by gene targeting in embryonic stem cells, *Proc Natl Acad Sci U S A* 89(10) (1992) 4471-5.
- [23] A.S. Plump, J.D. Smith, T. Hayek, K. Aalto-Setälä, A. Walsh, J.G. Verstuyft, E.M. Rubin, J.L. Breslow, Severe hypercholesterolemia and atherosclerosis in apolipoprotein E-deficient mice created by homologous recombination in ES cells, *Cell* 71(2) (1992) 343-53.
- [24] P.A. VanderLaan, C.A. Reardon, G.S. Getz, Site specificity of atherosclerosis: site-selective responses to atherosclerotic modulators, *Arterioscler Thromb Vasc Biol* 24(1) (2004) 12-22.
- [25] C. Silvestre-Roig, M.P. de Winther, C. Weber, M.J. Daemen, E. Lutgens, O. Soehnlein, Atherosclerotic plaque destabilization: mechanisms, models, and therapeutic strategies, *Circ Res* 114(1) (2014) 214-26.
- [26] J.C. Defesche, Low-density lipoprotein receptor--its structure, function, and mutations, *Semin Vasc Med* 4(1) (2004) 5-11.
- [27] S. Ishibashi, M.S. Brown, J.L. Goldstein, R.D. Gerard, R.E. Hammer, J. Herz, Hypercholesterolemia in low density lipoprotein receptor knockout mice and its reversal by adenovirus-mediated gene delivery, *J Clin Invest* 92(2) (1993) 883-93.
- [28] S. Ishibashi, J.L. Goldstein, M.S. Brown, J. Herz, D.K. Burns, Massive xanthomatosis and atherosclerosis in cholesterol-fed low density lipoprotein receptor-negative mice, *J Clin Invest* 93(5) (1994) 1885-93.
- [29] G.S. Getz, C.A. Reardon, Do the Apoe<sup>-/-</sup> and Ldlr<sup>-/-</sup> Mice Yield the Same Insight on Atherogenesis?, *Arterioscler Thromb Vasc Biol* 36(9) (2016) 1734-41.
- [30] M.M. Veniant, S. Withycombe, S.G. Young, Lipoprotein size and atherosclerosis susceptibility in Apoe<sup>-/-</sup> and Ldlr<sup>-/-</sup> mice, *Arterioscler Thromb Vasc Biol* 21(10) (2001) 1567-70.
- [31] E. Sehayek, J.G. Ono, E.M. Duncan, A.K. Batta, G. Salen, S. Shefer, L.B. Nguyen, K. Yang, M. Lipkin, J.L. Breslow, Hyodeoxycholic acid efficiently suppresses atherosclerosis formation and plasma cholesterol levels in mice, *J Lipid Res* 42(8) (2001) 1250-6.
- [32] R.E. Moore, M.A. Kawashiri, K. Kitajima, A. Secreto, J.S. Millar, D. Pratico, D.J. Rader, Apolipoprotein A-I deficiency results in markedly increased atherosclerosis in mice lacking the LDL receptor, *Arterioscler Thromb Vasc Biol* 23(10) (2003) 1914-20.
- [33] S.H. Zhang, R.L. Reddick, J.A. Piedrahita, N. Maeda, Spontaneous hypercholesterolemia and arterial lesions in mice lacking apolipoprotein E, *Science* 258(5081) (1992) 468-71.

- [34] K. Hartvigsen, C.J. Binder, L.F. Hansen, A. Rafia, J. Juliano, S. Horkko, D. Steinberg, W. Palinski, J.L. Witztum, A.C. Li, A diet-induced hypercholesterolemic murine model to study atherogenesis without obesity and metabolic syndrome, *Arterioscler Thromb Vasc Biol* 27(4) (2007) 878-85.
- [35] G.S. Getz, C.A. Reardon, Diet and murine atherosclerosis, *Arterioscler Thromb Vasc Biol* 26(2) (2006) 242-9.
- [36] P.A. VanderLaan, C.A. Reardon, R.A. Thisted, G.S. Getz, VLDL best predicts aortic root atherosclerosis in LDL receptor deficient mice, *J Lipid Res* 50(3) (2009) 376-85.
- [37] J.W. Knowles, N. Maeda, Genetic modifiers of atherosclerosis in mice, *Arterioscler Thromb Vasc Biol* 20(11) (2000) 2336-45.
- [38] M.M. Veniant, M.A. Sullivan, S.K. Kim, P. Ambroziak, A. Chu, M.D. Wilson, M.K. Hellerstein, L.L. Rudel, R.L. Walzem, S.G. Young, Defining the atherogenicity of large and small lipoproteins containing apolipoprotein B100, *J Clin Invest* 106(12) (2000) 1501-10.
- [39] Y. Ma, W. Wang, J. Zhang, Y. Lu, W. Wu, H. Yan, Y. Wang, Hyperlipidemia and atherosclerotic lesion development in Ldlr-deficient mice on a long-term high-fat diet, *PLoS One* 7(4) (2012) e35835.
- [40] H.H. Hobbs, D.W. Russell, M.S. Brown, J.L. Goldstein, The LDL receptor locus in familial hypercholesterolemia: mutational analysis of a membrane protein, *Annu Rev Genet* 24 (1990) 133-70.
- [41] Y.T. Lee, H.Y. Lin, Y.W. Chan, K.H. Li, O.T. To, B.P. Yan, T. Liu, G. Li, W.T. Wong, W. Keung, G. Tse, Mouse models of atherosclerosis: a historical perspective and recent advances, *Lipids Health Dis* 16(1) (2017) 12.
- [42] J.M. Ordovas, Lipoproteins, in: B. Caballero (Ed.) *Encyclopedia of Food Sciences and Nutrition*, Academic Press, San Diego, California, 2003, pp. 3543-3552.
- [43] G. Lo Sasso, W.K. Schlage, S. Boue, E. Veljkovic, M.C. Peitsch, J. Hoeng, The Apoe(-/-) mouse model: a suitable model to study cardiovascular and respiratory diseases in the context of cigarette smoke exposure and harm reduction, *J Transl Med* 14(1) (2016) 146.
- [44] K.R. Feingold, C. Grunfeld, Introduction to Lipids and Lipoproteins, in: K.R. Feingold, B. Anawalt, A. Boyce, G. Chrousos, W.W. de Herder, K. Dungan, A. Grossman, J.M. Hershman, H.J. Hofland, G. Kaltsas, C. Koch, P. Kopp, M. Korbonits, R. McLachlan, J.E. Morley, M. New, J. Purnell, F. Singer, C.A. Stratakis, D.L. Trencce, D.P. Wilson (Eds.), *Endotext*, South Dartmouth (MA), 2000.
- [45] I. Ramasamy, Recent advances in physiological lipoprotein metabolism, *Clin Chem Lab Med* 52(12) (2014) 1695-727.

- [46] M.S. Brown, J.L. Goldstein, Lipoprotein metabolism in the macrophage: implications for cholesterol deposition in atherosclerosis, *Annu Rev Biochem* 52 (1983) 223-61.
- [47] M.R. Diffenderfer, E.J. Schaefer, The composition and metabolism of large and small LDL, *Curr Opin Lipidol* 25(3) (2014) 221-6.
- [48] H.J. Pownall, C. Rosales, B.K. Gillard, A.M. Gotto, Jr., High-density lipoproteins, reverse cholesterol transport and atherogenesis, *Nat Rev Cardiol* (2021).
- [49] H. Dieplinger, R. Zechner, G.M. Kostner, The in vitro formation of HDL2 during the action of LCAT: the role of triglyceride-rich lipoproteins, *J Lipid Res* 26(3) (1985) 273-82.
- [50] C. Bruce, R.A. Chouinard, Jr., A.R. Tall, Plasma lipid transfer proteins, high-density lipoproteins, and reverse cholesterol transport, *Annu Rev Nutr* 18 (1998) 297-330.
- [51] S. Acton, A. Rigotti, K.T. Landschulz, S. Xu, H.H. Hobbs, M. Krieger, Identification of scavenger receptor SR-BI as a high density lipoprotein receptor, *Science* 271(5248) (1996) 518-20.
- [52] B.C. Kwan, F. Kronenberg, S. Beddhu, A.K. Cheung, Lipoprotein metabolism and lipid management in chronic kidney disease, *J Am Soc Nephrol* 18(4) (2007) 1246-61.
- [53] T.M.B. Page, Lipoproteins, Blood Lipids, and Lipoprotein Metabolism, 2021. <http://themedicalbiochemistrypage.org/lipoproteins-blood-lipids-and-lipoprotein-metabolism/>. (Accessed 23 June 2021 2021).
- [54] T.N. Tulenko, A.E. Sumner, The physiology of lipoproteins, *J Nucl Cardiol* 9(6) (2002) 638-49.
- [55] E.A. Fisher, J.E. Feig, B. Hewing, S.L. Hazen, J.D. Smith, High-density lipoprotein function, dysfunction, and reverse cholesterol transport, *Arterioscler Thromb Vasc Biol* 32(12) (2012) 2813-20.
- [56] W.S. Davidson, R.A. Silva, S. Chantepie, W.R. Lagor, M.J. Chapman, A. Kontush, Proteomic analysis of defined HDL subpopulations reveals particle-specific protein clusters: relevance to antioxidative function, *Arterioscler Thromb Vasc Biol* 29(6) (2009) 870-6.
- [57] K.-H. Cho, High-density lipoproteins as biomarkers and therapeutic tools, Springer, Singapore, 2019.
- [58] D. Rhoads, J.C. Tardif, From HDL-cholesterol to HDL-function: cholesterol efflux capacity determinants, *Curr Opin Lipidol* 30(2) (2019) 101-107.
- [59] M.P. Adorni, N. Ronda, F. Bernini, F. Zimetti, High Density Lipoprotein Cholesterol Efflux Capacity and Atherosclerosis in Cardiovascular Disease:



Pathophysiological Aspects and Pharmacological Perspectives, *Cells* 10(3) (2021).

[60] H.Y. Choi, A. Hafiane, A. Schwertani, J. Genest, High-Density Lipoproteins: Biology, Epidemiology, and Clinical Management, *Can J Cardiol* 33(3) (2017) 325-333.

[61] M. Navab, G.M. Ananthramaiah, S.T. Reddy, B.J. Van Lenten, B.J. Ansell, G.C. Fonarow, K. Vahabzadeh, S. Hama, G. Hough, N. Kamranpour, J.A. Berliner, A.J. Lusis, A.M. Fogelman, The oxidation hypothesis of atherogenesis: the role of oxidized phospholipids and HDL, *J Lipid Res* 45(6) (2004) 993-1007.

[62] F. Brites, M. Martin, I. Guillas, A. Kontush, Antioxidative activity of high-density lipoprotein (HDL): Mechanistic insights into potential clinical benefit, *BBA Clin* 8 (2017) 66-77.

[63] A. Kontush, S. Chantepie, M.J. Chapman, Small, dense HDL particles exert potent protection of atherogenic LDL against oxidative stress, *Arterioscler Thromb Vasc Biol* 23(10) (2003) 1881-8.

[64] M. Navab, S.Y. Hama, G.P. Hough, G. Subbanagounder, S.T. Reddy, A.M. Fogelman, A cell-free assay for detecting HDL that is dysfunctional in preventing the formation of or inactivating oxidized phospholipids, *J Lipid Res* 42(8) (2001) 1308-17.

[65] M. Navab, S.S. Imes, S.Y. Hama, G.P. Hough, L.A. Ross, R.W. Bork, A.J. Valente, J.A. Berliner, D.C. Drinkwater, H. Laks, et al., Monocyte transmigration induced by modification of low density lipoprotein in cocultures of human aortic wall cells is due to induction of monocyte chemotactic protein 1 synthesis and is abolished by high density lipoprotein, *J Clin Invest* 88(6) (1991) 2039-46.

[66] B.J. Van Lenten, S.Y. Hama, F.C. de Beer, D.M. Stafforini, T.M. McIntyre, S.M. Prescott, B.N. La Du, A.M. Fogelman, M. Navab, Anti-inflammatory HDL becomes pro-inflammatory during the acute phase response. Loss of protective effect of HDL against LDL oxidation in aortic wall cell cocultures, *J Clin Invest* 96(6) (1995) 2758-67.

[67] E.M. Tsompanidi, M.S. Brinkmeier, E.H. Fotiadou, S.M. Giakoumi, K.E. Kypreos, HDL biogenesis and functions: role of HDL quality and quantity in atherosclerosis, *Atherosclerosis* 208(1) (2010) 3-9.

[68] P. Penson, D.L. Long, G. Howard, V.J. Howard, S.R. Jones, S.S. Martin, D.P. Mikhailidis, P. Muntner, M. Rizzo, D.J. Rader, M.M. Safford, A. Sahebkar, P.P. Toth, M. Banach, Associations between cardiovascular disease, cancer, and very low high-density lipoprotein cholesterol in the REasons for Geographical and Racial Differences in Stroke (REGARDS) study, *Cardiovasc Res* 115(1) (2019) 204-212.

- [69] T. Hevonoja, M.O. Pentikainen, M.T. Hyvonen, P.T. Kovanen, M. Ala-Korpela, Structure of low density lipoprotein (LDL) particles: basis for understanding molecular changes in modified LDL, *Biochim Biophys Acta* 1488(3) (2000) 189-210.
- [70] A. Sommer, E. Prenner, R. Gorges, H. Stütz, H. Grillhofer, G.M. Kostner, F. Paltauf, A. Hermetter, Organization of phosphatidylcholine and sphingomyelin in the surface monolayer of low density lipoprotein and lipoprotein(a) as determined by time-resolved fluorometry, *J Biol Chem* 267(34) (1992) 24217-22.
- [71] S. Lund-Katz, M.C. Phillips, Packing of cholesterol molecules in human low-density lipoprotein, *Biochemistry* 25(7) (1986) 1562-8.
- [72] M. Dashty, M.M. Motazacker, J. Levels, M. de Vries, M. Mahmoudi, M.P. Peppelenbosch, F. Rezaee, Proteome of human plasma very low-density lipoprotein and low-density lipoprotein exhibits a link with coagulation and lipid metabolism, *Thromb Haemost* 111(3) (2014) 518-30.
- [73] H. Karlsson, P. Leanderson, C. Tagesson, M. Lindahl, Lipoproteomics I: mapping of proteins in low-density lipoprotein using two-dimensional gel electrophoresis and mass spectrometry, *Proteomics* 5(2) (2005) 551-65.
- [74] H. Karlsson, H. Mörtstedt, H. Lindqvist, C. Tagesson, M. Lindahl, Protein profiling of low-density lipoprotein from obese subjects, *Proteomics Clin Appl* 3(6) (2009) 663-71.
- [75] C.K. Mathews, K.E. Van Holde, K.G. Ahern, *Biochemistry*, 3rd ed., Benjamin Cummings, San Francisco, Calif., 2000.
- [76] J.L. Goldstein, M.S. Brown, The LDL receptor, *Arterioscler Thromb Vasc Biol* 29(4) (2009) 431-8.
- [77] J.L. Goldstein, M.S. Brown, A century of cholesterol and coronaries: from plaques to genes to statins, *Cell* 161(1) (2015) 161-172.
- [78] L. Zhang, K. Reue, L.G. Fong, S.G. Young, P. Tontonoz, Feedback regulation of cholesterol uptake by the LXR-IDOL-LDLR axis, *Arterioscler Thromb Vasc Biol* 32(11) (2012) 2541-6.
- [79] V.I. Summerhill, A.V. Grechko, S.F. Yet, I.A. Sobenin, A.N. Orekhov, The Atherogenic Role of Circulating Modified Lipids in Atherosclerosis, *Int J Mol Sci* 20(14) (2019).
- [80] D. Steinberg, In celebration of the 100th anniversary of the lipid hypothesis of atherosclerosis, *J Lipid Res* 54(11) (2013) 2946-9.
- [81] S.S. Martin, R.S. Blumenthal, M. Miller, LDL cholesterol: the lower the better, *Med Clin North Am* 96(1) (2012) 13-26.
- [82] F. Sala, A.L. Catapano, G.D. Norata, High density lipoproteins and atherosclerosis: emerging aspects, *J Geriatr Cardiol* 9(4) (2012) 401-7.

- [83] E.R. Zakiev, V.N. Sukhorukov, A.A. Melnichenko, I.A. Sobenin, E.A. Ivanova, A.N. Orekhov, Lipid composition of circulating multiple-modified low density lipoprotein, *Lipids Health Dis* 15(1) (2016) 134.
- [84] V.V. Tertov, V.V. Kaplun, I.A. Sobenin, A.N. Orekhov, Low-density lipoprotein modification occurring in human plasma possible mechanism of in vivo lipoprotein desialylation as a primary step of atherogenic modification, *Atherosclerosis* 138(1) (1998) 183-95.
- [85] V.V. Tertov, V.V. Kaplun, I.A. Sobenin, E.Y. Boytsova, N.V. Bovin, A.N. Orekhov, Human plasma trans-sialidase causes atherogenic modification of low density lipoprotein, *Atherosclerosis* 159(1) (2001) 103-15.
- [86] Z. Oztürk, H. Sönmez, F.M. Görgün, H. Ekmekçi, D. Bilgen, N. Ozen, V. Sözer, T. Altuğ, E. Kökoğlu, The Relationship Between Lipid Peroxidation and LDL Desialylation in Experimental Atherosclerosis, *Toxicol Mech Methods* 17(5) (2007) 265-73.
- [87] A.N. Orekhov, Y.V. Bobryshev, I.A. Sobenin, A.A. Melnichenko, D.A. Chistiakov, Modified low density lipoprotein and lipoprotein-containing circulating immune complexes as diagnostic and prognostic biomarkers of atherosclerosis and type 1 diabetes macrovascular disease, *Int J Mol Sci* 15(7) (2014) 12807-41.
- [88] E.A. Ivanova, Y.V. Bobryshev, A.N. Orekhov, LDL electronegativity index: a potential novel index for predicting cardiovascular disease, *Vasc Health Risk Manag* 11 (2015) 525-32.
- [89] A.N. Orekhov, I.A. Sobenin, Modified lipoproteins as biomarkers of atherosclerosis, *Front Biosci (Landmark Ed)* 23 (2018) 1422-1444.
- [90] E.A. Ivanova, V.A. Myasoedova, A.A. Melnichenko, A.V. Grechko, A.N. Orekhov, Small Dense Low-Density Lipoprotein as Biomarker for Atherosclerotic Diseases, *Oxid Med Cell Longev* 2017 (2017) 1273042.
- [91] A.V. Poznyak, N.G. Nikiforov, A.M. Markin, D.A. Kashirskikh, V.A. Myasoedova, E.V. Gerasimova, A.N. Orekhov, Overview of OxLDL and Its Impact on Cardiovascular Health: Focus on Atherosclerosis, *Front Pharmacol* 11 (2020) 613780.
- [92] H.S. Kruth, W. Huang, I. Ishii, W.Y. Zhang, Macrophage foam cell formation with native low density lipoprotein, *J Biol Chem* 277(37) (2002) 34573-80.
- [93] D. Harrison, K.K. Griendling, U. Landmesser, B. Hornig, H. Drexler, Role of oxidative stress in atherosclerosis, *Am J Cardiol* 91(3A) (2003) 7A-11A.
- [94] C. Khatana, N.K. Saini, S. Chakrabarti, V. Saini, A. Sharma, R.V. Saini, A.K. Saini, Mechanistic Insights into the Oxidized Low-Density Lipoprotein-Induced Atherosclerosis, *Oxid Med Cell Longev* 2020 (2020) 5245308.

- [95] R. Carnevale, S. Bartimoccia, C. Nocella, S. Di Santo, L. Loffredo, G. Illuminati, E. Lombardi, V. Boz, M. Del Ben, L. De Marco, P. Pignatelli, F. Violi, LDL oxidation by platelets propagates platelet activation via an oxidative stress-mediated mechanism, *Atherosclerosis* 237(1) (2014) 108-16.
- [96] M. Alique, C. Luna, J. Carracedo, R. Ramírez, LDL biochemical modifications: a link between atherosclerosis and aging, *Food Nutr Res* 59 (2015) 29240.
- [97] L. Toma, C.S. Stancu, A.V. Sima, Endothelial Dysfunction in Diabetes Is Aggravated by Glycated Lipoproteins; Novel Molecular Therapies, *Biomedicines* 9(1) (2020).
- [98] F.J. Tames, M.I. Mackness, S. Arrol, I. Laing, P.N. Durrington, Non-enzymatic glycation of apolipoprotein B in the sera of diabetic and non-diabetic subjects, *Atherosclerosis* 93(3) (1992) 237-44.
- [99] K.K. Berneis, R.M. Krauss, Metabolic origins and clinical significance of LDL heterogeneity, *J Lipid Res* 43(9) (2002) 1363-79.
- [100] S. Hirayama, T. Miida, Small dense LDL: An emerging risk factor for cardiovascular disease, *Clin Chim Acta* 414 (2012) 215-24.
- [101] C. Packard, M. Caslake, J. Shepherd, The role of small, dense low density lipoprotein (LDL): a new look, *Int J Cardiol* 74 Suppl 1 (2000) S17-22.
- [102] A.G. Basnakian, S.V. Shah, E. Ok, E. Altunel, E.O. Apostolov, Carbamylated LDL, *Adv Clin Chem* 51 (2010) 25-52.
- [103] T. Speer, F.O. Owala, E.W. Holy, S. Zewinger, F.L. Frenzel, B.E. Stahli, M. Razavi, S. Triem, H. Cvija, L. Rohrer, S. Seiler, G.H. Heine, V. Jankowski, J. Jankowski, G.G. Camici, A. Akhmedov, D. Fliser, T.F. Luscher, F.C. Tanner, Carbamylated low-density lipoprotein induces endothelial dysfunction, *Eur Heart J* 35(43) (2014) 3021-32.
- [104] F.H. Verbrugge, W.H. Tang, S.L. Hazen, Protein carbamylation and cardiovascular disease, *Kidney Int* 88(3) (2015) 474-8.
- [105] A. Rivas-Urbina, A. Rull, J. Ordonez-Llanos, J.L. Sanchez-Quesada, Electronegative LDL: An Active Player in Atherogenesis or a By- Product of Atherosclerosis?, *Curr Med Chem* 26(9) (2019) 1665-1679.
- [106] G. Cazzolato, P. Avogaro, G. Bittolo-Bon, Characterization of a more electronegatively charged LDL subfraction by ion exchange HPLC, *Free Radic Biol Med* 11(3) (1991) 247-53.
- [107] A.P. Mello, I.T. da Silva, D.S. Abdalla, N.R. Damasceno, Electronegative low-density lipoprotein: origin and impact on health and disease, *Atherosclerosis* 215(2) (2011) 257-65.

- [108] J.L. Sánchez-Quesada, S. Villegas, J. Ordóñez-Llanos, Electronegative low-density lipoprotein. A link between apolipoprotein B misfolding, lipoprotein aggregation and proteoglycan binding, *Curr Opin Lipidol* 23(5) (2012) 479-86.
- [109] S. Akyol, J. Lu, O. Akyol, F. Akcay, F. Armutcu, L.Y. Ke, C.H. Chen, The role of electronegative low-density lipoprotein in cardiovascular diseases and its therapeutic implications, *Trends Cardiovasc Med* 27(4) (2017) 239-246.
- [110] J.L. Sánchez-Quesada, S. Benítez, J. Ordóñez-Llanos, Electronegative low-density lipoprotein, *Curr Opin Lipidol* 15(3) (2004) 329-35.
- [111] J.L. Sánchez-Quesada, A. Pérez, A. Caixàs, M. Rigla, A. Payés, S. Benítez, J. Ordóñez-Llanos, Effect of glycemic optimization on electronegative low-density lipoprotein in diabetes: relation to nonenzymatic glycosylation and oxidative modification, *J Clin Endocrinol Metab* 86(7) (2001) 3243-9.
- [112] G. Niccoli, M. Baca, M. De Spirito, T. Parasassi, N. Cosentino, G. Greco, M. Conte, R.A. Montone, G. Arcovito, F. Crea, Impact of electronegative low-density lipoprotein on angiographic coronary atherosclerotic burden, *Atherosclerosis* 223(1) (2012) 166-70.
- [113] K. Oorni, M.O. Pentikainen, M. Ala-Korpela, P.T. Kovanen, Aggregation, fusion, and vesicle formation of modified low density lipoprotein particles: molecular mechanisms and effects on matrix interactions, *J Lipid Res* 41(11) (2000) 1703-14.
- [114] K. Oörni, P. Posio, M. Ala-Korpela, M. Jauhiainen, P.T. Kovanen, Sphingomyelinase induces aggregation and fusion of small very low-density lipoprotein and intermediate-density lipoprotein particles and increases their retention to human arterial proteoglycans, *Arterioscler Thromb Vasc Biol* 25(8) (2005) 1678-83.
- [115] S.L. Schissel, J. Tweedie-Hardman, J.H. Rapp, G. Graham, K.J. Williams, I. Tabas, Rabbit aorta and human atherosclerotic lesions hydrolyze the sphingomyelin of retained low-density lipoprotein. Proposed role for arterial-wall sphingomyelinase in subendothelial retention and aggregation of atherogenic lipoproteins, *J Clin Invest* 98(6) (1996) 1455-64.
- [116] S. Lehti, S.D. Nguyen, I. Belevich, H. Vihinen, H.M. Heikkila, R. Soliymani, R. Kakela, J. Saksi, M. Jauhiainen, G.A. Grabowski, O. Kummu, S. Horkko, M. Baumann, P.J. Lindsberg, E. Jokitalo, P.T. Kovanen, K. Oorni, Extracellular Lipids Accumulate in Human Carotid Arteries as Distinct Three-Dimensional Structures and Have Proinflammatory Properties, *Am J Pathol* 188(2) (2018) 525-538.

- [117] K. Oorni, J.K. Hakala, A. Annala, M. Ala-Korpela, P.T. Kovanen, Sphingomyelinase induces aggregation and fusion, but phospholipase A2 only aggregation, of low density lipoprotein (LDL) particles. Two distinct mechanisms leading to increased binding strength of LDL to human aortic proteoglycans, *J Biol Chem* 273(44) (1998) 29127-34.
- [118] K. Oorni, P.T. Kovanen, Aggregation Susceptibility of Low-Density Lipoproteins-A Novel Modifiable Biomarker of Cardiovascular Risk, *J Clin Med* 10(8) (2021).
- [119] S. Jayaraman, D.L. Gantz, O. Gursky, Effects of phospholipase A(2) and its products on structural stability of human LDL: relevance to formation of LDL-derived lipid droplets, *J Lipid Res* 52(3) (2011) 549-57.
- [120] M. Sneek, S.D. Nguyen, T. Pihlajamaa, G. Yohannes, M.L. Riekkola, R. Milne, P.T. Kovanen, K. Oörni, Conformational changes of apoB-100 in SMase-modified LDL mediate formation of large aggregates at acidic pH, *J Lipid Res* 53(9) (2012) 1832-9.
- [121] M.F. Lopes-Virella, G. Virella, T.J. Orchard, S. Koskinen, R.W. Evans, D.J. Becker, K.Y. Forrest, Antibodies to oxidized LDL and LDL-containing immune complexes as risk factors for coronary artery disease in diabetes mellitus, *Clin Immunol* 90(2) (1999) 165-72.
- [122] M.F. Lopes-Virella, M.B. McHenry, S. Lipsitz, E. Yim, P.F. Wilson, D.T. Lackland, T. Lyons, A.J. Jenkins, G. Virella, D.E.R. Group, Immune complexes containing modified lipoproteins are related to the progression of internal carotid intima-media thickness in patients with type 1 diabetes, *Atherosclerosis* 190(2) (2007) 359-69.
- [123] S. Yla-Herttuala, W. Palinski, S.W. Butler, S. Picard, D. Steinberg, J.L. Witztum, Rabbit and human atherosclerotic lesions contain IgG that recognizes epitopes of oxidized LDL, *Arterioscler Thromb* 14(1) (1994) 32-40.
- [124] S. Bettuzzi, Conclusions and perspectives, *Adv Cancer Res* 105 (2009) 133-50.
- [125] F. Rizzi, M. Coletta, S. Bettuzzi, Chapter 2: Clusterin (CLU): From one gene and two transcripts to many proteins, *Adv Cancer Res* 104 (2009) 9-23.
- [126] W.D. Stuart, B. Krol, S.H. Jenkins, J.A. Harmony, Structure and stability of apolipoprotein J-containing high-density lipoproteins, *Biochemistry* 31(36) (1992) 8552-9.
- [127] H.Y. Sun, S.F. Chen, M.D. Lai, T.T. Chang, T.L. Chen, P.Y. Li, D.B. Shieh, K.C. Young, Comparative proteomic profiling of plasma very-low-density and low-density lipoproteins, *Clin Chim Acta* 411(5-6) (2010) 336-44.

- [128] I.P. Trougakos, E.S. Gonos, Clusterin/apolipoprotein J in human aging and cancer, *Int J Biochem Cell Biol* 34(11) (2002) 1430-48.
- [129] E.M. Foster, A. Dangla-Valls, S. Lovestone, E.M. Ribe, N.J. Buckley, Clusterin in Alzheimer's Disease: Mechanisms, Genetics, and Lessons From Other Pathologies, *Front Neurosci* 13 (2019) 164.
- [130] S. Park, K.W. Mathis, I.K. Lee, The physiological roles of apolipoprotein J/clusterin in metabolic and cardiovascular diseases, *Rev Endocr Metab Disord* 15(1) (2014) 45-53.
- [131] B. Shannan, M. Seifert, K. Leskov, J. Willis, D. Boothman, W. Tilgen, J. Reichrath, Challenge and promise: roles for clusterin in pathogenesis, progression and therapy of cancer, *Cell Death Differ* 13(1) (2006) 12-9.
- [132] Y. Ishikawa, Y. Akasaka, T. Ishii, K. Komiyama, S. Masuda, N. Asuwa, N.H. Choi-Miura, M. Tomita, Distribution and synthesis of apolipoprotein J in the atherosclerotic aorta, *Arterioscler Thromb Vasc Biol* 18(4) (1998) 665-72.
- [133] I.C. Gelissen, T. Hochgrebe, M.R. Wilson, S.B. Easterbrook-Smith, W. Jessup, R.T. Dean, A.J. Brown, Apolipoprotein J (clusterin) induces cholesterol export from macrophage-foam cells: a potential anti-atherogenic function?, *Biochem J* 331 ( Pt 1)(Pt 1) (1998) 231-7.
- [134] P. Rohne, H. Prochnow, C. Koch-Brandt, The CLU-files: disentanglement of a mystery, *Biomol Concepts* 7(1) (2016) 1-15.
- [135] K.S. Leskov, D.Y. Klovov, J. Li, T.J. Kinsella, D.A. Boothman, Synthesis and functional analyses of nuclear clusterin, a cell death protein, *J Biol Chem* 278(13) (2003) 11590-600.
- [136] D.T. Humphreys, J.A. Carver, S.B. Easterbrook-Smith, M.R. Wilson, Clusterin has chaperone-like activity similar to that of small heat shock proteins, *J Biol Chem* 274(11) (1999) 6875-81.
- [137] A.R. Wyatt, J.J. Yerbury, P. Berghofer, I. Greguric, A. Katsifis, C.M. Dobson, M.R. Wilson, Clusterin facilitates in vivo clearance of extracellular misfolded proteins, *Cell Mol Life Sci* 68(23) (2011) 3919-31.
- [138] A. Londou, A. Mikrou, I.K. Zarkadis, Cloning and characterization of two clusterin isoforms in rainbow trout, *Mol Immunol* 45(2) (2008) 470-8.
- [139] A.R. Wyatt, J.J. Yerbury, M.R. Wilson, Structural characterization of clusterin-chaperone client protein complexes, *J Biol Chem* 284(33) (2009) 21920-21927.
- [140] T. Hochgrebe, G.J. Pankhurst, J. Wilce, S.B. Easterbrook-Smith, pH-dependent changes in the in vitro ligand-binding properties and structure of human clusterin, *Biochemistry* 39(6) (2000) 1411-9.

- [141] R.W. Bailey, A.K. Dunker, C.J. Brown, E.C. Garner, M.D. Griswold, Clusterin, a binding protein with a molten globule-like region, *Biochemistry* 40(39) (2001) 11828-40.
- [142] J. Lord, K. Morgan, Clusterin, in: K. Morgan, M.M. Carrasquillo (Eds.), *Genetic Variants in Alzheimer's Disease*, Springer New York, New York, NY, 2013, pp. 25-51.
- [143] B. Mackness, R. Hunt, P.N. Durrington, M.I. Mackness, Increased immunolocalization of paraoxonase, clusterin, and apolipoprotein A-I in the human artery wall with the progression of atherosclerosis, *Arterioscler Thromb Vasc Biol* 17(7) (1997) 1233-8.
- [144] T.C. Jordan-Starck, S.D. Lund, D.P. Witte, B.J. Aronow, C.A. Ley, W.D. Stuart, D.K. Swertfeger, L.R. Clayton, S.F. Sells, B. Paigen, et al., Mouse apolipoprotein J: characterization of a gene implicated in atherosclerosis, *J Lipid Res* 35(2) (1994) 194-210.
- [145] I.C. Gelissen, T. Hochgrebe, M.R. Wilson, S.B. Easterbrook-Smith, W. Jessup, R.T. Dean, A.J. Brown, Apolipoprotein J (clusterin) induces cholesterol export from macrophage-foam cells: a potential anti-atherogenic function?, *Biochem J* 331 ( Pt 1) (1998) 231-7.
- [146] M. Schwarz, L. Spath, C.A. Lux, K. Paprotka, M. Torzewski, K. Dersch, C. Koch-Brandt, M. Husmann, S. Bhakdi, Potential protective role of apoprotein J (clusterin) in atherogenesis: binding to enzymatically modified low-density lipoprotein reduces fatty acid-mediated cytotoxicity, *Thromb Haemost* 100(1) (2008) 110-8.
- [147] M. Martinez-Bujidos, A. Rull, B. Gonzalez-Cura, M. Perez-Cuellar, L. Montoliu-Gaya, S. Villegas, J. Ordonez-Llanos, J.L. Sanchez-Quesada, Clusterin/apolipoprotein J binds to aggregated LDL in human plasma and plays a protective role against LDL aggregation, *FASEB J* 29(5) (2015) 1688-700.
- [148] V. Apostolopoulos, J. Bojarska, T.T. Chai, S. Elnagdy, K. Kaczmarek, J. Matsoukas, R. New, K. Parang, O.P. Lopez, H. Parhiz, C.O. Perera, M. Pickholz, M. Remko, M. Saviano, M. Skwarczynski, Y. Tang, W.M. Wolf, T. Yoshiya, J. Zabrocki, P. Zielenkiewicz, M. AlKhazindar, V. Barriga, K. Kelaidonis, E.M. Sarasia, I. Toth, A Global Review on Short Peptides: Frontiers and Perspectives, *Molecules* 26(2) (2021).
- [149] P. Vlieghe, V. Lisowski, J. Martinez, M. Khrestchatsky, Synthetic therapeutic peptides: science and market, *Drug Discov Today* 15(1-2) (2010) 40-56.
- [150] D. Goodwin, P. Simerska, I. Toth, Peptides as therapeutics with enhanced bioactivity, *Curr Med Chem* 19(26) (2012) 4451-61.



- [151] E.A. Stein, F.J. Raal, Lipid-Lowering Drug Therapy for CVD Prevention: Looking into the Future, *Curr Cardiol Rep* 17(11) (2015) 104.
- [152] C. Costopoulos, M. Niespialowska-Steuden, N. Kukreja, D.A. Gorog, Novel oral anticoagulants in acute coronary syndrome, *Int J Cardiol* 167(6) (2013) 2449-55.
- [153] A. Wolska, M. Reimund, D.O. Sviridov, M.J. Amar, A.T. Remaley, Apolipoprotein Mimetic Peptides: Potential New Therapies for Cardiovascular Diseases, *Cells* 10(3) (2021).
- [154] G.M. Anantharamaiah, J.L. Jones, C.G. Brouillette, C.F. Schmidt, B.H. Chung, T.A. Hughes, A.S. Bhowan, J.P. Segrest, Studies of synthetic peptide analogs of the amphipathic helix. Structure of complexes with dimyristoyl phosphatidylcholine, *J Biol Chem* 260(18) (1985) 10248-55.
- [155] D.W. Garber, Y.V. Venkatachalapathi, K.B. Gupta, J. Ibdah, M.C. Phillips, J.B. Hazelrig, J.P. Segrest, G.M. Anantharamaiah, Turnover of synthetic class A amphipathic peptide analogues of exchangeable apolipoproteins in rats. Correlation with physical properties, *Arterioscler Thromb* 12(8) (1992) 886-94.
- [156] M. Navab, G.M. Anantharamaiah, S.T. Reddy, S. Hama, G. Hough, V.R. Grijalva, N. Yu, B.J. Ansell, G. Datta, D.W. Garber, A.M. Fogelman, Apolipoprotein A-I mimetic peptides, *Arterioscler Thromb Vasc Biol* 25(7) (2005) 1325-31.
- [157] M. Navab, G.M. Anantharamaiah, S. Hama, D.W. Garber, M. Chaddha, G. Hough, R. Lallone, A.M. Fogelman, Oral administration of an Apo A-I mimetic Peptide synthesized from D-amino acids dramatically reduces atherosclerosis in mice independent of plasma cholesterol, *Circulation* 105(3) (2002) 290-2.
- [158] X. Li, K.Y. Chyu, J.R. Faria Neto, J. Yano, N. Nathwani, C. Ferreira, P.C. Dimayuga, B. Cercek, S. Kaul, P.K. Shah, Differential effects of apolipoprotein A-I-mimetic peptide on evolving and established atherosclerosis in apolipoprotein E-null mice, *Circulation* 110(12) (2004) 1701-5.
- [159] L.T. Bloedon, R. Dunbar, D. Duffy, P. Pinell-Salles, R. Norris, B.J. DeGroot, R. Movva, M. Navab, A.M. Fogelman, D.J. Rader, Safety, pharmacokinetics, and pharmacodynamics of oral apoA-I mimetic peptide D-4F in high-risk cardiovascular patients, *J Lipid Res* 49(6) (2008) 1344-52.
- [160] B.J. Van Lenten, A.C. Wagner, C.L. Jung, P. Ruchala, A.J. Waring, R.I. Lehrer, A.D. Watson, S. Hama, M. Navab, G.M. Anantharamaiah, A.M. Fogelman, Anti-inflammatory apoA-I-mimetic peptides bind oxidized lipids with much higher affinity than human apoA-I, *J Lipid Res* 49(11) (2008) 2302-11.

- [161] C.E. Watson, N. Weissbach, L. Kjems, S. Ayalasomayajula, Y. Zhang, I. Chang, M. Navab, S. Hama, G. Hough, S.T. Reddy, D. Soffer, D.J. Rader, A.M. Fogelman, A. Schecter, Treatment of patients with cardiovascular disease with L-4F, an apo-A1 mimetic, did not improve select biomarkers of HDL function, *J Lipid Res* 52(2) (2011) 361-73.
- [162] A. Chattopadhyay, M. Navab, G. Hough, F. Gao, D. Meriwether, V. Grijalva, J.R. Springstead, M.N. Palgnachari, R. Namiri-Kalantari, F. Su, B.J. Van Lenten, A.C. Wagner, G.M. Anantharamaiah, R. Farias-Eisner, S.T. Reddy, A.M. Fogelman, A novel approach to oral apoA-I mimetic therapy, *J Lipid Res* 54(4) (2013) 995-1010.
- [163] M. Navab, G. Hough, G.M. Buga, F. Su, A.C. Wagner, D. Meriwether, A. Chattopadhyay, F. Gao, V. Grijalva, J.S. Danciger, B.J. Van Lenten, E. Org, A.J. Lusis, C. Pan, G.M. Anantharamaiah, R. Farias-Eisner, S.S. Smyth, S.T. Reddy, A.M. Fogelman, Transgenic 6F tomatoes act on the small intestine to prevent systemic inflammation and dyslipidemia caused by Western diet and intestinally derived lysophosphatidic acid, *J Lipid Res* 54(12) (2013) 3403-18.
- [164] A.T. Remaley, F. Thomas, J.A. Stonik, S.J. Demosky, S.E. Bark, E.B. Neufeld, A.V. Bocharov, T.G. Vishnyakova, A.P. Patterson, T.L. Eggerman, S. Santamarina-Fojo, H.B. Brewer, Synthetic amphipathic helical peptides promote lipid efflux from cells by an ABCA1-dependent and an ABCA1-independent pathway, *J Lipid Res* 44(4) (2003) 828-36.
- [165] Y. Uehara, S. Ando, E. Yahiro, K. Oniki, M. Ayaori, S. Abe, E. Kawachi, B. Zhang, S. Shioi, H. Tanigawa, S. Imaizumi, S. Miura, K. Saku, FAMP, a novel apoA-I mimetic peptide, suppresses aortic plaque formation through promotion of biological HDL function in ApoE-deficient mice, *J Am Heart Assoc* 2(3) (2013) e000048.
- [166] J.K. Bielicki, H. Zhang, Y. Cortez, Y. Zheng, V. Narayanaswami, A. Patel, J. Johansson, S. Azhar, A new HDL mimetic peptide that stimulates cellular cholesterol efflux with high efficiency greatly reduces atherosclerosis in mice, *J Lipid Res* 51(6) (2010) 1496-503.
- [167] O.F. Sharifov, G. Nayyar, D.W. Garber, S.P. Handattu, V.K. Mishra, D. Goldberg, G.M. Anantharamaiah, H. Gupta, Apolipoprotein E mimetics and cholesterol-lowering properties, *Am J Cardiovasc Drugs* 11(6) (2011) 371-81.
- [168] H. Gupta, C.R. White, S. Handattu, D.W. Garber, G. Datta, M. Chaddha, L. Dai, S.H. Gianturco, W.A. Bradley, G.M. Anantharamaiah, Apolipoprotein E mimetic Peptide dramatically lowers plasma cholesterol and restores endothelial function in watanabe heritable hyperlipidemic rabbits, *Circulation* 111(23) (2005) 3112-8.

- [169] C.R. White, D.W. Garber, G.M. Anantharamaiah, Anti-inflammatory and cholesterol-reducing properties of apolipoprotein mimetics: a review, *J Lipid Res* 55(10) (2014) 2007-21.
- [170] S.T. Reddy, G.M. Anantharamaiah, M. Navab, S. Hama, G. Hough, V. Grijalva, D.W. Garber, G. Datta, A.M. Fogelman, Oral amphipathic peptides as therapeutic agents, *Expert Opin Investig Drugs* 15(1) (2006) 13-21.
- [171] M. Navab, G.M. Anantharamaiah, S.T. Reddy, B.J. Van Lenten, A.C. Wagner, S. Hama, G. Hough, E. Bachini, D.W. Garber, V.K. Mishra, M.N. Palgunachari, A.M. Fogelman, An oral apoJ peptide renders HDL antiinflammatory in mice and monkeys and dramatically reduces atherosclerosis in apolipoprotein E-null mice, *Arterioscler Thromb Vasc Biol* 25(9) (2005) 1932-7.
- [172] V.K. Mishra, M.N. Palgunachari, J.S. Hudson, R. Shin, T.D. Keenum, N.R. Krishna, G.M. Anantharamaiah, Structure and lipid interactions of an anti-inflammatory and anti-atherogenic 10-residue class G(\*) apolipoprotein J peptide using solution NMR, *Biochim Biophys Acta* 1808(1) (2011) 498-507.
- [173] N.A. Mansukhani, Z. Wang, V.P. Shively, M.E. Kelly, J.M. Vercaamen, M.R. Kibbe, Sex Differences in the LDL Receptor Knockout Mouse Model of Atherosclerosis, *Artery Res* 20 (2017) 8-11.
- [174] R.J. Havel, H.A. Eder, J.H. Bragdon, The distribution and chemical composition of ultracentrifugally separated lipoproteins in human serum, *J Clin Invest* 34(9) (1955) 1345-53.
- [175] C.M. Radding, D. Steinberg, Studies on the synthesis and secretion of serum lipoproteins by rat liver slices, *J Clin Invest* 39 (1960) 1560-9.
- [176] C. Bancells, S. Villegas, F.J. Blanco, S. Benítez, I. Gállego, L. Beloki, M. Pérez-Cuellar, J. Ordóñez-Llanos, J.L. Sánchez-Quesada, Aggregated electronegative low density lipoprotein in human plasma shows a high tendency toward phospholipolysis and particle fusion, *J Biol Chem* 285(42) (2010) 32425-35.
- [177] M. KGaA, Introduction to SDS-PAGE - Separation of Proteins Based on Size, 2021. <https://www.sigmaaldrich.com/ES/es/technical-documents/protocol/protein-biology/gel-electrophoresis/sds-page>. (Accessed 02 July 2021 2021).
- [178] R. Brunelli, G. Mei, E.K. Krasnowska, F. Pierucci, L. Zichella, F. Ursini, T. Parasassi, Estradiol enhances the resistance of LDL to oxidation by stabilizing apoB-100 conformation, *Biochemistry* 39(45) (2000) 13897-903.
- [179] E. de Juan-Franco, A. Pérez, V. Ribas, J.A. Sánchez-Hernández, F. Blanco-Vaca, J. Ordóñez-Llanos, J.L. Sánchez-Quesada, Standardization of

a method to evaluate the antioxidant capacity of high-density lipoproteins, *Int J Biomed Sci* 5(4) (2009) 402-10.

[180] V. Ribas, J.L. Sánchez-Quesada, R. Antón, M. Camacho, J. Julve, J.C. Escolà-Gil, L. Vila, J. Ordóñez-Llanos, F. Blanco-Vaca, Human apolipoprotein A-II enrichment displaces paraoxonase from HDL and impairs its antioxidant properties: a new mechanism linking HDL protein composition and antiatherogenic potential, *Circ Res* 95(8) (2004) 789-97.

[181] C. Flood, M. Gustafsson, R.E. Pitas, L. Arnaboldi, R.L. Walzem, J. Boren, Molecular mechanism for changes in proteoglycan binding on compositional changes of the core and the surface of low-density lipoprotein-containing human apolipoprotein B100, *Arterioscler Thromb Vasc Biol* 24(3) (2004) 564-70.

[182] R.M. Stoekenbroek, E.S. Stroes, G.K. Hovingh, ApoA-I mimetics, *Handb Exp Pharmacol* 224 (2015) 631-48.

[183] M. Navab, G.M. Anantharamaiah, S.T. Reddy, S. Hama, G. Hough, V.R. Grijalva, A.C. Wagner, J.S. Frank, G. Datta, D. Garber, A.M. Fogelman, Oral D-4F causes formation of pre-beta high-density lipoprotein and improves high-density lipoprotein-mediated cholesterol efflux and reverse cholesterol transport from macrophages in apolipoprotein E-null mice, *Circulation* 109(25) (2004) 3215-20.

[184] G.S. Getz, G.D. Wool, C.A. Reardon, HDL apolipoprotein-related peptides in the treatment of atherosclerosis and other inflammatory disorders, *Curr Pharm Des* 16(28) (2010) 3173-84.

[185] I. Karalis, J.W. Jukema, HDL Mimetics Infusion and Regression of Atherosclerosis: Is It Still Considered a Valid Therapeutic Option?, *Curr Cardiol Rep* 20(8) (2018) 66.

[186] C.R. White, D.I. Goldberg, G.M. Anantharamaiah, Recent developments in modulating atherogenic lipoproteins, *Curr Opin Lipidol* 26(5) (2015) 369-75.

[187] M. Reimund, A. Wolska, R. Risti, S. Wilson, D. Sviridov, A.T. Remaley, A. Lookene, Apolipoprotein C-II mimetic peptide is an efficient activator of lipoprotein lipase in human plasma as studied by a calorimetric approach, *Biochem Biophys Res Commun* 519(1) (2019) 67-72.

[188] A. Wolska, Z.H. Yang, A.T. Remaley, Hypertriglyceridemia: new approaches in management and treatment, *Curr Opin Lipidol* 31(6) (2020) 331-339.

[189] M. Ruuth, S.D. Nguyen, T. Vihervaara, M. Hilvo, T.D. Laajala, P.K. Kondadi, A. Gistera, H. Lahteenmaki, T. Kittila, J. Huusko, M. Uusitupa, U. Schwab, M.J. Savolainen, J. Sinisalo, M.L. Lokki, M.S. Nieminen, A. Jula, M. Perola, S. Yla-Herttula, L. Rudel, A. Oorni, M. Baumann, A. Baruch, R.

- Laaksonen, D.F.J. Ketelhuth, T. Aittokallio, M. Jauhiainen, R. Kakela, J. Boren, K.J. Williams, P.T. Kovanen, K. Oorni, Susceptibility of low-density lipoprotein particles to aggregate depends on particle lipidome, is modifiable, and associates with future cardiovascular deaths, *Eur Heart J* 39(27) (2018) 2562-2573.
- [190] S.P. Heffron, M.K. Ruuth, Y. Xia, G. Hernandez, L. Aikas, C. Rodriguez, K. Oorni, J.S. Berger, Low-density lipoprotein aggregation predicts adverse cardiovascular events in peripheral artery disease, *Atherosclerosis* 316 (2021) 53-57.
- [191] S.D. Nguyen, M. Javanainen, S. Rissanen, H. Zhao, J. Huusko, A.M. Kivela, S. Yla-Herttuala, M. Navab, A.M. Fogelman, I. Vattulainen, P.T. Kovanen, K. Oorni, Apolipoprotein A-I mimetic peptide 4F blocks sphingomyelinase-induced LDL aggregation, *J Lipid Res* 56(6) (2015) 1206-21.
- [192] M. Ruuth, L. Aikas, F. Tigistu-Sahle, R. Kakela, H. Lindholm, P. Simonen, P.T. Kovanen, H. Gylling, K. Oorni, Plant Stanol Esters Reduce LDL (Low-Density Lipoprotein) Aggregation by Altering LDL Surface Lipids: The BLOOD FLOW Randomized Intervention Study, *Arterioscler Thromb Vasc Biol* 40(9) (2020) 2310-2321.
- [193] Z. Feng, B. Xu, Inspiration from the mirror: D-amino acid containing peptides in biomedical approaches, *Biomol Concepts* 7(3) (2016) 179-87.
- [194] S.J. Nicholls, K. Bubb, The mystery of evacetrapib - why are CETP inhibitors failing?, *Expert Rev Cardiovasc Ther* 18(3) (2020) 127-130.
- [195] A.R. Tall, Plasma high density lipoproteins: Therapeutic targeting and links to atherogenic inflammation, *Atherosclerosis* 276 (2018) 39-43.
- [196] E. Jarauta, A.M. Bea-Sanz, V. Marco-Benedi, I. Lamiquiz-Moneo, Genetics of Hypercholesterolemia: Comparison Between Familial Hypercholesterolemia and Hypercholesterolemia Nonrelated to LDL Receptor, *Front Genet* 11 (2020) 554931.
- [197] S. Oppi, T.F. Luscher, S. Stein, Mouse Models for Atherosclerosis Research-Which Is My Line?, *Front Cardiovasc Med* 6 (2019) 46.
- [198] D.L. Tribble, Lipoprotein oxidation in dyslipidemia: insights into general mechanisms affecting lipoprotein oxidative behavior, *Curr Opin Lipidol* 6(4) (1995) 196-208.
- [199] A. Zerrad-Saadi, P. Therond, S. Chantepie, M. Couturier, K.A. Rye, M.J. Chapman, A. Kontush, HDL3-mediated inactivation of LDL-associated phospholipid hydroperoxides is determined by the redox status of apolipoprotein A-I and HDL particle surface lipid rigidity: relevance to inflammation and atherogenesis, *Arterioscler Thromb Vasc Biol* 29(12) (2009) 2169-75.

- [200] M. Estruch, J.L. Sanchez-Quesada, J. Ordonez Llanos, S. Benitez, Electronegative LDL: a circulating modified LDL with a role in inflammation, *Mediators Inflamm* 2013 (2013) 181324.
- [201] W.Y. Chen, F.Y. Chen, A.S. Lee, K.H. Ting, C.M. Chang, J.F. Hsu, W.S. Lee, J.R. Sheu, C.H. Chen, M.Y. Shen, Sesamol reduces the atherogenicity of electronegative L5 LDL in vivo and in vitro, *J Nat Prod* 78(2) (2015) 225-33.
- [202] Y.S. Lai, T.C. Yang, P.Y. Chang, S.F. Chang, S.L. Ho, H.L. Chen, S.C. Lu, Electronegative LDL is linked to high-fat, high-cholesterol diet-induced nonalcoholic steatohepatitis in hamsters, *J Nutr Biochem* 30 (2016) 44-52.
- [203] E.P. Stahl, D.S. Dhindsa, S.K. Lee, P.B. Sandesara, N.P. Chalasani, L.S. Sperling, Nonalcoholic Fatty Liver Disease and the Heart: JACC State-of-the-Art Review, *J Am Coll Cardiol* 73(8) (2019) 948-963.
- [204] C. Ju, F. Tacke, Hepatic macrophages in homeostasis and liver diseases: from pathogenesis to novel therapeutic strategies, *Cell Mol Immunol* 13(3) (2016) 316-27.
- [205] D.P. Koonen, R.L. Jacobs, M. Febbraio, M.E. Young, C.L. Soltys, H. Ong, D.E. Vance, J.R. Dyck, Increased hepatic CD36 expression contributes to dyslipidemia associated with diet-induced obesity, *Diabetes* 56(12) (2007) 2863-71.
- [206] A. Rivas-Urbina, A. Rull, L. Montoliu-Gaya, M. Perez-Cuellar, J. Ordonez-Llanos, S. Villegas, J.L. Sanchez-Quesada, Low-density lipoprotein aggregation is inhibited by apolipoprotein J-derived mimetic peptide D-[113-122]apoJ, *Biochim Biophys Acta Mol Cell Biol Lipids* 1865(2) (2020) 158541.
- [207] Y. Xu, H. Liu, M. Liu, F. Li, L. Liu, F. Du, D. Fan, H. Yu, A human apolipoprotein E mimetic peptide reduces atherosclerosis in aged apolipoprotein E null mice, *Am J Transl Res* 8(8) (2016) 3482-92.
- [208] M. Fernandez-Sendin, C.A. Di Trani, A. Bella, M. Vasquez, N. Ardaiz, C. Gomar, L. Arrizabalaga, S. Ciordia, F.J. Corrales, F. Aranda, P. Berraondo, Long-Term Liver Expression of an Apolipoprotein A-I Mimetic Peptide Attenuates Interferon-Alpha-Induced Inflammation and Promotes Antiviral Activity, *Front Immunol* 11 (2020) 620283.
- [209] K.C. McGrath, X. Li, S.M. Twigg, A.K. Heather, Apolipoprotein-AI mimetic peptides D-4F and L-5F decrease hepatic inflammation and increase insulin sensitivity in C57BL/6 mice, *PLoS One* 15(1) (2020) e0226931.
- [210] M. Peng, Q. Zhang, Y. Cheng, S. Fu, H. Yang, X. Guo, J. Zhang, L. Wang, L. Zhang, Z. Xue, Y. Li, Y. Da, Z. Yao, L. Qiao, R. Zhang, Apolipoprotein A-I

mimetic peptide 4F suppresses tumor-associated macrophages and pancreatic cancer progression, *Oncotarget* 8(59) (2017) 99693-99706.

[211] T.M. Nowacki, A.T. Remaley, D. Bettenworth, M. Eisenblatter, T. Vowinkel, F. Becker, T. Vogl, J. Roth, U.J. Tietge, A. Lugerling, J. Heidemann, J.R. Nofer, The 5A apolipoprotein A-I (apoA-I) mimetic peptide ameliorates experimental colitis by regulating monocyte infiltration, *Br J Pharmacol* 173(18) (2016) 2780-92.

## ▪ ACKNOWLEDGEMENTS





Siempre pensaba si iba a llegar el momento de escribir este apartado de tesis y ahora es realidad. Y es realidad gracias a muchas personas que estuvieron presentes todo este tiempo. ¡Por dónde comenzar a escribir cuando hay tantas personas maravillosas que se han cruzado en tu camino!

Quiero agradecer a Jordi Ordóñez por estar allí cuando llegué por primera vez a Sant Pau y por guiarme cuando le dije que quería hacer el doctorado. Gracias por aceptarme en tu grupo y por esas palabras que uno necesita escuchar para no venirse abajo cuando no todo va bien. Gracias Jordi por estar ahí en cada momento. Gracias también por enlazarme con José Luis o JL, como yo le digo, para que fuera mi responsable directo de este trabajo.

JL, que quieres que te diga que no sepa. No se me olvida la primera vez que te escribí un correo y te dije Doctor y tu respuesta fue que no te dijera Doctor, un comentario muy tuyo jajajaja. Gracias por ser pieza fundamental de esta tesis, por confiar en mí desde el momento cero y por permitirme crecer profesional y personalmente. Me has enseñado no solo de lipoproteínas, me has enseñado que no hay que estresarse porque siempre todo termina saliendo y por enseñarme que no hay nada mejor e importante que las pachangas y la cerveza que se hace en casa. Eres una de las mejores personas que he conocido en mucho tiempo y te mereces todo lo bueno que la vida puede tener. ¡Gracias por estar allí siempre!

Gracias a Nuria y a Karen. Mis compañeras del lab y del día a día. Dos personas que ahora son parte de mi vida, qué suerte haberlas encontrado en este camino. Gracias por aguantarme, por las risas, los chismes y por todo. ¡Las quiero y extraño!

Sonia y Nuria P, las que han visto a la Andrea feliz, triste, sonriente, molesta o en cualquier estado de ánimo porque siempre estaban allí para comprenderme, reír conmigo o molestarnos todas por alguna injusticia jajaja. Gracias por ayudarme en todo lo que era posible ayudar en este proyecto y por enseñarme que uno puede ser feliz en su trabajo, solo basta tener compañeras como ustedes.

Joan Carles o JC. Gracias por nunca decirme no cuando te preguntaba algo. Siempre disponible, siempre amable, siempre allí para ayudar. Gracias por enseñarme mucho de lo que hoy presento en esta tesis. Gracias por confiar en mí y porque mi PFIS fue gracias a ti.

Xisco, gracias también por creer en mí todo este tiempo, por tus consejos y ayuda. Por reír en las fotos cuando te lo pedí, la prueba esta impresa jejeje.

Josep, a pesar de que siempre estabas ocupado con mucho trabajo jamás me dabas un no por respuesta. Siempre dispuesto a ayudar aún cuando no fuera algo de tu especialidad. Nunca he visto persona tan apasionada por lo que hace como tú, gracias por enseñarme que hay que querer lo que uno hace a pesar de las dificultades.

David, siempre digo que sin ti el laboratorio sería muy aburrido y no hay verdad mas pura que esa. Los días de trabajo siempre eran mas amenos contigo, tus chistes, tus bromas, tu libro, tu conocimiento. Gracias por tu apoyo infinito.

Gracias al resto de mis compis del lab que de alguna u otra manera hicieron de mi tiempo allí una de las mejores experiencias que he tenido. Gracias Lidia, Noe, Marina, Elena, Raquel, Margarida, Rosa, Susana. ¡Gracias TOTALES!

A mis amigos de siempre, los de toda la vida. Greis, Carmen, Joha, Jonathan (el feo), Deli, Esthy, Faby, Gus! Gracias porque no importa la hora, la distancia o el día SIEMPRE están en mi vida haciéndola más bonita.

Gracias también a Joi, gracias por necesitar un TFM y por aceptar hacerlo conmigo. Fuiste pieza fundamental de este trabajo experimental. Creo que sin ti no hubiera sido posible acabar todo. Gracias por llegar a mi vida también porque eres una persona increíble. Te has convertido en una amiga que jamás quisiera perder. Gracias nenita bella por estar siempre.

El motor que me mueve cada día mi familia. Gracias mamita por ser lo más maravilloso que tengo en la vida, por creer siempre en mí. No tengo palabras para agradecerte el gran trabajo que has hecho como madre, ojalá pueda ser tan solo un poquito como tú. Gracias por levantarte siempre, por no decaer por esa fuerza que me transmites. ¡Te amo!

Gracias manito (mi monito) no solo por acompañarme en esta aventura, sino por ser un ejemplo de vida siendo tan jovencito. Me motivas y llenas de amor mi existencia todos los días. Gracias por permitir tenerte tan cerca. ¡Te amo!

A ti papito gracias. Porque donde quieras que estés sé que me observas con orgullo, porque todo lo que soy te lo debo a ti. Porque fue tanto lo que me diste en vida que se me llena el alma todos los días con tantos recuerdos a tu lado. Créeme, no hay día que no te piense. Te dedico esta tesis papito ¡Te amo!

Gracias a ti negrito, por ser mi sostén diario. Porque creo que no lo hubiera logrado sin ti, sin tu amor, sin tu apoyo, sin tus palabras, sin tu guía. Eres lo que siempre soñé y mucho más. Cuando te miro a los ojos el mundo se

paraliza, soy afortunada de compartir mi vida contigo. Gracias por cada segundo de felicidad que me das, por caminar a mi lado, por ayudarme tanto con esta tesis y por darme el MEJOR regalo del mundo, ERIC mi príncipe, mi pequeño gran motor que me cambió la vida. Gracias hijo porque ahora sé y siento muchas cosas que no sabía antes de tu llegada. Me transformaste totalmente, eres lo más importante de mi vida y prometo hacerte feliz siempre.

Al resto de mi familia GRACIAS, son la mejor familia que puede existir. Los amo inmensamente.

Gracias Diosito por permitir estar aquí y escribir estas palabras.